

SEQUENCE-STRATIGRAPHIC CONTROL ON THE NONMARINE FOSSIL RECORD: A
TEST IN THE JUDITH RIVER FORMATION OF NORTH-CENTRAL MONTANA

by

ANIK REGAN

(Under the Direction of Steven M. Holland)

ABSTRACT

Simulating the nonmarine fossil record within a sequence-stratigraphic framework is important for understanding stratigraphic control on the distribution of fossils. The empirical model presented here simulates a stratigraphic column with occurrences of plant, invertebrate, and vertebrate fossils based on data from the Judith River Formation of north-central Montana. The model uses an embedded Markov chain to simulate stratigraphy, based on calculated transition probabilities among facies and the thickness distribution across facies. Facies transition probabilities and their thickness and frequency distribution are used to numerically compare systems tracts. The numerical comparisons match the qualitative expectations from previous studies of nonmarine stratigraphy. Fossil occurrences in the simulated columns are based on observed probabilities of occurrence of each taxon within each facies. Although sample size is insufficient in some cases, the probabilities of occurrence of fossils varies among facies, systems tracts, and the elevation gradient.

INDEX WORDS: Judith River Formation, sequence stratigraphy, Markov chain, nonmarine, fossil preservation, Cretaceous

SEQUENCE-STRATIGRAPHIC CONTROL ON THE NONMARINE FOSSIL RECORD: A
TEST IN THE JUDITH RIVER FORMATION OF NORTH-CENTRAL MONTANA

by

ANIK REGAN

B.A., Macalester College, 2017

A Thesis Submitted to the Graduate Faculty of The University of Georgia in Partial Fulfillment
of the Requirements for the Degree

MASTER OF SCIENCE

ATHENS, GEORGIA

2021

© 2021

Anik Regan

All Rights Reserved

SEQUENCE-STRATIGRAPHIC CONTROL ON THE NONMARINE FOSSIL RECORD: A
TEST IN THE JUDITH RIVER FORMATION OF NORTH-CENTRAL MONTANA

by

ANIK REGAN

Major Professor:	Steven M. Holland
Committee:	Raymond R. Rogers
	David F. Porinchu

Electronic Version Approved:

Ron Walcott
Vice Provost for Graduate Education and Dean of the Graduate School
The University of Georgia
December 2021

DEDICATION

This work is dedicated to all the strong, intelligent, weird, and wonderful women in my life. Ariana Garcia Callahan, Brooke Hunter, Sarah Silbert, Izzy Ballet, Lea Davidson, Kelly MacGregor, Kristi Curry Rogers, Samantha Khatri, Kelsey Mueller, Hoai-Nam Bui, and Judy Lutter. You all, among many others, inspire me with your passion, empathy, and friendship. Much love.

ACKNOWLEDGEMENTS

I would like to express my sincere gratitude to Steve Holland for his guidance on this project. His incredible editing and baking skills, his wisdom and kindness, and the enthusiasm he brings to his work and the lab made this project fun and successful. This work would not have happened without Ray Rogers, who inspired my interest in geology, brought me to the field, gave me a job, helped me get into grad school, and continuously supports my path as a scientist and as a human. Thank you both.

I would like to thank my field assistant Alex “Sun Rash” Johanson for his excellence and enthusiasm. I couldn’t have asked for a better partner to work with this summer. Thank you Dave Porinchu for taking the time to serve on my committee. I am grateful to the people in the UGA Geology Department, past and current Strat Lab members, housemates, my wonderful frisbee teammates, and my friends and family (Marla, John, and Caitlin) for your academic, mental, and emotional support over the years. I also thank Zane Fulbright, Ellie Fulbright, Kandy Walton, Jim Mitchell, Jack Carr, Tom Philp, Heidi Tungesvick, Dan Noskog, Jerry Magda, and the folks at the Rising Trout and the Winifred Tavern for making my fieldwork in Montana possible. Finally, thank you Ian Hahn for always being there for me.

This work was partially supported by the NSF/GSA Graduate Student Geoscience Grant #12773-20, which is funded by NSF Award #194990. In addition, funding was provided by the Paleontological Society, Sigma Xi, and the Miriam Watts-Wheeler Fund.

TABLE OF CONTENTS

	Page
ACKNOWLEDGEMENTS	v
LIST OF TABLES	viii
LIST OF FIGURES	ix
CHAPTER	
1 INTRODUCTION AND LITERATURE REVIEW	1
2 SEQUENCE-STRATIGRAPHIC CONTROL ON THE NONMARINE FOSSIL RECORD: A TEST IN THE JUDITH RIVER FORMATION OF NORTH-CENTRAL MONTANA	4
Introduction.....	5
Background.....	6
Geologic Setting.....	17
Hypotheses	22
Methods.....	23
Stratigraphic Framework	26
Quantitative Analysis of Stratigraphy.....	28
Probability of Occurrence of Fossils.....	31
Discussion	34
Conclusions.....	43
3 CONCLUSIONS AND FUTURE WORK.....	45

REFERENCES	48
------------------	----

APPENDICES

A LOCALITIES OF MEASURED COLUMNS AND FOSSIL COLLECTIONS	104
B STRATIGRAPHIC COLUMNS	106
C FOSSIL COUNTS	112
D COLUMN KEY	121
E TRANSITION MATRICES	122
F PROPORTIONAL FACIES THICKNESS AND FREQUENCIES	124
G PROBABILITIES OF OCCURRENCE	127
H R CODE FOR MODEL, CALCULATIONS, AND FIGURES	133
I R CODE FOR HELPER FUNCTIONS	149

LIST OF TABLES

	Page
Table 1: Semi-quantitative log scale used for counting fossil abundances	64
Table 2: Nonmarine facies of the Judith River Formation	65
Table 3: Comparison of probability of occurrence among systems tracts.....	68
Table 4: Comparison of the probability of occurrence along an environmental gradient	69

LIST OF FIGURES

	Page
Figure 1: Accommodation to sedimentation ratio	70
Figure 2: Stratigraphic architecture of nonmarine settings.....	72
Figure 3: Summary of occurrence of nonmarine fossils.....	73
Figure 4: Theoretical Eh–pH stability fields for fossils preserved in paleosols	74
Figure 5: Species response curve.....	75
Figure 6: Map of study area.....	76
Figure 7: Paleogeographic map	78
Figure 8: Regional stratigraphic framework.....	79
Figure 9: Floodplain facies association plate.....	81
Figure 10: Channel facies association plate.....	83
Figure 11: Woodhawk Bottom study area	85
Figure 12: Woodhawk Bottom measured columns.....	86
Figure 13: Stafford Ferry study area.....	88
Figure 14: Stafford Ferry measured columns	89
Figure 15: HAST and LAST facies transitions.....	91
Figure 16: Comparison of HAST and LAST facies transitions.....	92
Figure 17: Numerical comparison of thickness and frequency of HAST and LAST facies.....	93
Figure 18: Probability of occurrence among channel and floodplain facies	94
Figure 19: Probability of occurrence among individual facies associations.....	95

Figure 20: Probability of occurrence in floodplain and channel facies among systems tracts96

Figure 21: Probability of occurrence in individual facies association among systems tracts.....97

Figure 22: Probability of occurrence in floodplain and channel facies in the HAST updip and
downdip.....98

Figure 23: Probability of occurrence in individual facies associations in the HAST updip and
downdip.....99

Figure 24: Sampling methods to compare updip and downdip probabilities of occurrence100

Figure 25: Simulated and measured stratigraphic columns101

Figure 26: Simulated gradual transitions between systems tracts103

CHAPTER 1

INTRODUCTION AND LITERATURE REVIEW

This thesis is organized into three chapters. The first gives background and motivation for this work. Chapter two is written as a stand-alone manuscript to be submitted to *PALAIOS* and comprises an introduction, geologic background, methods, results, discussion, and conclusions. The final chapter offers suggestions for future research. Several appendices provide supporting data and code.

The fossil record is a natural archive of macroevolutionary and macroecological phenomenon. However, the fossil record not only reflects biological history but also the processes relating to fossilization and sediment accumulation (Behrensmeyer and Kidwell, 1985; Behrensmeyer and Hook, 1992; Kidwell and Flessa, 1995; Behrensmeyer et al., 2000; Kidwell and Holland, 2002; Purnell et al., 2018; Holland and Loughney, 2020). It is therefore important to disentangle these processes from biological history (Holland, 2000; Fraser, 2017). One important set of processes relate to stratigraphic architecture, which controls many patterns of fossil occurrence (Brett, 1995; Holland, 1995, 2000; Patzkowsky and Holland, 2012; Holland and Loughney, 2020).

Modeling is one technique that can be used to systematically evaluate the fossil record and explore underlying processes of fossil preservation. Models of the fossil record provide a way to control some of the variance seen in the natural record and then generate hypotheses on the observed patterns of fossil occurrences. These models must be grounded in a sequence-stratigraphic framework, as stratigraphic architecture controls the distribution and preservation of

fossils. Most previous models have focused on the relationships between fossil preservation and sequence stratigraphy in marine systems (Brett, 1995; Scarponi and Kowalewski, 2007; Peters et al., 2009; Patzkowsky and Holland, 2012; Holland and Patzkowsky, 2015).

One early example of simulating the marine fossil record combines models of basin-scale stratigraphy, species originations and extinctions, and probabilities of occurrence of fossils in facies to simulate stratigraphic patterns and fossil distributions (Holland and Patzkowsky, 1999). The results of the model demonstrated sequence-stratigraphic control on range offset as well as a method for partitioning the controls on fossil occurrences. This work spurred further investigation of the stratigraphic context of fossil occurrences and the subsequent interpretations of biotic change (i.e., Holland and Patzkowsky, 2015).

The research on marine systems has shown that stratigraphic architecture is predictable and that fossil concentrations occur at predictable stratigraphic locations. The same principles should hold true for nonmarine systems, but few studies in nonmarine systems have interpreted fossil occurrences within a sequence-stratigraphic framework (but see Rogers and Kidwell, 2000; Straight and Eberth, 2002; Colombi et al., 2017), and no study has developed a stratigraphic model of the nonmarine fossil record. This presents a great opportunity to develop models that incorporate stratigraphy and fossil preservation to enhance our understanding of biodiversity on land at any scale.

One of the few examples from the nonmarine realm uses a model of fossilization of North American mammals to address if latitudinal richness gradients are detectable in the nonmarine fossil record (Fraser, 2017). For this model, fossil localities are simulated based on the probability of occurrence, which is a function of body size and geographic range. The latitudinal diversity gradient is estimated for the simulated fossil localities based on the slope of

the richness gradient and the degree of species turnover. The results of the model indicated that at low preservation rates the gradients are not detectable. However, at medium to high preservation rates, the diversity gradient can be reliably estimated. This study, although not incorporating stratigraphic processes, demonstrates the utility of using models to explore the fossil record. With these results, future researchers can test these predictions in nonmarine basins.

Given the paucity of stratigraphic models of the nonmarine fossil record as well as the utility of putting fossils in a sequence-stratigraphic context, there is a clear need for research in this area. This work begins to fill that niche. The purpose of this study is to combine fieldwork and empirical modeling to describe the variability of fossil occurrences in the Judith River Formation of north-central Montana with respect to facies, systems tracts, and an elevation gradient.

CHAPTER 2

SEQUENCE-STRATIGRAPHIC CONTROL ON THE NONMARINE FOSSIL RECORD: A TEST IN THE JUDITH RIVER FORMATION OF NORTH-CENTRAL MONTANA¹

¹ Regan, A.K., Rogers, R.R., and Holland, S.M. To be submitted to PALAIOS

Introduction

Sequence-stratigraphic architecture is well known to control the distribution and preservation of fossils in marine systems, where it affects interpretations of ecological and evolutionary patterns (Brett, 1995; Scarponi and Kowalewski, 2007; Peters et al., 2009; Patzkowsky and Holland, 2012; Holland and Patzkowsky, 2015). For example, the last occurrences of marine invertebrate fossils tend to cluster at significant surfaces such as subaerial unconformities and major flooding surfaces (Holland and Patzkowsky, 2015; Nawrot et al., 2018). Marine vertebrates follow a similar pattern, where fossils occur most commonly in stratigraphically condensed intervals (such as marine flooding surfaces), and the taxonomic composition of assemblages varies with position in the sequence (Peters et al., 2009; McMullen et al., 2014). In addition, species richness and diversity of Quaternary marine mollusks closely track sequence-stratigraphic architecture (Scarponi and Kowalewski, 2007; Wittmer et al., 2014).

In contrast, interpretations of the nonmarine fossil record are limited by a scarcity of similar quantitative studies that incorporate sequence stratigraphy into paleobiologic interpretations (but see Rogers and Kidwell, 2000; Straight and Eberth, 2002; Colombi et al., 2017). Furthermore, existing numerical models of nonmarine deposition either incorporate parameters that are difficult to measure in the field (Allen, 1978; Leeder, 1978; Bridge and Leeder, 1979), or they focus on the geomorphology and landscape dynamics of the system and not on the resulting stratigraphic architecture (Salles et al., 2018). This makes it difficult to use these models to make predictions about the stratigraphic distribution of nonmarine fossils.

An important pattern that must be captured in any model of the nonmarine fossil record is that preservation of plant, molluscan invertebrate (from here on referred to as “invertebrate”), and vertebrate fossils varies among channel and floodplain facies (e.g., Bown and Kraus, 1981;

Koster et al., 1987; Eberth, 1990; Behrensmeyer and Hook, 1992; Rogers and Brady, 2010; Colombi et al., 2012; Loughney and Badgley, 2017). Moreover, the nature and relative proportion of these facies differs among nonmarine systems tracts (Shanley and McCabe, 1994; Martinsen et al., 1999). This combination raises the question of how fossil preservation varies among nonmarine systems tracts.

The goal of this project is to develop an empirical model of the nonmarine fossil record and calibrate it with stratigraphic and fossil data from the Judith River Formation of north-central Montana. The model requires three main components: a tabulation of transitions between facies (a transition matrix), the distribution of facies thicknesses, and the probability of occurrence of plant, invertebrate, and vertebrate fossils in each facies. The calculated transition probabilities and the facies thickness and frequencies are used to compare differences in nonmarine systems tracts. The calculated probability of preservation of fossils is evaluated among facies, systems tracts, as well as along an elevation gradient to understand patterns of nonmarine fossil preservation within a sequence-stratigraphic framework in the Judith River Formation.

Background

Nonmarine sequence stratigraphy

Modeling the nonmarine fossil record should be grounded in the long-term controls on the stratigraphic record, namely, sequence stratigraphy. Sequence stratigraphy itself is based on the inferred ratio of accommodation to sedimentation (A:S; Figure 1). Accommodation is the combined rate of tectonic subsidence (or uplift) and eustatic sea-level change. Early studies explicitly tied nonmarine systems tracts to changes in base level and eustatic sea level, and they applied marine systems-tract terminology to nonmarine strata (Posamentier and Vail, 1988;

Shanley and McCabe, 1993; Wright and Marriott, 1993; Shanley and McCabe, 1994). More recent studies have moved toward terminology that reflects observable features in nonmarine systems and has severed the necessity of a direct connection to eustasy. This is significant because many nonmarine basins are either unconnected to the shoreline (Scherer et al., 2015; Colombi et al., 2017) or are so far depositionally up dip that they are beyond the influence of changes in sea level (Holbrook et al., 2006).

Different models have been developed to portray the range of nonmarine stratigraphic architectures. One of the earliest and most widely used models divides alluvial architecture into a high-accommodation systems tract (HAST) and a low-accommodation systems tract (LAST; Martinsen et al., 1999; Catuneanu, 2006; Figure 2). Another approach packages fluvial aggradation cycles into equivalents to the transgressive systems tract and highstand/falling-stage systems tracts used in marine systems (Atchley et al., 2004; Cleveland et al., 2007). In this study, I use the Martinsen et al. (1999) model of HAST and LAST but recognize that these systems tracts represent a spectrum and may include a wider range of possible features and architectural elements (Boyd et al., 2000; Allen et al., 2014; Holland and Loughney, 2020).

There are three general states of the A:S ratio to consider in nonmarine stratigraphic architecture: negative, low positive, and high positive (Figure 1). While the actual A:S ratio in any given basin is seldom known, these general states have been inferred using a suite of characteristics such as channel stacking patterns and paleosol type and development (Burns et al., 1997; Martinsen et al., 1999; Atchley et al., 2004; Catuneanu, 2006; Cleveland et al., 2007; reviewed in Holland and Loughney, 2020).

A negative value of the A:S ratio forms a subaerial unconformity (Martinsen et al., 1999). In this scenario, rivers at or near the shore incise to create landward-growing valleys. This also

fosters the development of paleosols on the interfluves between these valleys (Martinsen et al., 1999; Blum et al., 2013). Paleosols may also form on terraces as the river continues to incise. Paleosols developed during this time have a low likelihood of preservation, but if preserved, will be well-developed and oxidized.

Low but positive values of the A:S ratio create a LAST (Martinsen et al., 1999). At or near the shore, fluvial channel deposits in a LAST are multistory and multilateral, with little to no floodplain preservation (Martinsen et al., 1999; Catuneanu, 2006; Scherer et al., 2015). These thick sandstone bodies can be traced laterally over long distances. Lateral channel migration reworks the floodplain, hindering the preservation of floodplain deposits (Wright and Marriott, 1993). Paleosols in the LAST are uncommon, owing to the lack of floodplain deposits, but when preserved they tend to be well-developed and oxidized, owing to a low local or regional water table (Gastaldo and Demko, 2011).

Higher values of the A:S ratio create a HAST (Martinsen et al., 1999). At or near the shore, HAST channel deposits are isolated within thicker floodplain deposits. These channel deposits may display evidence of tidal influence in coastal areas (Shanley and McCabe, 1993). Multistory channel deposits may be present, but the channel belts are seldom laterally continuous. Given the relatively high water table that accompanies high rates of accommodation (Gastaldo and Demko, 2011), floodplain deposits of a HAST may preserve ponds, lakes, mires, and immature, hydromorphic paleosols (Currie, 1997). Thick, well-developed coal seams are more likely to form in the HAST (Wadsworth et al., 2002; Catuneanu, 2006).

Transitions between the three states of the A:S ratio can be abrupt or gradational. The expansion surface marks an abrupt increase in the A:S ratio and the upward switch from a LAST to a HAST (Martinsen et al., 1999). This surface can be recognized by a sharp change in channel

architecture, from amalgamated, multistory, multilateral channel deposits to isolated channel deposits surrounded by thick floodplain deposits. An abrupt decrease in the A:S ratio marks a sequence boundary and the upward switch from a HAST to a LAST (Martinsen et al., 1999). The sequence boundary is placed at the subaerial unconformity, and it can lie at the base of an incised valley or at a well-developed, oxidized paleosol on the interfluves (e.g., Aitkin and Flint, 1995).

The boundaries of systems tracts are often imprecise and most likely vary in basins with different overall rates of accommodation and A:S ratios. An upward gradational transition from a LAST to a HAST may manifest in an expansion zone, rather than an expansion surface. Similarly, the sequence boundary can fall between two LAST deposits, indicating the possibility of a gradational change in alluvial architecture from HAST to LAST, without a distinct surface separating the two systems tracts (Figure 1).

Even so, depositional sequences tend to have a predictable architecture (Figure 2; Martinsen et al., 1999). Starting at the base of the section, the interpreted A:S ratio is positive and low (LAST) and steadily decreases upward as the sequence boundary is approached. This steady decrease is represented by the increasing amalgamation of the fluvial channel deposits. Once the A:S ratio becomes negative, a subaerial unconformity develops and rivers incise to form valleys (commonly referred to as incised valleys). As the A:S ratio becomes positive, the rivers begin to aggrade again. The channel deposits are multistory and multilateral under these low rates of accommodation, forming a LAST. The A:S ratio remains low as the valley is filled, preserving minimal floodplain deposits. As rates of accommodation increase, an expansion surface marks the abrupt increase in the A:S ratio and the switch to a HAST, with isolated fluvial channel deposits and thick intervals of floodplain. As accommodation rates begin to decrease and the A:S ratio decreases gradually, the HAST grades upward into the LAST without a sharp

surface separating them. At the top of the section the A:S ratio again becomes negative, initiating a subaerial unconformity. If this is followed by a rapid increase in the A:S ratio the sequence boundary and the expansion surface will coincide.

Variables in the HAST, LAST framework

Changes to the A:S ratio result from a variety of downstream and upstream processes (Blum and Tornqvist, 2000; Catuneanu, 2006).

Downstream control mainly reflects eustasy in basins that have a marine connection, and its influence declines with increasing distance from the shoreline. As a result, eustatic sea-level change has potentially negligible effects far inland (Burns et al., 1997; Blum and Tornqvist, 2000), making tectonic subsidence a dominant control on accommodation in many nonmarine systems (Bridge and Leeder, 1979). The landward limit of sea-level influence depends on many factors, including the drainage area of the basin, hinterland sediment supply, and the gradient of the floodplain, making this control difficult to quantify in the record (Blum and Tornqvist, 2000; Gugliotta et al., 2016).

Upstream control on sediment supply depends on climate and source area (relief, slope, and lithology), with the rate of sedimentation responding to changes in eustasy, climate, source-area tectonism, and basin subsidence (Catuneanu, 2006). Although many workers emphasize the importance of varying rates of accommodation in driving nonmarine architecture, sediment supply can be at least as important (Leeder et al., 1998; Huerta et al., 2011; Allen et al., 2014; Ainsworth et al., 2020).

Additional complicating factors affect nonmarine architecture. Internally generated (autogenic) fluvial processes, such as dune migration, channel meandering, channel bifurcation,

and avulsion, drive fluvial architecture and mimic the architecture of the HAST and LAST (Hajek et al., 2012; Hajek and Straub, 2017). The architecture of the HAST and LAST also vary in updip and downdip areas due to the complex interaction between upstream versus downstream controls (Holbrook et al., 2006). All of these factors underscore the need to characterize the HAST, LAST, expansion surface, and sequence boundary not just on channel stacking patterns, but also on a suite of recognizable characteristics such as evidence of tidal influence, degree of paleosol development and drainage, presence and complexity of coals, and presence of lakes (Colombera et al., 2015; Holland and Loughney, 2020) .

Nonmarine fossil preservation

Modeling the nonmarine fossil record requires an understanding of the controls on preservation of organic material. The occurrence of plant, invertebrate, and vertebrate fossils differs among depositional environments (Figure 3) because of the suitability of the original habitat for each organism and the potential for organic remains to be preserved in that habitat (Bown and Kraus, 1981; Koster et al., 1987; Eberth, 1990; Behrensmeyer and Hook, 1992; Rogers and Brady, 2010; Loughney and Badgley, 2017). The taphonomic modes of taxa depend on the supply of organic material, climate, the position of the water table, and the rates of accommodation, sedimentation, and decay (i.e., weathering, dissolution, and recycling; Behrensmeyer et al., 2000). In particular, the Eh and pH conditions of the burial environment are a key factor in the probability of preservation of the organic material (Retallack, 1998; Figure 4). Eh indicates the oxidation status of the sediments, with low Eh corresponding with reducing conditions. pH refers to the acidity or basicity, with low pH being more acidic. Given the overall controls on the preservation of plants, invertebrates, and vertebrates, it follows that environments

have varying potential to preserve taxa, and different facies will therefore have variable probabilities of occurrence of those fossil taxa (Behrensmeyer and Hook, 1992).

Plant fossils are best preserved in dysoxic or anoxic settings where the rate of sedimentation exceeds the rate of decay (Gastaldo and Demko, 2011; Figure 3). Wet and cool climates tend to favor these conditions by lowering microbial rates of respiration (Behrensmeyer et al., 2000). Fossil plant material, which includes preserved leaves and petals, root casts, seed pods, pollen, wood, amber, and carbonaceous debris, is most often found in lakes, ponds, abandoned channels, and poorly-drained floodplain deposits (Behrensmeyer and Hook, 1992). In these environments, decay is hindered by a high water table, itself promoted by a high A:S ratio (Gastaldo and Demko, 2011). Pollen is more robust than most other plant material, but it can also be affected by oxidation, desiccation, and degradation by bacteria and fungi (Campbell, 1999; Li et al., 2007).

Invertebrate fossils (mollusks) are preserved most readily in carbonate-rich (alkaline) sediments, where dissolution of calcite and aragonite is minimal (Cadée, 1999; Figure 3). Bioturbated, carbonate paleosols in arid to semi-arid environments facilitate the formation of a carbonate crust on the shell, which adds to the durability of the shell and its likelihood of preservation (Yanes et al., 2008). Invertebrates are commonly found in abandoned channel fills and oxygenated ponds and lakes (Behrensmeyer and Hook; 1982). They are also present in channel lag and floodplain deposits, although their abundance is not commonly reported in either setting.

Vertebrate assemblages are formed in four main settings: long-term sites of mortality (attrition), fluvial accumulation, carnivore and scavenger accumulation, and mass-death events (Loughney and Badgley, 2020; Figure 3). For bone to fossilize, the rate of recrystallization must

exceed the rate of dissolution and loss of bone mineral (Trueman, 1999). Preservation of bone in floodplain environments is controlled largely by Eh and pH conditions (Retallack, 1984, 1998) whereas Eh, pH, channel form, and sedimentation rate influence the likelihood of bone preservation in channels (Behrensmeyer, 1988). Bone is best preserved in floodplain deposits with neutral to high pH and low overall moisture (Behrensmeyer, 1982). Drier and warmer conditions generally favor bone preservation (Behrensmeyer et al., 2000). Vertebrate fossils are most commonly found in channel lags and bars, abandoned channels, pond/lakes deposits, and they are also present in floodplain deposits (Behrensmeyer and Hook, 1982).

Simulating the fossil record: past endeavors

Simulating the fossil record encourages the testing and development of new hypotheses on the quality of the fossil record and changes in the ecology and evolution of organisms through time. Existing models for simulating the fossil record are based on three components (Holland, 1995; Holland and Patzkowsky, 1999). The first is basin-scale stratigraphy, created through accommodation and sedimentation. The second component is a model of species originations and extinctions. The third component is the probability of species occurrence in each sedimentary facies.

Basin-scale stratigraphy has been modeled using many approaches that simulate accommodation, erosion, and sediment accumulation (Falivene et al., 2019). Some significant previous models of marine stratigraphy include STRATA (Flemings and Grotzinger, 1996), sedflux (Hutton and Syvitski, 2008), and SimClast (Dalman and Weltje, 2012). These models incorporate tectonic subsidence, eustasy, and sedimentation, to varying degrees of complexity to generate 2-D cross sections (generally onshore–offshore) of a continental margin.

A variety of nonmarine stratigraphic models also exist. The 2-D numerical Leeder-Allen-Bridge (LAB) models (Allen, 1978; Leeder, 1978; Bridge and Leeder, 1979) simulate alluvial architecture using estimates of geomorphic and tectonic parameters (i.e., avulsion rate, subsidence rate, channel dimensions, time, etc.). These models are useful for simulating a range of potential nonmarine stratigraphic architectures, but values for the parameters are difficult to obtain in the field. Process-based models of nonmarine systems, such as pyBadlands (Salles and Hardiman, 2016; Salles et al., 2018) and the modeling platform Landlab (Hobley et al., 2017), typically focus on landscape evolution, which encompasses the terrain and the flow of mass (i.e., ice, water, or nutrients) across that terrain (Hobley et al., 2017). Models such as these do not differentiate between channel and floodplain sedimentation and are therefore difficult to use within the HAST and LAST framework of nonmarine stratigraphy.

Species originations and extinctions can be computed by a variety of evolutionary models that describe change in diversity over time (Raup, 1985). Variation in these models arises from either maintaining a constant diversity through time or allowing the rate of speciation and extinction to change in a gradual or punctuated way. Previous simulations of the stratigraphic distribution of marine fossils used a time-homogenous random branching method to simulate a suite of species (Holland, 1995). This method allows for stochastic originations and extinctions of species based on a constant empirical probability.

Finally, the probability of species occurrence can be estimated using species-response curves (Holland, 1995; Holland and Patzkowsky, 1999; Figure 5). The probability of occurrence for any species can be approximated as normally distributed along an environmental gradient, or alternatively, as constant within each facies. For marine species, where water depth is the primary environmental gradient controlling species distribution, the species response curve

specifies the probability of occurrence at a given water depth (Figure 5). Since depth can be estimated from marine facies, the probability of occurrence for a suite of species can be determined using the species response curve. Elevation is an established principle environmental gradient that describes nonmarine species distribution (see review in Holland and Loughney, 2020), but it cannot be easily estimated from nonmarine facies. Therefore, species response curves are not yet a viable option for establishing the probability of occurrence in nonmarine systems.

An alternate approach: building an empirical model

The objective of this project is to create a 1-D empirical model of the nonmarine fossil record and apply it to the Judith River Formation to simulate stratigraphic columns and fossil occurrences. My approach differs from previous stratigraphic and paleobiologic models in several ways. I use an embedded Markov-chain method to simulate nonmarine stratigraphy, which bypasses the need for a numerical or process-based model of nonmarine systems. Instead, inputs to the model are based on field data of facies transitions and thickness. I do not simulate evolution at the species or genus level and instead use broad categories of taxonomic rank (i.e., class or higher), which do not originate or go extinct over the timescale this model. Finally, I base the probability of occurrence for each taxon on its presence in each facies in the Judith River Formation, instead of describing the probabilities using species response curves.

Markov chains are a way to model a series of random events and have been used to simulate nonmarine stratigraphy (Carr et al., 1966; Potter and Blakely, 1968; Krumbein and Dacey, 1969; Dindarloo et al., 2015). The chains consist of a series of discrete-time (as opposed to continuous-time) stochastic events, where transitions to each state depend only on the

preceding state, and not on earlier ones. In other words, the transition from one facies to the next in a stratigraphic column depends only on the current facies and is independent of any previous facies. Markov chains are built from transition matrices that contain the probabilities of moving between any combination of facies. The advantage of using a Markov chain, versus a process-based model, is the ability to create columns based on field data instead of based on assumptions about the theoretical behavior of the system.

Using Markov chains to simulate a stratigraphic column has one drawback: they can cause unreasonable thicknesses of units because there is a high probability of continuously transitioning to the same facies (Dindarloo et al., 2015). Consequently, simulated columns are built here using an embedded Markov chain (Krumbein and Dacey, 1969; Dindarloo, 2015), which disallows transitions to the same facies. To build the stratigraphic column using an embedded Markov chain, a starting facies is chosen at random, and its thickness is randomly drawn from a distribution of thicknesses for that facies type. The next unit is selected based on the transition matrix and its corresponding thickness is assigned. This process repeats until the desired column thickness is reached.

Fossil occurrences in the stratigraphic column are based on a probability matrix, where each taxon has a corresponding probability of occurrence in each facies. This matrix is built by tabulating the number of occurrences of a taxon in a particular facies divided by the total number of occurrences of that taxon. The occurrence of fossils in the column is assigned based on comparing the probability of occurrence for a given taxon and facies to a randomly generated number. If the random number is less than or equal to the probability of occurrence, it will be recorded as an occurrence in the column. This comparison happens at a specified sampling interval (e.g., every meter of the column) for plant, invertebrate, and vertebrate fossils.

Geologic Setting

Stratigraphy of the Judith River Formation

This model will be evaluated in the Campanian (Upper Cretaceous) Judith River Formation of north-central Montana. The formation is well-exposed in the badlands flanking the Missouri River in the Upper Missouri River Breaks National Monument (Figure 6) making this an ideal place to develop a model of the nonmarine fossil record. The Judith River Formation contains distal nonmarine and shallow marine strata, with a diverse array of fossils, deposited in the Western Interior Foreland Basin during the regression of the Claggett Sea and subsequent transgression of the Bearpaw Sea (Robinson Roberts and Kirschbaum, 1995; Rogers et al., 2016). These deposits thin eastward where the underlying Claggett Formation and the overlying Bearpaw Formation merge to form the Pierre Shale. The Judith River Formation correlates to the west with the nonmarine Two Medicine Formation, to the north with the Foremost, Oldman, and Dinosaur Park formations of the Belly River Group in Canada, and to the south as parts of the Mesaverde Group in Wyoming, the Wahweap and Kaiparowits Formations in southern Utah, the Fruitland Formation in New Mexico, and the Aguja Formation in West Texas (Rogers et al., 2016).

Paleogeography and paleoclimate

From the Early Cretaceous through the middle Paleocene, the Western Interior Foreland Basin was filled with a montage of marine and nonmarine sediments deposited during transgressions and regressions of the Western Interior Seaway (Gill and Cobban, 1973; Roberts and Kirschbaum, 1995; Fuentes et al., 2011; Slattery et al., 2013). The Western Interior Foreland Basin in northwestern Montana during the Campanian was bound to the west by the Cordilleran

Orogenic Belt and to the east by the North American craton (Slattery et al., 2013; Figure 7). The regression of the Claggett Sea and the transgression of the Bearpaw Sea impacted sediment distribution in the Judith River Formation (Gill and Cobban, 1973; Rogers, 1994, 1998; Slattery et al., 2013), while regional scale sediment distribution in the basin was controlled by dynamic subsidence from mantle downwelling (Chang and Liu, 2021). Sediments filling the basin during the Late Cretaceous originated from thrust sheets involving the Belt Supergroup as well as older, recycled foreland basin deposits (Fuentes et al., 2011). Bentonites (altered volcanic ash beds) and volcanoclastic material found throughout the Judith River Formation are thought to be derived from Late Cretaceous volcanism in the nearby Elkhorn Mountains and Adel Mountains (Smedes, 1966; Gill and Cobban, 1973; Foreman et al., 2008; Rogers et al., 2016).

The climate of the coastal plain during the Cretaceous is considered to have been warm, humid, and relatively stable (Wolfe and Upchurch, 1987). However, from the mid-Cretaceous to the Paleogene, temperatures may have cooled gradually. Paleoclimate reconstructions from carbonate nodules in paleosols in the updip Two Medicine Formation have yielded temperatures between 21–27° C (Burgener et al., 2019). Models of atmospheric circulation have indicated the possibility of monsoonal weather patterns and associated seasonal rainfall in the region (Fricke et al., 2010).

Members of the Judith River Formation

The Judith River Formation consists of four members (Figure 8). The lowermost Parkman Sandstone Member and the uppermost Woodhawk Member are shallow-marine strata and will not be discussed here in detail (see Rogers et al., 2016). The focus of this study is the

McClelland Ferry Member and Coal Ridge Member, which comprise a mix of coastal plain and paralic strata.

The McClelland Ferry Member is a ~70 m thick sandstone-dominated alluvial succession with architecture resembling that of a LAST. This member was deposited during the regression of the Claggett Sea (Rogers, 1998, 1994; Rogers et al., 2016). The basal contact with the underlying Parkman Sandstone Member shows no evidence of an unconformity. The fluvial channel deposits of the McClelland Ferry Member are commonly amalgamated, multistory and multilateral, creating sheet-like geometries. Internal scour surfaces are marked by lags containing clay rip-ups, ironstone pebbles, shell, and bone. Internally, the channel deposits display upward-fining sets of large-scale cross bedding and, where not eroded, are capped by rippled or planar-laminated beds. Lateral accretion surfaces are relatively rare, suggesting decreased rates of lateral migration of the fluvial channels and increased channel-bank stability (Allen, 1965). The overbank facies of the McClelland Ferry Member are gray-green to tan mudstone (Munsell colors 2.5Y 6/2, 5Y 4/1, 5Y 5/2) and siltstone with abundant rooting and evidence of pedogenesis. This coloration is typical of soils formed in reducing, water-logged, or anoxic environments (Tabor et al., 2017). Vertebrate and invertebrate fossil concentrations and bentonites are present, but they are both notably less abundant than in the overlying Coal Ridge Member.

The Coal Ridge Member is a ~90 m thick mudstone-dominated, alluvial and paralic succession with architecture resembling that of a HAST. The member interfingers with the shallow marine Woodhawk Member to the east and was deposited during the transgression of the Bearpaw Sea (Rogers, 1994, 1998; Rogers et al., 2016). The fluvial channel deposits of the Coal Ridge Member are commonly thinner and more lenticular than those of the McClelland Ferry

Member. Similar to the McClelland Ferry Member, these channel deposits are dominated by large-scale trough cross beds. In contrast, lateral accretion surfaces and inclined heterolithic strata are common. Thin laminae of clay and carbonaceous debris commonly drape foresets, indicating tidal influence within the channels. The overbank deposits of the Coal Ridge Member are dark gray to olive green (Munsell colors 5Y 5/2, 10YR 3/2, 5Y 4/3), generally more hydromorphic, and are often carbonaceous or interspersed with lignites, suggesting a high water table and higher probability of preserving organic material. In addition, bentonite beds, thin ironstone beds, and fossil concentrations containing plants, invertebrates, and vertebrates are abundant.

The contact between the McClelland Ferry Member and the overlying Coal Ridge Member is the mid-Judith discontinuity (Figure 8), which is a nonerosional, regionally traceable surface that is interpreted to reflect an abrupt increase in the rate of accommodation (Rogers, 1994, 1998; Rogers and Kidwell, 2000; Rogers et al., 2016). The mid-Judith discontinuity is an expansion surface, which marks the transition from a LAST to a HAST. In outcrop, the discontinuity is characterized by a change in channel architecture, from the multistory and multilateral channel deposits in the underlying McClelland Ferry Member, to thinner, isolated channel deposits in the Coal Ridge Member. The transition from the McClelland Ferry Member to the Coal Ridge Member is also marked by a change in slope and color. The mid-Judith discontinuity is easily recognized in subsurface log data, where spontaneous potential and resistivity decrease abruptly, and gamma ray radiation increases in intensity (Rogers, 1994, 1998; Rogers et al., 2016). The simultaneous changes in amplitude of the logs reflect a regional shift to mudstone-dominated facies and define the regressive-transgressive turnaround in the Judith River Formation (Rogers, 1998; Rogers et al., 2016). The discontinuity can be correlated

outside the study area to the east to a maximum regressive surface at the base of the Woodhawk Member. To the west, the mid-Judith discontinuity potentially correlates with lacustrine carbonate deposits in the Two Medicine Formation (Rogers, 1994, 1998; Rogers and Kidwell, 2000). The abrupt increase in accommodation marked by the discontinuity is attributed to Late Campanian tectonic subsidence (Gill and Cobban, 1973; Rogers, 1998; Sears, 2001; Fuentes et al., 2011).

The terms HAST and LAST were initially designed to describe inland settings, isolated from the effects of eustasy (Catuneanu, 2006); however, they can also be applied to coastal settings like the Judith River Formation. In coastal settings, where the position of the shoreline can be correlated updip into nonmarine strata, it is possible to apply marine systems tracts to nonmarine strata (i.e. Figure 2). For example, the McClelland Ferry Member could be considered a lowstand systems tract and the Coal Ridge Member, which contains multiple small-scale episodes of transgression and regression, could be considered a transgressive systems tract, particularly since both can be correlated downdip to shorefaces. Equivalently, the mid-Judith discontinuity could be called a maximum regressive surface (=transgressive surface), which separates the lowstand and transgressive systems tracts. Here, the terms HAST and LAST are applied to the nonmarine strata of the Judith River Formation to reflect the observed fluvial architecture, even though this may oversimplify some internal complexity. The use of this terminology will ideally facilitate comparison stratigraphy in other nonmarine basins, including those unconnected to the shoreline.

Fossils in the Judith River Formation

The Judith River Formation is abundantly fossiliferous, with vertebrates including amphibians, fish, reptiles, mammals, and dinosaurs (e.g., Dodson, 1971; Sahni, 1972; Béland and Russell, 1978; Brinkman, 1990; Rogers and Brady, 2010). Relatively few studies have examined the plants and pollen of the formation (Knowlton, 1905; Bell, 1965; Hall, 1968, 1969; Tschudy, 1973) or the invertebrates (Rogers and Brady, 2010; Rogers et al., 2018; Taylor and Rogers, 2021), but both are common. Most previous studies focus on the identification and description of new species (e.g., Arbour and Evans, 2017; Taylor and Rogers, 2021) and the origin, taphonomy, and ecological utility of large vertebrate quarries and vertebrate microfossil bonebeds (Wood et al., 1988; Fiorillo, 1990; Eberth and Brinkman, 1997; Rogers and Brady, 2010; Rogers et al., 2017).

Fossil preservation in the Judith River Formation varies with facies (Rogers and Brady, 2010). Pond and lake deposits contain abundant carbonaceous plant debris, amber blebs, freshwater invertebrates, and aquatic to semi-aquatic vertebrate fossils. Fluvial channel deposits contain silicified wood fragments, carbonaceous debris, carbon-draped foresets, invertebrate shell debris, and bone. The majority of vertebrate material is interpreted to have initially accumulated in floodplain ponds and lakes but was subsequently reworked and redeposited in the channels (Rogers, 1993; Rogers and Kidwell, 2000; Rogers et al., 2010; Rogers and Brady, 2010; Rogers et al., 2016).

Hypotheses

The Coal Ridge Member is reportedly more fossiliferous than the underlying McClelland Ferry Member (Rogers, 1993; Rogers et al., 2016). There are three reasons why this might be

true, which I will test by comparing the probabilities of occurrence. First, it may be because the Coal Ridge Member (a HAST) is thicker and therefore has a greater area over which fossils could be found. Second, it could be because the Coal Ridge Member has proportionally more floodplain deposits, in which fossils may be more likely to be preserved. Third, faster burial rates and less channel reworking in a HAST would generally elevate the preservation potential of organisms in the floodplain, and therefore the probability of occurrence of fossils in HAST floodplain facies would be greater than floodplain facies in the LAST (McClelland Ferry Member).

I predict that plant, invertebrate, and vertebrate fossils will have higher probabilities of occurrence in all floodplain facies of the HAST (Coal Ridge Member) versus the LAST (McClelland Ferry Member). However, in channel facies, I predict the patterns may differ slightly. For example, there may be a higher probability of collecting vertebrate, invertebrate, or durable plant material in LAST channels, because all the reworked floodplain could end up being incorporated into the channel lags and bars. Since channel deposits in the HAST are more isolated, fossil material in HAST channel lags and bars may be sparse.

Methods

Field

Stratigraphic columns of the nonmarine members of the Judith River Formation were measured in the Upper Missouri River Breaks National Monument in north-central Montana (Figure 6). Localities were chosen to follow known paths through accessible and fossiliferous rocks based on previous work (Rogers et al., 2016; Table 1A in Appendix A). One column (3-JRS-21) spans the entire thickness of the McClelland Ferry and Coal Ridge members (151.5 m),

while the other six columns capture partial exposures of each member. Columns were measured in two main areas, Stafford Ferry and Woodhawk Bottom, along a roughly east/west transect to capture both the updip and downdip expression of the Judith River Formation.

At each column, color, lithology, bedding, and sedimentary structures were described to interpret facies associations (Appendix B). The occurrence of plant, invertebrate, and vertebrate fossils was counted in each facies (Appendix C). Fossils were counted for five minutes for each facies one meter or less in thickness. For facies thicker than one meter, fossils were counted for five minutes over one-meter intervals. Fossils were counted on the surface about 1.5 m laterally on either side of the column line and, where possible, in a small (~0.5 m) trenched interval. Unless immediately obvious, no attempt was made to trace loose fossils higher in the column. Therefore, fossils occurring on the surface at any given interval were attributed to the facies identified in that interval. Fossils were scored on a semi-quantitative log scale for abundance (Table 1). An area was deemed unsuitable for searching if it was too steep, narrow, vegetated, or weathered. Abundance information was collected for the following categories of fossils: carbonaceous debris, amber, carbonized wood, silicified wood, seeds, leaf impressions, gastropods, bivalves, indeterminate shell hash, teeth, gar scales, turtle shell, ossified tendons, crocodile scutes, fish vertebrae, and all other bone. Six fossil localities were collected and submitted for curation at the Science Museum of Minnesota (Table 2A in Appendix A). All fossil and stratigraphic localities are on land administered by the Bureau of Land Management, and fieldwork was conducted under the Paleontological Resources Use Permit MTM 110471-21 issued to R. Rogers.

Analyses

A table of facies transition probabilities was produced for use in the 1-D model, but also as a method to compare the stratigraphy of the HAST and LAST (Appendix E). To generate the table, the number of transitions from one facies to another was summed, and then divided by the total number of transitions to that facies, generating a probability of transition for that facies. Transitions within facies (i.e. from floodplain mud to floodplain mud) are disallowed.

To explore trends in facies thickness and frequency, values of proportional average facies thickness and proportional number of bodies were calculated (Appendix F). Values of average facies thickness were scaled as a proportion of the thickness of the systems tracts of the columns in which they occurred. Values for the total number of bodies were scaled to the total number of facies in the systems tract. This scaling corrects for differences in measured column thickness and uneven sample sizes of HAST and LAST facies and allows for a more even comparison of the systems tracts.

To evaluate trends in fossil preservation in the Judith River Formation, probability of occurrence was calculated and compared among facies, systems tracts, and along an elevation gradient (Appendix G). For analysis, fossil types were grouped into broader categories of plants, invertebrates, and vertebrates. For plants, only occurrences of amber, silicified wood, seeds, and leaf impressions were included. Probabilities of occurrence were calculated by summing the total number of occurrences for each fossil category in each facies and dividing by the total number of times that particular facies was sampled. They were compared using 95% confidence intervals (Raup, 1991), which is a conservative method to evaluate differences in the estimates.

The empirical model presented here uses the transition matrix to generate synthetic columns, which simulate an expansion surface, a sequence boundary, and a gradual transition

from HAST to LAST and vice versa. The model also uses the observed probabilities of occurrence to simulate the distribution of fossils. Code for all analyses, figures, and the model is included in Appendices H and I.

Stratigraphic Framework

Facies associations

Seven facies associations occur in the nonmarine members of the Judith River Formation (Table 2). Facies are defined by distinct lithologies, colors, bedding, and sedimentary structures. For the purpose of this paper, the terms facies and facies associations are used interchangeably.

Four floodplain facies associations are identified in the study area: mire, pond/lake, floodplain mud, and floodplain sand (Figure 9). Floodplain environments in the Judith River Formation were generally poorly drained and the floodplain facies associations described in this study represent a spectrum of ponding, differentiated by lithology, color, bedding, and amount of organic material. Mire facies are recognizable by their dark reddish brown to black color and by the high amount of carbonaceous debris and carbonized wood, relative to the amount of mud or clay (Figure 9A, B). Pond/lake facies are distinguished from mire facies by their lighter and often more variable color, the lower proportion of carbonaceous debris to mudstone, and by the presence of invertebrate fossils (Figure 9C, D, E). Floodplain mud facies are light gray to olive gray to brown and either have unorganized, fine bits of organic matter or lack carbonaceous debris altogether (Figure 9F, G). Root traces are common in the floodplain mud facies. In some cases, the only distinguishing factor between the floodplain mud and the pond/lake facies is the presence of in-situ invertebrate shell material. Floodplain sand facies are identified by their lithology and sedimentary structures (ripple-scale lamination and rare large-scale trough cross

bedding). They are distinguished from fluvial channel bars by their relative thinness (floodplain sand < 2 m, channel bar \geq 2 m; Figure 9H). These thin sandy deposits are interpreted as originating from crevasse splays (cf. Burns et al., 2017). Contacts between the mire, pond/lake, and floodplain mud facies are generally gradational. Floodplain sand facies are commonly sharp-based and grade upwards into floodplain mud or pond/lake facies.

Three channel facies associations are identified in the study area: fluvial channel lags, fluvial channel bars, and tidally influenced channel bars (Figure 10). Channel lag facies are composed of gravel to cobble sized clasts of cemented sand or mud, with less frequent shell, bone, wood, and carbonaceous debris (Figure 10A, B). These lags are laterally discontinuous, and although observed in outcrop, were not often encountered in the path of the measured columns. Fluvial channel bar facies are identified based on their lithology (very fine to fine grained sand), sedimentary structures (abundant large-scale trough cross bedding), and thickness (Figure 10C, D). Tidal influence is identified primarily by carbonaceous-draped, large-scale trough cross beds and uncommonly by upward thinning, alternating beds of sand and mud (inclined heterolithic strata; Figure 10E, F; cf. Gugliotta et al., 2016). It is likely that some fluvial channel bar facies record tidal influence, but the inaccessibility of outcrop limited the ability to recognize those features. Tidally influenced channel bar facies are identified here only in the Coal Ridge Member.

Stratigraphy

A total of 364 meters of stratigraphic column of the Judith River Formation was measured for this study. At the Woodhawk Bottom study area (Figure 11A), the McClelland Ferry Member is thin to absent and the Coal Ridge Member is truncated by the marine

Woodhawk Member (Figure 11B). The position of the mid-Judith discontinuity at Woodhawk Bottom is not well constrained because of the paucity of nearby subsurface data and is therefore based solely on the WHB1-11 bentonite, changes in slope, and color of the beds (R. Rogers pers. comm.). The WHB1-11 bentonite at Woodhawk Bottom has been dated to 76.17 ± 0.07 Ma, within error of the STI-03 bentonite at Stafford Ferry (76.24 ± 0.18 Ma; Rogers et al., 2016). These marker beds are used in this study, as in previous work, to approximate the location of the mid-Judith discontinuity in outcrop. 114.3 meters of stratigraphic column was measured at Woodhawk Bottom (90.1 m of HAST, 24.2 m of LAST; Figure 12).

At the Stafford Ferry study area (Figure 13A), the full thickness of the nonmarine members of the Judith River Formation is exposed, with a clear distinction between the McClelland Ferry Member and the Coal Ridge Member (Figure 13B). The position of the mid-Judith discontinuity is most conspicuous at a distance, where it is made obvious by changes in color, slope, and dominant lithologies. Up close, the position of the discontinuity can be more obscure. The position of the discontinuity is estimated based on the STI-03 bentonite and by previous estimates of the thickness of the McClelland Ferry Member from subsurface data (Rogers et al., 2016). 249.7 meters of stratigraphic column was measured at Stafford Ferry (128.2 m of HAST, 121.5 m of LAST; Figure 14).

Quantitative Analysis of Stratigraphy

The following sections take a quantitative approach to describing the stratigraphy of the Judith River Formation by comparing transitions between facies (Appendix E) and the thickness and frequency with which they occur (Appendix F). Patterns in facies transition probabilities help reveal the internal organization of nonmarine architecture. Proportional thickness and

frequency alone do not convey stacking patterns or the vertical distribution of facies, but they help to compare the facies composition of these systems tracts. When combined, the transition probabilities and thickness distribution of facies can be used to simulate nonmarine stratigraphy.

Facies transition probabilities

Facies in the HAST show a propensity to transition to floodplain facies, regardless of the starting facies (Figure 15A; Table E1 in Appendix E). For example, the most common transitions are from floodplain mud to pond/lake (63% probability of transition), from mires to pond/lake (62%), and from tidally influenced channel bars to either floodplain mud (43%) or pond/lake (43%). Transitions to channel facies are less common overall, however, transitions from fluvial channel lags to tidally influenced channel bars are very high (100%), albeit with a low sample size (n=2).

Facies transitions in the LAST do not show as strong a pattern as those in the HAST, although the most common ending facies are fluvial channel bars, floodplain sands, and floodplain muds (Figure 15B; Table E2 in Appendix E). The transitions that are most common in the LAST are from mires to floodplain mud (100%), from fluvial channel lags to fluvial channel bars (80%), and from floodplain mud, pond/lake, and fluvial channel lags to floodplain sands (56%, 42%, 20%).

To directly compare which transitions are more common in the HAST versus the LAST, the LAST facies transition probabilities are subtracted from the HAST facies transition probabilities (Figure 16; Table E3 in Appendix E). Transitions from floodplain facies to fluvial channel bars, lags, and floodplain sand are more common in the LAST. Conversely, transitions from floodplain facies in the HAST show a wetting-up trend (Wadsworth et al., 2002), where

floodplain muds transition to pond/lakes, and pond/lakes transition to mires. For channel facies, transitions to and from tidally influenced channel bars are necessarily more common in the HAST, given the lack of tidally influenced channels in the LAST. In addition, transitions from fluvial channel bars to fluvial channel lags are more common in the LAST, indicating the prevalence of stacked, multistory channels.

Thickness of facies

Floodplain facies in the HAST and channel facies in the LAST have a higher proportional average thickness (Figure 17A; Table F1 in Appendix F). For example, mire, pond/lake, and floodplain mud facies represent 56% of HAST deposits and only 40% of LAST deposits. Fluvial channel lag and bar facies comprise 40% of LAST deposits and only 6% of HAST deposits. In contrast floodplain sand facies were proportionally twice as thick in the LAST (16%) than the HAST (8%). In addition, the tidally influenced channel bar facies was not identified in the LAST, so it is necessarily thicker in the HAST (14%).

Frequency of facies

Similar to trends in thickness, floodplain facies in the HAST and channel facies in the LAST occur more frequently (Figure 17B; Tables F2 and F3 in Appendix F). For example, mire, pond/lake, and floodplain mud facies represent 70% of the total number of HAST bodies and only 45% of LAST bodies. Fluvial channel lag and bar facies comprise 25% of the total number of LAST bodies and only 5% of HAST bodies. In contrast, floodplain sand facies occur more frequently in the LAST (24%) versus the HAST (12%). Tidally influenced channel bars occurred more frequently in the HAST (6%) since there were no occurrences in the LAST.

Probability of Occurrence of Fossils

The following sections examine trends in fossil preservation in the Judith River Formation by comparing the probability of occurrence of plant, invertebrate, and vertebrate fossils in facies, systems tracts, and along an elevation gradient (Appendix G). The probability of occurrence is compared broadly, between channel and floodplain facies, and narrowly, among individual facies associations. The calculated probabilities are also used in the model to simulate occurrences of fossils in a stratigraphic column.

Channel versus floodplain facies

Fossils are compared at the broadest level between all Judith River channel and floodplain facies (Figure 18; Table G1 in Appendix G). The probability of occurrence of vertebrate and invertebrate fossils is indistinguishable between channel and floodplain facies (as indicated by broadly overlapping confidence intervals). However, vertebrate fossils tend to be more common in floodplain facies and invertebrate fossils tend to be more common in channel facies. The probability of occurrence for plant fossils is greater in floodplain facies than in channel facies (as indicated by non-overlapping confidence intervals).

Invertebrate and plant fossils show some statistically significant differences in probability of occurrence when compared among individual facies associations (Figure 19; Table G2 in Appendix G). Invertebrates have a higher probability of occurrence in the pond/lake facies than in floodplain sand and fluvial channel bar facies, and they tend to have the highest probability of occurrence in pond/lake and fluvial channel lag facies. Invertebrate fossils were not found in the mire or floodplain mud facies. Plants are more commonly found in pond/lake and floodplain

sand facies relative to fluvial channel bar facies, but overall tend to have their highest probability of occurrence in mire facies. Although not statistically significant, vertebrate fossils tend to occur more frequently in floodplain mud and fluvial channel lag facies. In addition, vertebrate fossils were not found in the mire facies.

HAST versus LAST

The probability of occurrence of vertebrate fossils in channel facies and plant fossils in floodplain and channel facies differs among the HAST and the LAST (Figure 20; Table G3 in Appendix G). Vertebrates have a higher probability of occurrence in LAST channel facies and that tends to hold true for LAST floodplain facies as well. Plant fossils occur more frequently in both floodplain and channel facies in the HAST than the LAST. Differences in the probability of occurrence of invertebrate fossils between systems tracts cannot be demonstrated, however, they tend to be more commonly found in LAST floodplain facies and HAST channel facies.

Owing to the large confidence intervals caused by small sample size, differences in the probability of occurrence cannot be distinguished among systems tracts at the individual facies-association level (Figure 21; Table G4 in Appendix G). However, there are two exceptions. Vertebrate fossils occur more frequently in fluvial channel bar facies in the LAST, and plant fossils have a higher probability of occurrence in pond/lake facies in the HAST. In addition, vertebrate fossils tend to be found more often in LAST facies. Although not statistically significant, invertebrate fossils tend to occur more frequently in HAST facies. Plant fossils also tend to have a higher probability of occurrence in HAST facies but did not occur in HAST fluvial channel lag facies or in LAST fluvial channel bar facies.

HAST updip versus downdip

Probabilities of occurrence are indistinguishable in the HAST updip (Stafford Ferry) and downdip (Woodhawk Bottom; Figure 22; Table G5 in Appendix G). Although not statistically significant, vertebrate fossils tend to have a higher probability of occurrence in updip floodplain and channel facies. Invertebrates tend to be more commonly found downdip for both floodplain and channel facies, although the estimates for updip and downdip floodplain facies are almost identical. Plant fossils tend to occur more frequently updip for both floodplain and channel facies. Owing to a lack of LAST facies at Woodhawk Bottom, a similar comparison was not made.

Because of the small sample size, the probability of occurrence cannot be distinguished between updip and downdip locations for any taxa among individual facies associations (Figure 23; Table G6 in Appendix G). However, trends tend to mirror those discussed above. Vertebrate fossils tend to be found more frequently in updip facies, with the exception of floodplain sand facies. Vertebrates were not found in downdip fluvial channel lag or fluvial channel bar facies. Invertebrates tend to have a higher probability of occurrence downdip, with the exception of pond/lake facies. Invertebrate fossils did not occur in downdip fluvial channel lag facies. Plant fossils tend to occur more commonly updip, also with the exception of pond/lake facies. There were no occurrences of plant fossils in downdip floodplain mud, floodplain sand, or fluvial channel bar facies.

Discussion

Comparison with previous studies of the Judith River Formation stratigraphy

The stratigraphy of the Judith River Formation described here is consistent with descriptions from Rogers et al. (2016). Specifically, there are no large inconsistencies observed between column 3-JRS-21 (this study, Figure 14) and column 91-JRT-8 (Rogers et al., 2016, Figure 3), which were measured in the same location. More broadly, the characteristics and distribution of the facies in each member are consistent between studies. The McClelland Ferry Member is dominated by thick, trough-cross bedded sandstone bodies, interpreted as multistory and multilateral fluvial channel bars, without evidence of tidal influence. The Coal Ridge Member has thicker intervals of mudstones and lignites, interpreted as floodplain muds, ponds/lakes, and mires, and many of the thick sandstone bodies have evidence of tidal influence.

The principal difference in this study is the use of nonmarine sequence-stratigraphic nomenclature to describe the architecture of the Judith River Formation. The McClelland Ferry Member is interpreted here as a LAST, the Coal Ridge Member is interpreted as a HAST, and the mid-Judith discontinuity is identified as an expansion surface. These interpretations were made possible by Rogers et al. (2016), who stated the same concepts using slightly different terminology. He inferred a low- and high-accommodation record, separated by a discontinuity, using highly detailed analysis of stratigraphic columns, sandstone petrography, clay mineralogy, and subsurface data. In this study, terminology from Martinsen et al. (1999) is used to emphasize how the Judith River Formation fits in a nonmarine sequence-stratigraphic framework, which enables comparisons to other nonmarine basins. In addition, two new bonebeds were identified and collected in the McClelland Ferry Member (Table A2 in Appendix A), expanding the knowledge of fossils in the lower nonmarine member.

Numerical observations of HAST and LAST

Based on theoretical and field studies of nonmarine stratigraphy (Leeder, 1978; Allen, 1978; Bridge and Leeder, 1979; Posamentier and Vail, 1988; Shanley and McCabe, 1993; Wright and Marriott, 1993; Shanley and McCabe, 1994; Aitkin and Flint, 1995; Martinsen et al., 1999; Colombera et al., 2015), strata in a LAST are expected to contain multistory, multilateral channel deposits and thin floodplain deposits, whereas those in a HAST are expected to have single-story channel deposits encased in thicker floodplain deposits. Despite this, no quantitative methods have been proposed for describing or separating systems tracts. Characteristics of the HAST and LAST can be numerically evaluated by comparing facies transitions and the thickness and frequency of facies. In addition, examining stratigraphy from a numerical perspective helps illuminate trends that can be used to distinguish and correlate systems tracts.

The facies transitions (Figure 16) and the facies thicknesses and frequencies (Figure 17) of the systems tracts in the Judith River Formation generally confirm that the LAST has more multistory, multilateral channel deposits and thin floodplain deposits whereas the HAST has more single-story channel deposits encased in thicker floodplain deposits. With few exceptions, transitions between the facies also follow these expectations. Transitions between floodplain facies are common in the HAST, creating thick floodplain intervals. Transitions from fluvial channel bar facies to fluvial channel lag facies, creating multistory channels, are more common in the LAST. In addition, floodplain facies are mostly proportionally thicker and more common in the HAST than in the LAST and channel facies are proportionally thicker and more common in the LAST. Although systems tracts should not be defined exclusively on ratios of channel to floodplain facies and channel stacking patterns (Colombera et al., 2015; Holland and Loughney,

2020), these comparisons provide a means to describe the stratigraphy and, in this case, test the predictions and expected relationships.

Vertical variation in probabilities of occurrence

Channel versus floodplain—Although channel and floodplain environments differ in their potential for organic remains to be preserved (Bown and Kraus, 1981; Behrensmeyer and Hook, 1992), the results presented in this study do not support differences in the probability of occurrence between channel and floodplain facies for vertebrate and invertebrate fossils (Figure 18). One possible explanation for this disparity is the method by which the fossil concentrations in the Judith River Formation form. Vertebrate material initially accumulates in the floodplain through attrition and is then exhumed and redeposited in channels (Behrensmeyer, 1982; Rogers, 1993; Rogers and Kidwell, 2000; Rogers and Brady, 2010; Rogers et al., 2010; Rogers et al., 2016). This may hold true for invertebrate fossils as well and would lead to similar probabilities of occurrence in channel and floodplain facies, even if the remains have a higher initial chance of burial in floodplain facies. In contrast, plant fossils are more common in floodplain facies than channel facies, which is consistent with the narrow conditions that need to be met for plant remains to be preserved (Gastaldo and Demko, 2011). Once fossilized, only the sturdier plant material, such as silicified wood, will survive getting reworked by channels, leading to a low probability of occurrence in channel facies.

HAST versus LAST—The Coal Ridge Member has been described as having a higher frequency of skeletal concentrations than the McClelland Ferry Member and containing most of the microfossil bonebeds (Rogers and Brady 2010; Rogers et al., 2016). These differences raise

the possibility that these patterns might be generally true for HAST units like the Coal Ridge Member. Three potential reasons were proposed to account for this: the Coal Ridge Member is thicker, has proportionally more floodplain facies, or HAST floodplain facies have a intrinsically higher preservation potential than LAST floodplain facies. I therefore hypothesized that the probability of occurrence of plant, invertebrate, and vertebrate fossils would be higher in all HAST floodplain facies, and that the probability of occurrence for all categories would be higher in all LAST channel facies. There is presently no evidence that preservation potential between facies in the HAST and LAST can be distinguished, owing to small sample sizes and the overwhelming majority of overlapping confidence intervals. Increased sample size, however, may reveal differences in future studies. Although not statistically significant, several trends seen in the estimates are relevant to the initial reasoning.

The first possibility addresses the relative thickness of the systems tracts in the Judith River Formation. The numerical comparison of the stratigraphy reveals that the Coal Ridge Member (a HAST) has proportionally thicker floodplain facies and the McClelland Ferry Member (a LAST) has proportionally thicker channel facies (Figure 17A). Therefore, a higher probability of occurrence of fossils in HAST floodplain facies and LAST channel facies could be attributed simply to differences in the amount of suitable search area.

The second possibility addresses the relative frequency of channel and floodplain facies in the Judith River Formation. In general, floodplain facies in the HAST and channel facies in the LAST occur more frequently (Figure 17B). So once again, a higher probability of occurrence could be attributed to suitable search area. The trends in facies thickness and facies frequency do not adequately address cases in which the observed pattern does not match the predictions, so it is therefore likely that differences reflect more than simply the amount of exposed rock.

The third possibility, regarding fundamental preservation potential in the HAST and LAST, is more difficult to evaluate with the current data. Vertebrate fossils are more commonly found in LAST fluvial channel bar facies and plant fossils have a higher probability of occurrence in HAST pond/lake facies (Figure 21). These results support the hypothesis that HAST floodplain facies and LAST channel facies are intrinsically more fossiliferous.

Results that are not statistically significant are substantially more variable, and many do not follow the predicted pattern that HAST floodplain facies and LAST channel facies would be more fossiliferous. Only two out of six comparisons between HAST and LAST floodplain and channel facies follow the predicted pattern (Figure 20). At the facies-association level, six out of nine floodplain facies have a higher probability of occurrence in the HAST (Table 3). Three out of six channel facies (not including tidally influenced channels, which were not observed in the LAST), have higher probabilities of occurrence in the LAST.

In many cases, the observed pattern is the opposite of what is expected. Vertebrate fossils in floodplain sand facies, and both vertebrate and invertebrate fossils in pond/lake facies, all have a higher probability of occurrence in the LAST (Table 3). Plant fossils in fluvial channel bar facies, and invertebrate fossils in fluvial channel lag and bar facies, are found more commonly in the HAST. This could be due to small sample size (low power and high probability of a type two error) or it could reflect a more complex pattern in preservation than was initially hypothesized.

Using a 95% confidence interval comparison is a conservative test to evaluate differences in the probabilities of occurrence, and the confidence intervals presented here are very broad owing to small sample size. An obvious question arises from this problem: how large of a sample size is needed to distinguish the probabilities of occurrence? The probability for invertebrates in the pond/lake facies can be used to assess this (Figure 21). This facies has only barely

overlapping confidence intervals and is the most sampled facies in the study (n=86). The probability of occurrence in the HAST is 31.7% with confidence intervals of 20.4–43.5% and a sample size of 63. The probability in the LAST is 47.8% with confidence intervals of 27.4–68.4% and a sample size of 23. If the sample size is doubled, the confidence intervals would still overlap (23.7–40.0% and 33.4–62.3%). If the sample size is quadrupled (252/92), the confidence intervals would not overlap (26.0–37.5% and 37.6–58.0%). With facies that have a much lower sample size (i.e., fluvial channel lags or mires), quadrupling the sample size would still not be adequate. Similar tests for other facies suggest that each facies would need to be sampled ~150–200 times to produce non-overlapping confidence intervals.

The probabilities of occurrence reveal a more complex answer to the original predictions that the Coal Ridge Member is more fossiliferous than the McClelland Ferry Member. Other possible explanations may explain this pattern. The McClelland Ferry Member is exposed on steep slopes, as a result of its multistory and multilateral channels, making it often more difficult to prospect than the Coal Ridge Member. Even if fossils are highly abundant in facies of the McClelland Ferry Member, the likelihood of discovering bonebeds is low, purely for accessibility reasons, favoring a perception that fossils are more common in the Coal Ridge Member.

Another possible explanation lies in the definition of ‘fossiliferous’. Although relative abundance was measured, the data analysis is conducted on presence/absence of fossils. Therefore, concentrations of fossils are treated the same as single fossils. As a consequence, this study does not compare presence/absence of microfossil bone beds as was done in Rogers and Brady (2010). The Coal Ridge Member may have higher total numbers of fossils, but they occur as concentrations. In contrast, the McClelland Ferry Member may have fewer total fossils, but

they occur more regularly throughout the column, leading to a higher overall probability of occurrence throughout the column.

Lateral variation in probabilities of occurrence

In modern coastal settings, precipitation, temperature, nutrient availability, soil texture, salinity, and stream gradient are correlated with elevation and distance from the shore, and these factors control community composition and richness (see review in Holland and Loughney, 2020). The presence of these environmental gradients has also been demonstrated in the fossil record (Gunnell and Bartels, 2001; Lehman, 2001; DiMichele et al., 2007). For example, a drop in the diversity of Pennsylvanian forest plant species, specifically a loss of shrubs and ground cover, was observed in the channel dominated facies on the seaward side of a mire relative to the siltstone dominated facies on the landward side of the same mire (DiMichele et al., 2007). Because of these gradients, it is important to differentiate changes in community composition that are solely a result of changing elevation (or distance from the shore) as separate from temporal changes in climate, ecosystem structure, and species pool (Holland and Loughney, 2020).

The Stafford Ferry study area is approximately 35 km updip from the Woodhawk Bottom study area. Comparing the probability of occurrence of fossils in the HAST of these two areas is used to assess if there is a detectable ecological gradient tied to distance from the shoreline. Unlike the comparison between HAST and LAST facies, it is unclear what the initial predictions would be. For example, ecological considerations might suggest that a taxon should be more common downdip, but taphonomic considerations might suggest the opposite. Although in all cases the confidence intervals on the probability of occurrence overlap (Figure 23), plant and

vertebrate fossils tend to have higher probabilities of occurrence updip versus downdip (Table 4). In contrast, the probability of occurrence of invertebrate fossils tends to increase downdip in the channel bar and floodplain sand facies.

More data and better stratigraphic resolution are needed to assess if ecological gradients are detectable at this scale in the Judith River Formation. The comparison made in this study between the HAST updip (Figure 24; orange shaded column) and HAST downdip (red shaded column) does not capture a consistent distance from the shore, because the shore was undergoing net inland movement through time (i.e., net transgression). Sampling with regards to distance from the shoreline (Figure 24; red and orange stars), instead of just updip versus downdip, may reveal clearer patterns in the data.

This study also uses broad taxonomic categories (plants, invertebrates, and vertebrates), which are likely too crude to address changes at the community level. There are suggestions of differences in the probability of occurrence updip and downdip, however, the ideal would be to assess changes in preservation at the species level. This raises many questions for further research. For example, does the assemblage of plant species, turtles, or freshwater clams change from Stafford Ferry to Woodhawk Bottom? Is a greater distance required to observe such changes?

Ecological gradients are as important from a taphonomic perspective as they are from a community composition and richness perspective, since taphonomic traits change along environmental gradients (Holz and Simões, 2005). It is possible that the presence of an ecological gradient in community richness or composition may be overprinted by a taphonomic signature. The taphonomy of microfossil bonebeds in the Judith River Formation has been studied extensively (Rogers and Kidwell, 2000; Rogers and Brady, 2010; Rogers et al., 2017),

but many future avenues exist for comparing taphonomy with respect to HAST and LAST as well as updip versus downdip.

Implications for simulating the nonmarine fossil record

Using the facies transitions and probabilities of occurrence calculated from the field data, multiple synthetic columns with fossil occurrences are generated using the 1-D empirical model. Four examples of synthetic columns are shown: a sharp transition from LAST to HAST (expansion surface), a sharp transition from HAST to LAST (sequence boundary; Figure 25), a gradual transition from HAST to LAST, and a gradual transition from LAST to HAST (Figure 26).

These simulated columns are compared to the measured columns from the Judith River Formation and qualitatively evaluated for similarity. The stratigraphy in the simulated expansion surface and the measured column 3-JRS-21 appear similar (Figure 25A). The LAST in both has thick, multistory fluvial channel bar facies and the HAST has more tidally influenced channel bar facies and long intervals of different floodplain facies. The stratigraphy of the sequence boundary cannot be compared to an actual sequence boundary in the Judith River Formation but is instead compared to columns where only the LAST or the HAST were measured (4-JRS-21 and 3-JRS-21; Figure 25B). As expected, no obvious visual differences are seen between the simulated and measured columns. The correspondence between the measured and simulated columns is good, because it demonstrates the model is functional. It is also expected, since the model uses transitions probabilities and facies thicknesses from the measured columns.

The patterning of fossil occurrences in both the synthetic and real columns looks quite similar. The fossil occurrences in these simulations are based on the combined probabilities for

HAST and LAST because only 2 of 21 results show a significant difference in the probabilities of occurrence between systems tracts. From a modeling perspective, it is a simpler solution to combine the probabilities of occurrence for the simulation, as was done here. However, if fossil preservation truly differs based on an elevation gradient or among systems tracts, those differences would need to be reflected in the model.

The advantage to having a model like this is that scenarios not observed in the field can be simulated, like a gradual transition from HAST to LAST or vice-versa (Figure 26). The ability to simulate different scenarios allows future studies to then make predictions about what the fossil record may look like for cases outside of this study area.

Conclusions

1. The stratigraphy of the Judith River Formation described in this study is consistent with previous work by Rogers et al. (2016), although new nonmarine systems tract nomenclature is applied, facilitating comparisons to other nonmarine basins. New fossil localities in the McClelland Ferry Member add to the overall understanding of fossils in the Judith River Formation.
2. Numerical comparisons of the stratigraphy reveal that the HAST (Coal Ridge Member) and LAST (McClelland Ferry Member) in Judith River Formation conform with qualitative descriptions of nonmarine stratigraphy. Floodplain facies in the Coal Ridge Member are on average thicker and more numerous. Fluvial channel bar and lag facies in the McClelland Ferry Member are also thicker on average and occur more frequently. Transitions between facies also follow expectations leading to thicker intervals of floodplain facies in the HAST and stacked channel facies in the LAST. Although channel architecture is the primary characteristic used in

this study to differentiate HAST and LAST, incorporating more characteristics of nonmarine stratigraphy is recommended for future studies.

3. Floodplain facies in the HAST and channel facies in the LAST do not universally have higher probabilities of occurrence of plant, invertebrate and vertebrate fossils, making the degree to which stratigraphic architecture controls the distribution of fossils unclear. Floodplain facies in the HAST and channel facies in the LAST are generally thicker and more numerous, meaning that higher probabilities of occurrence may just be due to suitable search area. To confidently address the question of whether HAST floodplain facies and LAST channel facies are truly better suited to preserve fossils, the amount of data collected needs to be quadrupled.

4. Probabilities of occurrence are indistinguishable in the updip HAST and downdip HAST, although the probability is generally higher for plant and vertebrate fossils in the updip and higher for invertebrates in the downdip. Substantially greater sampling efforts are needed to address the presence of ecological gradients in nonmarine fossil assemblages. Additionally, samples would need to be compared at similar distances from the shore through time, and at a finer taxonomic scale.

5. The embedded Markov-chain model presented here is able to recreate realistic stratigraphy and the distribution of fossils using the observed facies and fossil data from the field. The model provides a potential method for simulating a range of stratigraphic architectures not observed in the field area. This allows the formation of testable hypothesis for understanding the interplay of stratigraphic architecture and the stratigraphic distribution of fossils in this and other nonmarine basins.

CHAPTER 3

CONCLUSIONS AND FUTURE WORK

Three main conclusions can be drawn from this work. First, both the qualitative and quantitative expectations of nonmarine stratigraphy in the Judith River Formation are upheld. Second, the probability of occurrence of fossils is more variable and complex among facies, systems tracts, and along an elevation gradient than originally hypothesized. Third, embedded Markov chains can be used effectively to simulate columns with reasonable architectures. These conclusions open many potential avenues for future field work and modeling.

The numerical comparison of the Judith River Formation generally supports the architectural expectations of a LAST with multistory, multilateral channel deposits and thin floodplain deposits, as well as a HAST with thick intervals of floodplain deposits with thinner, isolated channel deposits. More work is needed, however, to quantify and describe other important elements of nonmarine systems tracts, such as paleosol type and development, the presence and complexity of coals, and indications of tidal influence. Future work should focus on describing nonmarine basins within a sequence-stratigraphic context to explore the range of expressions of nonmarine architecture from coastal systems to inland settings lacking the influence of changing sea level. This would ideally lead to more robust criteria for discerning and correlating nonmarine systems tracts.

The probability of occurrence of fossils was used in the Judith River Formation to evaluate preservation in facies, systems tracts, and along an elevation gradient. Most of these probabilities are indistinguishable, owing to small sample size. A logical avenue for future work

would be to collect more data. This could be carried out in multiple ways, depending on the research question at hand. The methods described in this study could be used to explore whether probabilities of occurrence are distinguishable among facies or systems tracts. Simply, more columns with fossil counts throughout the basin would need to be measured with approximately 150-200 of each facies sampled. The sampling methods would need to differ slightly from this study to evaluate if elevation gradients are detectable in the study area. Sampling for that should be done along a transect, from updip to downdip, and samples would need to be compared at relatively consistent distances from the shoreline.

Another avenue to explore elevation gradients in the record would be to use plant biomarkers to investigate paleoelevation in the basin. Variations in the bacterial membrane lipids in fossil plant material can be used to reconstruct soil temperature and then calibrated to estimate paleotemperature (Weijers et al., 2006; Anderson et al., 2015; de Bar et al., 2019). This method could potentially be used to establish if there is an elevation gradient in the Judith River Formation. However, the resolution of this method may be too coarse to capture the gradient on the coastal plain.

The model presented here was able to produce realistic stratigraphic architectures for a single column. The utility in this model is the ability to produce architectures not observed in the field (i.e., a sequence boundary) and explore what the fossil distribution would look like. This model could also be used to simulate thousands of columns and explore the range of potential stratigraphic architectures and fossil distributions.

This model has many limitations due to its simplicity. The primary limitation is the inability to correlate columns and explore a cross section of a nonmarine basin. Future work in this area could involve using geometric or numeric models to simulate a cross section and

generate individual columns for analysis, as was done in the marine record in Holland and Patzkowsky (1999).

REFERENCES

- Ainsworth, R.B., Vonk, A.J., Wellington, P., and Paumard, V., 2020, Out-of-phase cyclical sediment supply: a potential causal mechanism for generating stratigraphic asymmetry and explaining sequence stratigraphic spatial variability: *Journal of Sedimentary Research*, v. 90, p. 1706–1733.
- Aitkin, J.F., and Flint, S.S., 1995, The application of high-resolution sequence stratigraphy to fluvial systems: a case study from the Upper Carboniferous Breathitt Group, eastern Kentucky, USA: *Sedimentology*, v. 42, p. 3–30.
- Allen, J.P., Fielding, C.R., Gibling, M.R., and Rygel, M.C., 2014, Recognizing products of palaeoclimate fluctuation in the fluvial stratigraphic record: an example from the Pennsylvanian to Lower Permian of Cape Breton Island, Nova Scotia: *Sedimentology*, v. 61, p. 1332–1381.
- Allen, J.R.L., 1965, A review of the origin and characteristics of recent alluvial sediments: *Sedimentology*, v. 5, p. 89–191.
- Allen, J.R.L., 1978, Studies in fluvial sedimentation: an exploratory quantitative model for the architecture of avulsion-controlled alluvial suites: *Sedimentary Geology*, v. 21, p. 129–147.
- Anderson, V.J., Saylor, J.E., Shanahan, T.M., and Horton, B.K., 2015, Paleoelevation records from lipid biomarkers: application to the tropical Andes: *GSA Bulletin*, v. 127, p. 1604–1616.
- Arbour, V.M., and Evans, D.C., 2017, A new ankylosaurine dinosaur from the Judith River Formation of Montana, USA, based on an exceptional skeleton with soft tissue preservation: *Royal Society Open Science*, v. 4, p. 1–28.

- Atchley, S.C., Nordt, L.C., and Dworkin, S.I., 2004, Eustatic control on alluvial sequence stratigraphy: a possible example from the Cretaceous–Tertiary transition of the Tornillo Basin, Big Bend National Park, west Texas, U.S.A.: *Journal of Sedimentary Research*, v. 74, p. 391–404.
- Behrensmeier, A.K., 1982, Time resolution in vertebrate assemblages: *Paleobiology*, v. 8, p. 211–227.
- Behrensmeier, A.K., 1988, Vertebrate preservation in fluvial channels: *Palaeogeography, Palaeoclimatology, Palaeoecology*, v. 63, p. 183–199.
- Behrensmeier, A.K., and Kidwell, S.M., 1985, Taphonomy's contributions to paleobiology: *Paleobiology*, v. 11, p. 105–119.
- Behrensmeier, A.K., and Hook, R.W., 1992, Paleoenvironments contexts and taphonomic modes, *in* Behrensmeier, A.K., Damuth, J.D., DiMichele, W.A., Potts, R., Sues, H.D., and Wing, S.L., eds., *Terrestrial Ecosystems Through Time: Evolutionary Paleocology of Terrestrial Plants and Animals*: Chicago, The University of Chicago Press, p. 15–93.
- Behrensmeier, A.K., Kidwell, S.M., and Gastaldo, R.A., 2000, Taphonomy and paleobiology: *Paleobiology*, v. 26, p. 103–147.
- Béland, P., and Russell, D.A., 1978, Paleocology of Dinosaur Provincial Park (Cretaceous), Alberta, interpreted from the distribution of articulated vertebrate remains: *Canadian Journal of Earth Sciences*, v. 15, p. 1012–1024.
- Bell, W.A., 1965, Upper Cretaceous and Paleocene plants of western Canada: Geological Survey of Canada, Department of Mines and Technical Surveys, Paper 65-35, 44 p.

- Blakey, R.C., 2014, Paleogeography and paleotectonics of the Western Interior Seaway, Jurassic–Cretaceous of North America: American Association of Petroleum Geologists, Search and Discovery Article 30392, 72 pp.
- Blum, M., Martin, J., Milliken, K., and Garvin, M., 2013, Paleovalley systems: insights from Quaternary analogs and experiments: *Earth-Science Reviews*, v. 116, p. 128–169.
- Blum, M.D., and Tornqvist, T.E., 2000, Fluvial response to climate and sea-level change: a review and look forward: *Sedimentology*, v. 47, p. 2–48.
- Bown, T.M., and Kraus, M.J., 1981, Vertebrate fossil-bearing paleosol units (Willwood Formation, Lower Eocene, northwest Wyoming, U.S.A.): implications for taphonomy, biostratigraphy, and assemblage analysis: *Palaeogeography, Palaeoclimatology, Palaeoecology*, v. 34, p. 31–56.
- Boyd, R., Diessel, C., Wadsworth, J., Leckie, D., and Zaitlin B.A., 2000, Developing a model for non-marine sequence stratigraphy—application to the Western Canada Sedimentary Basin: GeoCanada 2000, The Millennium Geosciences Summit Conference, Calgary, Alberta, Canada, Abstract 138, 4 p.
- Brett, C.E., 1995, Sequence stratigraphy, biostratigraphy, and taphonomy in shallow marine environments: *PALAIOS*, v. 10, p. 597–616.
- Bridge, J.S., and Leeder, M.R., 1979, A simulation model of alluvial stratigraphy: *Sedimentology*, v. 26, p. 617–644.
- Brinkman, D.B., 1990, Paleocology of the Judith River Formation (Campanian) of Dinosaur Provincial Park, Alberta, Canada: evidence from vertebrate microfossil localities: *Palaeogeography, Palaeoclimatology, Palaeoecology*, v. 78, p. 37–54.

- Burgener, L., Hyland, E., Huntington, K.W., Kelson, J.R., and Sewall, J.O., 2019, Revisiting the equable climate problem during the Late Cretaceous greenhouse using paleosol carbonate clumped isotope temperatures from the Campanian of the Western Interior Basin, USA: *Palaeogeography, Palaeoclimatology, Palaeoecology*, v. 516, p. 244–267.
- Burns, B.A., Heller, P.L., Marzo, M., and Paola, C., 1997, Fluvial response in a sequence stratigraphic framework: example from the Montserrat fan delta, Spain: *Journal of Sedimentary Research*, v. 67, p. 311–321.
- Burns, C.E., Mountney, N.P., Hodgson, D.M., and Colombero, L., 2017, Anatomy and dimensions of fluvial crevasse-splay deposits: Examples from the Cretaceous Castlegate Sandstone and Neslen Formation, Utah, U.S.A: *Sedimentary Geology*, v. 351, p. 21–35.
- Cadée, G.C., 1999, Bioerosion of shells by terrestrial gastropods: *Lethaia*, v. 32, p. 253–260.
- Campbell, I.D., 1999, Quaternary pollen taphonomy: examples of differential redeposition and differential preservation: *Palaeogeography, Palaeoclimatology, Palaeoecology*, v. 149, p. 245–256.
- Carr, D.D., Horowitz, A., Hrabar, S.V., Ridge, K.F., Rooney, R., Straw, W.T., Webb, W., and Potter, P.E., 1966, Stratigraphic sections, bedding sequences, and random processes: *Science*, v. 154, p. 1162–1164.
- Catuneanu, O., 2006, *Principles of Sequence Stratigraphy*: Amsterdam, Elsevier, 375 p.
- Chang, C., and Liu, L., 2021, Investigating the formation of the Cretaceous Western Interior Seaway using landscape evolution simulations: *Geological Society of America Bulletin*, v. 133, p. 347–361.
- Cleveland, D.M., Atchley, S.C., and Nordt, L.C., 2007, Continental sequence stratigraphy of the Upper Triassic (Norian–Rhaetian) Chinle strata, northern New Mexico, U.S.A: *allocyclic*

- and autocyclic origins of paleosol-bearing alluvial successions: *Journal of Sedimentary Research*, v. 77, p. 909–924.
- Colombera L., Mountney, N.P., and McCaffrey, W.D., 2015, A meta-study of relationships between fluvial channel-body stacking pattern and aggradation rate: Implications for sequence stratigraphy: *Geology*, v. 43, p. 283–286.
- Colombi, C.E., Limarino, C.O., and Alcober, O.A., 2017, Allogenic controls on the fluvial architecture and fossil preservation of the Upper Triassic Ischigualasto Formation, NW Argentina: *Sedimentary Geology*, v. 362, p. 1–16.
- Colombi, C.E., Rogers, R.R., and Alcober, O.A., 2012, Vertebrate taphonomy of the Ischigualasto Formation: *Journal of Vertebrate Paleontology*, v. 32, p. 31–50.
- Currie, B.S., 1997, Sequence stratigraphy of nonmarine Jurassic–Cretaceous rocks, central Cordilleran foreland-basin system: *Geological Society of America Bulletin*, v. 109, p. 1206–1222.
- Dalman, R.A.F., and Weltje, G.J., 2012, SimClast: an aggregated forward stratigraphic model of continental shelves: *Computers & Geosciences*, v. 38, p. 115–126.
- De Bar, M.W., Rampen, S.W., Hopmans, E.C., Sinninghe Damsté, J.S., and Schouten, S., 2019, Constraining the applicability of organic paleotemperature proxies for the last 90 Myrs: *Organic Geochemistry*, v. 128, p. 122–136.
- DiMichele, W.A., Falcon-Lang, H.J., Nelson, W.J., Elrick, S.D., and Ames, P.R., 2007, Ecological gradients within a Pennsylvanian mire forest: *Geology*, v. 35, p. 415–418.
- Dindarloo, S.R., Bagherieh, A., Hower, J.C., Calder, J.H., and Wagner, N.J., 2015, Coal modeling using Markov Chain and Monte Carlo simulation: analysis of microlithotype and lithotype succession: *Sedimentary Geology*, v. 329, p. 1–11.

- Dodson, P., 1971, Sedimentology and taphonomy of the Oldman Formation (Campanian), Dinosaur Provincial Park, Alberta (Canada): *Palaeogeography, Palaeoclimatology, Palaeoecology*, v. 10, p. 21–74.
- Eberth, D.A., 1990, Stratigraphy and sedimentology of vertebrate microfossil sites in the uppermost Judith River Formation (Campanian), Dinosaur Provincial Park, Alberta, Canada: *Palaeogeography, Palaeoclimatology, Palaeoecology*, v. 78, p. 1–36.
- Eberth, D.A., and Brinkman, D.B., 1997, Paleocology of an estuarine, incised-valley fill in the Dinosaur Park Formation (Judith River Group, Upper Cretaceous) of southern Alberta, Canada: *PALAIOS*, v. 12, p. 43–58.
- Falivene, O., Frascati, A., Pittaluga, M.B., and Martin, J., 2019, Three-dimensional reduced complexity simulation of fluvio-deltaic clastic stratigraphy: *Journal of Sedimentary Research*, v. 89, p. 46–65.
- Fiorillo, A.R., 1990, Taphonomy and depositional setting of Careless Creek Quarry (Judith River Formation), Wheatland County, Montana, U.S.A.: *Palaeogeography, Palaeoclimatology, Palaeoecology*, v. 81, p. 281–311.
- Flemings, P.B., and Grotzinger, J.P., 1996, STRATA: freeware for analyzing classic stratigraphic problems: *GSA Today*, v. 6, p. 1–7.
- Foreman, B.Z., Rogers, R.R., Deino, A.L., Wirth, K.R., and Thole, J.T., 2008, Geochemical characterization of bentonite beds in the Two Medicine Formation (Campanian, Montana), including a new $^{40}\text{Ar}/^{39}\text{Ar}$ age: *Cretaceous Research*, v. 29, p. 373–385.
- Fricke, H.C., Foreman, B.Z., and Sewall, J.O., 2010, Integrated climate model-oxygen isotope evidence for a North American monsoon during the Late Cretaceous: *Earth and Planetary Science Letters*, v. 289, p. 11–21.

- Fuentes, F., DeCelles, P.G., Constenius, K.N., and Gehrels, G.E., 2011, Evolution of the Cordilleran foreland basin system in northwestern Montana, U.S.A.: *Geological Society of America Bulletin*, v. 123, p. 507–533.
- Fraser, D., 2017, Can latitudinal richness gradients be measured in the terrestrial fossil record?: *Paleobiology*, v. 43, p. 479–494.
- Gastaldo, R.A., and Demko, T.M., 2011, The relationship between continental landscape evolution and the plant fossil record: long term hydraulic controls on preservation, *in* Allison P.A., and Bottjer D.J., eds., *Taphonomy, Second Edition: Topics in Geobiology Book Series*, v. 32, p. 250–285.
- Gill, J.R., and Cobban, W.A., 1973, Stratigraphy and geologic history of the Montana Group and equivalent rocks, Montana, Wyoming, and North and South Dakota: *U.S. Geological Survey Professional Paper 776*, 37 p.
- Gugliotta, M., Flint, S.S., Hodgson, D.M., and Veiga, G.D., 2016, Recognition criteria, characteristics and implications of the fluvial to marine transition zone in ancient deltaic deposits (Lajas Formation, Argentina): *Sedimentology*, v. 63, p. 1971–2001.
- Gunnell, G.F., and Bartels, W.S., 2001, Basin margins, biodiversity, evolutionary innovation, and the origin of new taxa, *in* Gunnell, G.F., ed., *Eocene Biodiversity: Unusual Occurrences and Rarely Sampled Habitats: Kluwer Academic/Plenum, New York*, p. 403–432.
- Hajek, E.A., Heller, P.L., and Shur, E.L., 2012, Field test of autogenic control on alluvial stratigraphy (Ferris Formation, Upper Cretaceous–Paleogene, Wyoming): *Geological Society of America Bulletin*, v. 124, p. 1898–1912.

- Hajek, E.A., and Straub, K.M., 2017, Autogenic sedimentation in clastic stratigraphy: Annual Review of Earth and Planetary Sciences, v. 45, p. 681–709.
- Hall, J.W., 1968, A new genus of Salviniaceae and a new species of *Azolla* from the Late Cretaceous: American Fern Journal, v. 58, p. 77–88.
- Hall, J.W., 1969, Studies on fossil *Azolla*: primitive types of megaspores and massulae from the Cretaceous: American Journal of Botany, v. 56, p. 1173–1180.
- Hobley, D.E.J., Adams, J.M., Nudurupati, S.S., Hutton, E.W.H., Gasparini, N.M., Istanbuluoglu, E., and Tucker, G.E., 2017, Creative computing with Landlab: an open-source toolkit for building, coupling, and exploring two-dimensional numerical models of Earth-surface dynamics: Earth Surface Dynamics, v. 5, p. 21–46.
- Holbrook, J., Scott, R.W., and Oboh-Ikuenobe, F.E., 2006, Base-level buffers and buttresses: a model for upstream versus downstream control on fluvial geometry and architecture within sequences: Journal of Sedimentary Research, v. 76, p. 162–174.
- Holland, S.M., 1995, The stratigraphic distribution of fossils: Paleobiology, v. 21, p. 92–109.
- Holland, S.M., 2000, The quality of the fossil record: a sequence stratigraphic perspective: Paleobiology, v. 25, p. 148–168.
- Holland, S.M., and Loughney, K.M., 2020, The Stratigraphic Paleobiology of Nonmarine Systems: Elements in Paleontology: Cambridge, Cambridge University Press, 79 p.
- Holland, S.M., and Patzkowsky, M.E., 1999, Models for simulating the fossil record: Geology, v. 27, p. 491–494.
- Holland, S.M., and Patzkowsky, M.E., 2015, Stratigraphy of mass extinction: Palaeontology, v. 58, p. 903–924.

- Holz, M., and Simões, M.G., 2005, Taphonomy – Overview of Main Concepts and Applications to Sequence Stratigraphic Analysis, *in* Koutsoukos, E.A.M., ed., *Applied Stratigraphy*, Springer, New York, p. 249–278.
- Huerta, P., Armenteros, I., and Silva, P.G., 2011, Large-scale architecture in non-marine basins: the response to the interplay between accommodation space and sediment supply: *Sedimentology*, v. 58, p. 1716–1736.
- Hunt, D., and Tucker, M.E., 1992, Stranded parasequences and the forced regressive wedge systems tract: deposition during base-level fall: *Sedimentary Geology*, v. 81, p. 1–9.
- Hutton, S.M., and Syvitski, J.P.M., 2008, Seflux 2.0: an advanced process-response model that generates three-dimensional stratigraphy: *Computers & Geosciences*, v. 34, p. 1319–1337.
- Kidwell, S.M., and Flessa, K.W., 1996, The quality of the fossil record: populations, species, and communities: *Annual Review of Earth and Planetary Science*, v. 24, p. 433–464.
- Kidwell, S.M., and Holland, S.M., 2000, The quality of the fossil record: implications for evolutionary analysis: *Annual Review of Ecology and Systematics*, v. 33, p. 561–588.
- Knowlton, F.H., 1905, Fossil plants of the Judith River Beds, *in*, Stanton, T.W., and Hatcher, J.B., eds., *Geology and Paleontology of the Judith River Beds: United States Geological Survey Bulletin 257*, p. 129–168.
- Koster, E.H., Currie, P.J., Brinkman, D.B., Johnston, P.A., and Braman, D.R., 1987, Sedimentology and paleontology of the Upper Cretaceous Judith River/Bearpaw formations at Dinosaur Provincial Park, Alberta, *in* Geological Society of Canada Mineralogical Association of Canada Joint Annual Meeting, Field Trip Guidebook No. 10, 130 p.

- Krumbein, W.C., and Dacey, M.F., 1969, Markov chains and embedded Markov chains in geology: *Mathematical Geology*, v. 1, p. 79–96.
- Leeder, M.R., 1978, A quantitative stratigraphic model for alluvium, with special reference to channel deposit density and interconnectedness, *in* Miall, A.D., ed., *Fluvial Sedimentology: Canadian Society of Petroleum Geologists Memoir 5*, p. 587–596.
- Leeder, M.R., Harris, T., and Kirkby, M.J., 1998, Sediment supply and climate change: implications for basin stratigraphy: *Basin Research*, v. 10, p. 7–18.
- Lehman, T.M., 2001, Late Cretaceous dinosaur provinciality, *in* Tanke, D.H., and Carpenter, K., eds., *Mesozoic Vertebrate Life: Indiana University Press, Bloomington*, p. 310–328.
- Li, Y.C., Xu, Q.H., Yang, X.L., Chen, H., and Lu, X.M., 2007, Pollen-vegetation relationship and pollen preservation on the Northeastern Qinghai-Tibetan Plateau: *Grana*, v. 44, p. 160–171.
- Loughney, K.M., and Badgley, C., 2017, Facies, environments, and fossil preservation in the Barstow Formation, Mojave Desert, California: *PALAIOS*, v. 32, p. 396–412.
- Loughney, K.M., and Badgley, C., 2020, The influence of depositional environment and basin history on the taphonomy of mammalian assemblages from the Barstow Formation (middle Miocene), California: *PALAIOS*, v. 35, p. 175–190.
- Martinsen, O.J., Ryseth, A., Helland-Hansen, W., Flesche, H., Torkildsen, G., and Idil, S., 1999, Stratigraphic base level and fluvial architecture: Ericsson Sandstone (Campanian), Rock Springs Uplift, SW Wyoming, USA: *Sedimentology*, v. 46, p. 235–259.
- McMullen, S.K., Holland, S.M., and O’Keefe, R.F., 2014, The occurrence of vertebrate and invertebrate fossils in a sequence stratigraphic context: the Jurassic Sundance Formation, Bighorn Basin, Wyoming, U.S.A.: *PALAIOS*, v. 29, p. 277–294.

- Nawrot, R., Scarponi, D., Azzarone, M., Dexter, T.A., Kusnerik, K.M., Wittmer, J.M., Amorosi, A., and Kowalewski, M., 2018, Stratigraphic signatures of mass extinctions: ecological and sedimentary determinants: *Proceedings of the Royal Society B*, v. 285, 20181191.
- Patzkowsky, M.E., and Holland, S.M., 2012, *Stratigraphic Paleobiology: Understanding the Distribution of Fossil Taxa in Time and Space*: Chicago, University of Chicago Press, 256 p.
- Peters, S.E., Antar, M.S.M., Zalmout, I.S., and Gingerich, P.D., 2009, Sequence stratigraphic control on preservation of late Eocene whales and other vertebrates at Wadi Al-Hitan, Egypt: *PALAIOS*, v. 24, p. 290–302.
- Posamentier, H.W., and Vail, P., 1988, Eustatic controls on clastic deposition II—sequence and systems tract models, *in* Wilgus, C.K., Hastings, B.S., Kendall, C.G.St.C., Posamentier, H.W., Ross, C.A., and Van Wagoner, J.C., eds., *Sea-Level Changes: an Integrated Approach*: Society of Economic Paleontologists and Mineralogists Special Publication 42, p. 125–154.
- Potter, P.E., and Blakely, R.F., 1968, Random processes and lithologic transitions: *The Journal of Geology*, v. 76, p. 59–78.
- Purnell, M.A., Donoghue, P.J., Gabbott, S.E., McNamara, M.E., Murdock, D.J.E., and Sansom, R.S., 2018, Experimental analysis of soft-tissue fossilization: opening the black box: *Palaeontology*, v. 61, p. 317–323.
- Raup, D.M., 1985, Mathematical models of cladogenesis: *Paleobiology*, v. 11, p. 42–52.
- Raup, D.M., 1991, The future of analytical paleobiology, *in* Gilinsky, N.L., and Signor, P.W., eds., *Analytical Paleobiology*, Paleontological Society Short Course in Paleontology, No. 4, p. 207–216.

- Retallack, G., 1984, Completeness of the rock and fossil record: some estimates using fossil soils: *Paleobiology*, v. 10, p. 59–78.
- Retallack, G., 1998, Fossil soils and completeness of the rock and fossil records, *in* Donovan, S.K., and Paul, C.R.C., eds., *The Adequacy of the Fossil Record*: Chichester, Wiley, p. 132–163.
- Robinson Roberts, L.N., and Kirschbaum, M.A., 1995, Paleogeography of the Late Cretaceous of the Western Interior of middle North America—coal distribution and sediment accumulation: U.S. Geological Survey Professional Paper 1561, 115 p.
- Rogers, R.R., 1993, Systematic patterns of time-averaging in the terrestrial vertebrate record: A Cretaceous case study, *in*, Kidwell, S.M., and Behrensmeier, A.K., eds., *Taphonomic Approaches to Time Resolution in Fossil Assemblages*, Short Courses in Paleontology Number 6, p. 228–249.
- Rogers, R.R., 1994, Nature and origin of through-going discontinuities in nonmarine foreland basin strata, Upper Cretaceous Montana: implications for sequence analysis: *Geology*, v. 22, p. 1119–1122.
- Rogers, R.R., 1998, Sequence analysis of the Upper Cretaceous Two Medicine and Judith River Formations, Montana: nonmarine response to the Claggett and Bearpaw Marine cycles: *Journal of Sedimentary Research*, v. 68, p. 615–631.
- Rogers, R.R., and Brady, M.E., 2010, Origins of microfossil bonebeds: insights from the Upper Cretaceous Judith River Formation of north-central Montana: *Paleobiology*, v. 36, p. 80–112.
- Rogers, R.R., Carrano, M.T., Curry Rogers, K.A., Perez, M., and Regan, A.K., 2017, *Isotaphonomy in concept and practice: an exploration of vertebrate microfossil bonebeds*

- in the Upper Cretaceous (Campanian) Judith River Formation, north-central Montana: *Paleobiology*, v. 43, p. 248–273.
- Rogers, R.R., Curry Rogers, K.A., Bagley, B.B., Goodin, J.J., Hartman, J.H., Thole, J.T., and Zaton, M., 2018, Pushing the record of trematode parasitism of bivalves upstream and back to the Cretaceous: *Geology*, v. 46, p. 431–434.
- Rogers, R.R., Fricke, H.C., Addona, V., Canavan, R.R., Dwyer, C.N., Harwood, C.L., Koenig, A.E., Murray, R., Thole, J.T., and Williams, J., 2010, Using laser ablation-inductively coupled plasma-mass spectrometry (LA-ICP-MS) to explore geochemical taphonomy of vertebrate fossils in the Upper Cretaceous Two Medicine and Judith River Formations of Montana: *PALAIOS*, v. 25, p. 183–195.
- Rogers, R.R., and Kidwell, S.M., 2000, Associations of vertebrate skeletal concentrations and discontinuity surfaces in terrestrial and shallow marine records: a test in the Cretaceous of Montana: *The Journal of Geology*, v. 108, p. 131–154.
- Rogers, R.R., Kidwell, S.M., Deino, A.L., Mitchell, J.P., Nelson, K., and Thole, J.T., 2016, Age, correlation, and lithostratigraphic revision of the Upper Cretaceous (Campanian) Judith River Formation in its type area (north-central Montana), with a comparison of low- and high-accommodation alluvial records: *The Journal of Geology*, v. 124, p. 99–135.
- Sahni, A., 1972, The vertebrate fauna of the Judith River Formation, Montana: *Bulletin of the American Museum of Natural History*, v. 147, p. 321–412.
- Salles, T., Ding, X., and Brocard, G., 2018, pyBadlands: a framework to simulate sediment transport, landscape dynamics and basin stratigraphic evolution through space and time: *PLoS ONE*, v. 13, p. 1–24.

- Salles, T., and Hardiman, L., 2016, Badlands: an open-source, flexible and parallel framework to study landscape dynamics: *Computers & Geosciences*, v. 91, p. 77–89.
- Scarponi, D., and Kowalewski, M., 2007, Sequence stratigraphic anatomy of diversity patterns: late Quaternary benthic mollusks of Po Plain, Italy: *PALAIOS*, v. 22, p. 296–305.
- Scherer, C.M.S., Goldberg, K., and Bardola, T., 2015, Facies architecture and sequence stratigraphy of an early post-rift fluvial succession, Aptian Barbalha Formation, Araripe Basin, northeastern Brazil: *Sedimentary Geology*, v. 322, p. 43–62.
- Sears, J.W., 2001, Emplacement and denudation history of the Lewis–Eldorado–Hoadley thrust slab in the northern Montana Cordillera, USA: implications for steady-state orogenic processes: *American Journal of Science*, v. 301, p. 359–373.
- Shanley, K.W., and McCabe, P.J., 1993, Alluvial architecture in a sequence stratigraphic framework: a case history from the Upper Cretaceous of southern Utah, USA, *in* Flint, S., and Bryant, I., eds., *Quantitative Modelling of Clastic Hydrocarbon Reservoirs and Outcrop Analogues: International Association of Sedimentologists Special Publication*, v. 15, p. 21–55.
- Shanley, K.W., and McCabe, P.J., 1994, Perspectives on the sequence stratigraphy of continental strata: *American Association of Petroleum Geologists Bulletin*, v. 78, p. 544–568.
- Slattery, J.S., Cobban, W.A., McKinney, K.C., Harries, P.J., and Sandness, A.L., 2013, Early Cretaceous to Paleocene paleogeography of the Western Interior Seaway: the interaction of eustasy and tectonism, *in* Bingle-Davis, M., ed., *Casper, Wyoming, Wyoming Geological Association, 68th Annual Field Conference, Guidebook*, p. 22–60.

- Smedes, H.W., 1966, Geology and igneous petrology of the northern Elkhorn Mountains, Jefferson and Broadwater Counties, Montana: U.S. Geological Survey Professional Paper 510, 116 p.
- Straight, W.H., and Eberth, D.A., 2002, Testing the utility of vertebrate remains in recognizing patterns in fluvial deposits: an example from the lower Horseshoe Canyon Formation, Alberta: *PALAIOS*, v. 17, p. 472–256.
- Tabor, N.J., Myers, T.S., and Michel, L.A., 2017, Sedimentologist's guide for recognition, description, and classification of paleosols, *in* Zeigler, K.E., and Parker, W.G., eds., *Terrestrial Depositional Systems*: Amsterdam, Elsevier, p. 165–208.
- Taylor, P.D., and Rogers, R.R., 2021, A new cheilostome bryozoan from a dinosaur site in the Upper Cretaceous (Campanian) Judith River Formation of Montana: *Journal of Paleontology*, v. 95, p. 965–973.
- Trueman, C.N., 1999, Rare earth element geochemistry and taphonomy of vertebrate assemblages: *PALAIOS*, v. 14, p. 555–568.
- Tschudy, B.D., 1973, Palynology of the Upper Campanian (Cretaceous) Judith River Formation, north-central Montana: U.S. Geological Survey Professional Paper 770, 42 p.
- Wadsworth, J., Diessel, C., Boyd, R., Leckie, D., and Zaitlin, B.A., 2002, Stratigraphic style of coal and non-marine strata in a tectonically influenced intermediate accommodation setting: the Mannville Group of the Western Canadian Sedimentary Basin, south-central Alberta: *Bulletin of Canadian Petroleum Geology*, v. 50, p. 507–541.
- Weijers, J.W.H., Schouten, S., Spaargaren, O.C., and Sinninghe Damsté, J.S., 2006, Occurrence and distribution of tetraether membrane lipids in soils: implications for the use of the TEX₈₆ proxy and the BIT index: *Organic Geochemistry*, v. 37, p. 1680–1693.

- Wittmer, J.M., Dexter, T.A., Scarponi, D., Amorosi, A., and Kowalewski, M., 2014, Quantitative bathymetric models for late Quaternary transgressive-regressive cycles of the Po Plain, Italy: *The Journal of Geology*, v. 122, p. 649–670.
- Wolfe, J.A., and Upchurch, G.R., 1987, North American nonmarine climates and vegetation during the Late Cretaceous: *Palaeogeography, Palaeoclimatology, Palaeoecology*, v. 61, p. 33–77.
- Wood, J.M., Thomas, R.G., and Visser, J., 1988, Fluvial processes and vertebrate taphonomy: the Upper Cretaceous Judith River Formation, south-central Dinosaur Provincial Park, Alberta, Canada: *Palaeogeography, Palaeoclimatology, Palaeoecology*, v. 66, p. 127–143.
- Wright, V.P., and Marriott, S.B., 1993, Sequence stratigraphy of fluvial depositional systems: the role of floodplain sediment storage: *Sedimentary Geology*, v. 86, p. 203–210.
- Yanes, Y., Tomašových, A., Kowalewski, M., Castillo, C., Aguirre, J., Alonso, M.R., and Ibáñez, M., 2008, Taphonomy and compositional fidelity of Quaternary fossil assemblages of terrestrial gastropods from carbonate-rich environments of the Canary Islands: *Lethaia*, v. 4, p. 235–256.

Table 1. Semi-quantitative log-scale used for counting fossil abundances

Number of specimens	Fossil abundance code	Ecological descriptor
1000 +	3	Very abundant
300–1000	2.5	Abundant
100–300	2	Common
30–100	1.5	Frequent
10–30	1	Occasional
3–10	0.5	Rare
1–3	0	Very rare
0	-1	Absent
Unsuitable search area	NS	-

Table 2. Sedimentologic characteristics of the nonmarine facies of the Judith River Formation

Facies Association	Lithology	Bedding	Sedimentary Structures	Other
Mire	Lignite to argillaceous (impure) lignite	Fissile to blocky. Laterally continuous over 10's of meters. 30 cm–2 m thick		Dark reddish brown (5YR 2.5/2, 7.5YR 4/3) to black (7.5YR 2.5/1, 5YR 3/1) with abundant organic material (carbonaceous debris, carbonized wood). Common selenite veins. Locally poorly cemented and well indurated
Pond/Lake	Mudstone and carbonaceous shale	Horizontally laminated to blocky. Laterally continuous although locally, facies pinch out into floodplain. 50 cm–5.5 m thick		Abundant horizontally aligned carbonaceous debris. Dark brown (7.5YR 3/2) to very dark grey (2.5Y 3/1). When gray (5Y 6/1) or olive gray (5Y 5/2) and without carbonaceous debris, facies was identified by invertebrate material

Floodplain mud	Mudstone and siltstone	Laterally continuous. 50 cm–5 m thick. Blocky (common) to horizontally laminated (rare).		Rare randomly oriented carbonaceous debris. Occurs in range of gray, olive, and brown colors (2.5Y 4/1, 5Y 6/1, 2.5Y 6/2, 2.5Y 7/1). Locally well indurated, except powdery where weathered. Abundant root traces and waxy root traces
Floodplain sands	Fine grained sandstone often interbedded with mudstone or siltstone	0.5–2 m thick. Laterally continuous over short distances (~5–10 m). Commonly grades horizontally or vertically into floodplain mudstone	Abundant ripple-scale lamination and rare large-scale trough cross bedding	Has well cemented and poorly cemented intervals
Channel lag	Gravel to cobble sized clasts of cemented sand or mud, with rare shell, bone, wood, or carbonaceous debris	10–20 cm coarse material in channel sands. Laterally continuous over 1–2 meters		
Fluvial channel bars	Very fine to fine grained sandstone	2–8.5 m thick. Laterally continuous over 10's of meters	Large-scale trough cross bedding. Tabular and trough ripple-scale lamination	Many bodies capped by ironstone or include ironstone layers. Variably cemented. Bioturbation common

Tidally influenced channel bars	Very fine to fine grained sandstone and mudstone	0.5–1 m beds of sand and mud, thinning upward (~1–7 m total thickness)	Inclined heterolithic strata (IHS). Large-scale trough cross bedding with organic drapes	Local dark, indurated ironstone layers with abundant leaf and wood impressions
---------------------------------	--	--	--	--

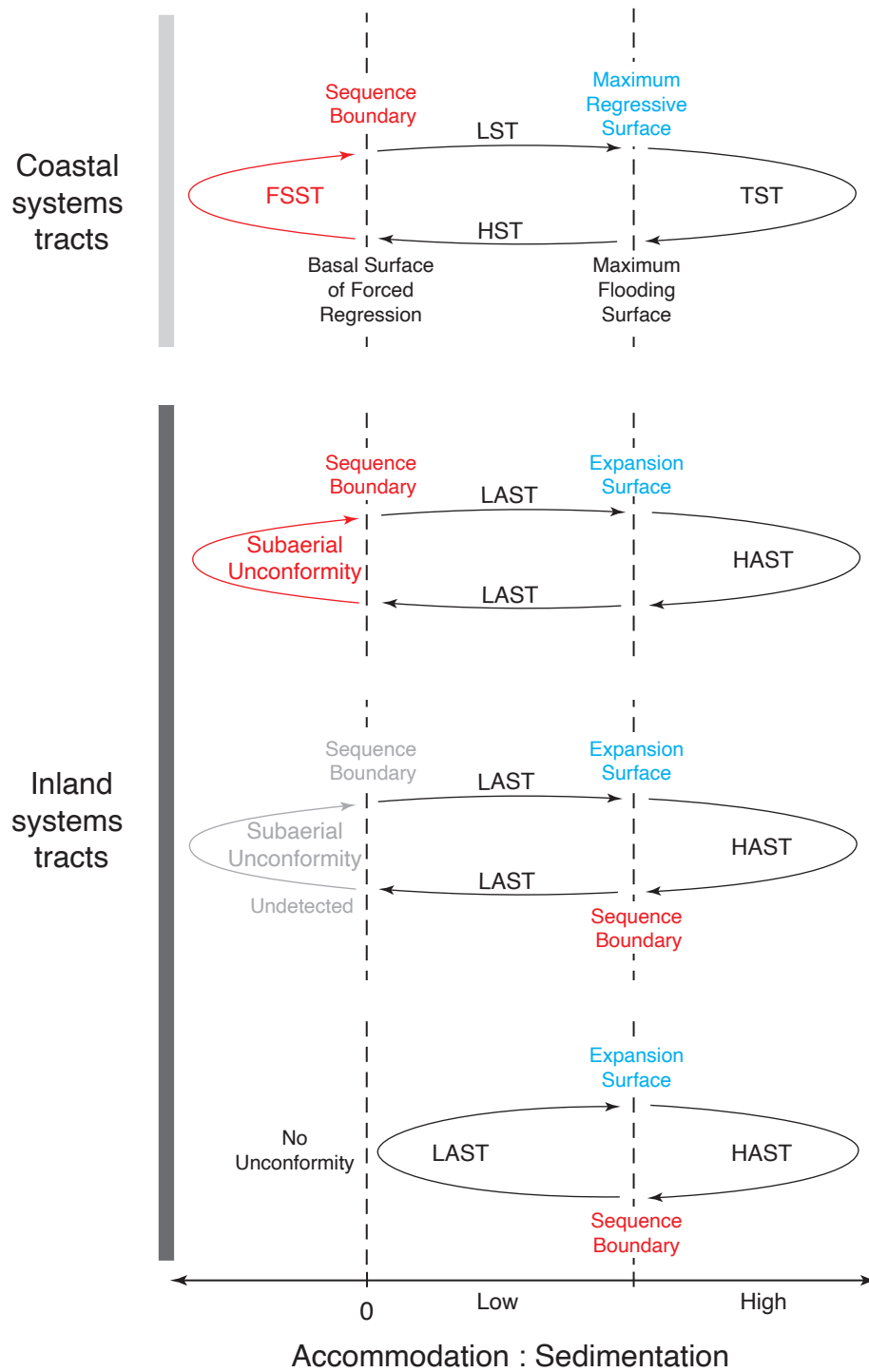
Table 3. The difference in the HAST and LAST probabilities of occurrence. Positive values indicate higher probabilities in the HAST, and negative values indicate higher probabilities in the LAST. Bolded values indicate statistical significance based on non-overlapping 95% confidence intervals.

Facies	Plants	Invertebrates	Vertebrates
Mire	0.020	0	0
Pond/Lake	0.354	-0.303	-0.136
Floodplain mud	0.122	0	0.021
Floodplain sand	0.034	0.114	-0.188
Fluvial channel lag	-0.200	0.100	-0.100
Fluvial channel bar	0.133	0.068	-0.376
Tidally influenced channel bar	0.265	0.353	0.294

Table 4. The difference in probabilities of occurrence between HAST updip (Stafford Ferry) and HAST downdip (Woodhawk Bottom). Positive values indicate higher probabilities updip and negative values indicate higher probabilities downdip. No values are statistically significant based on non-overlapping 95% confidence intervals.

Facies	Plants	Invertebrates	Vertebrates
Mire	0.288	0	0
Pond/Lake	-0.197	0.157	0.055
Floodplain mud	0.343	0	0.067
Floodplain sand	0.286	-0.190	-0.047
Fluvial channel lag	0	0.500	0.500
Fluvial channel bar	0.182	-0.409	0.182
Tidally influenced channel bar	0.310	-0.290	0.110

Figure 1. Relationship between the accommodation:sedimentation ratio and systems tracts of coastal settings (Hunt and Tucker, 1992) and inland settings (Martinsen et al., 1999). LAST: low-accommodation systems tract. HAST: high-accommodation systems tract. FSST: falling stage systems tract. LST: lowstand systems tract. HST: highstand systems tract. TST: transgressive systems tract.



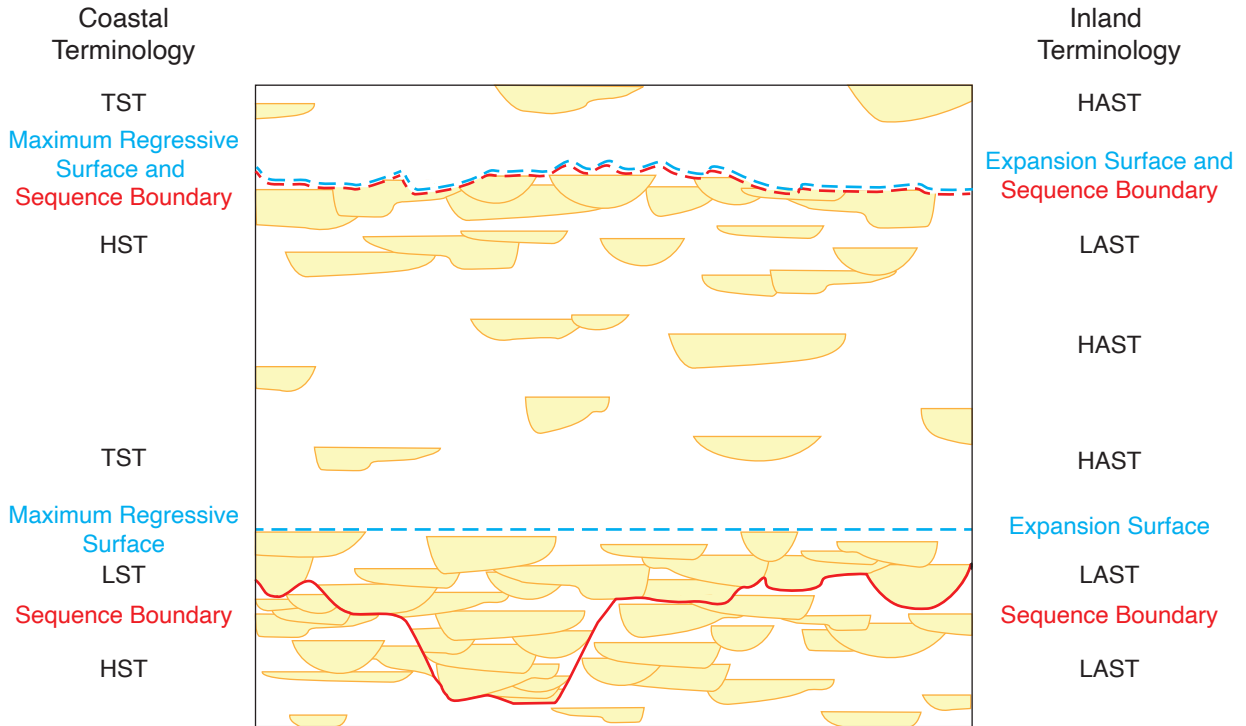


Figure 2. Stratigraphic architecture of nonmarine settings along depositional strike. Coastal terminology follows the Hunt and Tucker (1992) model. Inland terminology follows the Martinsen et al., (1999) model. LST: lowstand systems tract. HST: highstand systems tract. TST: transgressive systems tract. HAST: high-accommodation systems tract. LAST: low-accommodation systems tract. The falling stage systems tract (not shown) would be expressed farther down dip from this cross section.

	Macroplant fossils	Invertebrate fossils	Vertebrate fossils
Channel lags and bars	●	+	●
Abandoned channel fill	●	●	●
Levee	●	●	●
Poorly-drained floodplain	●	+	+
Well-drained floodplain	+	●	+
Oxygenated pond/lake	●	●	●
Low-oxygen pond/lake	●	●	●

Figure 3. Summary of occurrence of nonmarine fossils. Larger circles correspond with higher frequency of occurrence. Plus signs indicate presence, with no estimate of abundance. Modified from Behrensmeyer and Hook (1982).

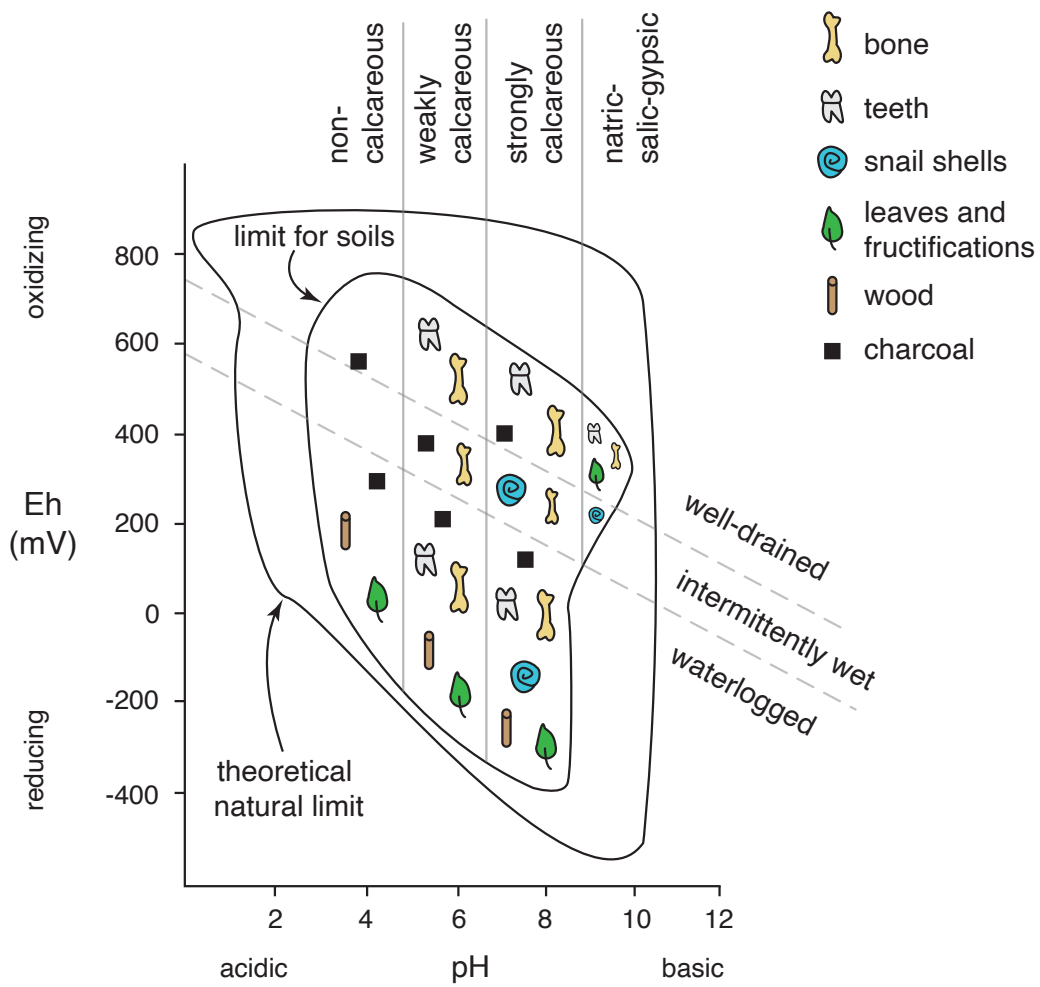


Figure 4. Theoretical Eh–pH stability fields for plant, invertebrate, and vertebrate fossils preserved in paleosols. Modified from Retallack (1998).

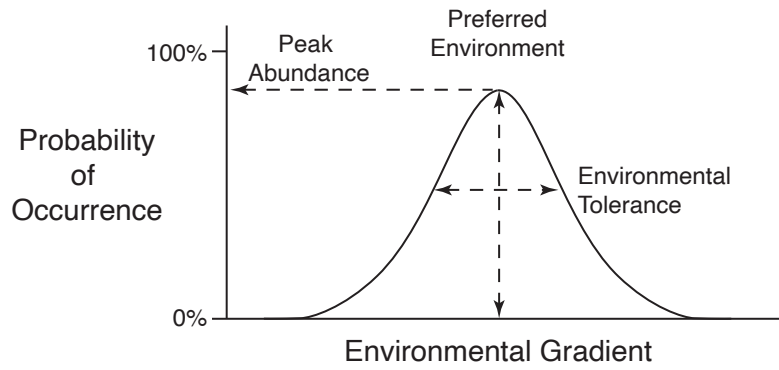
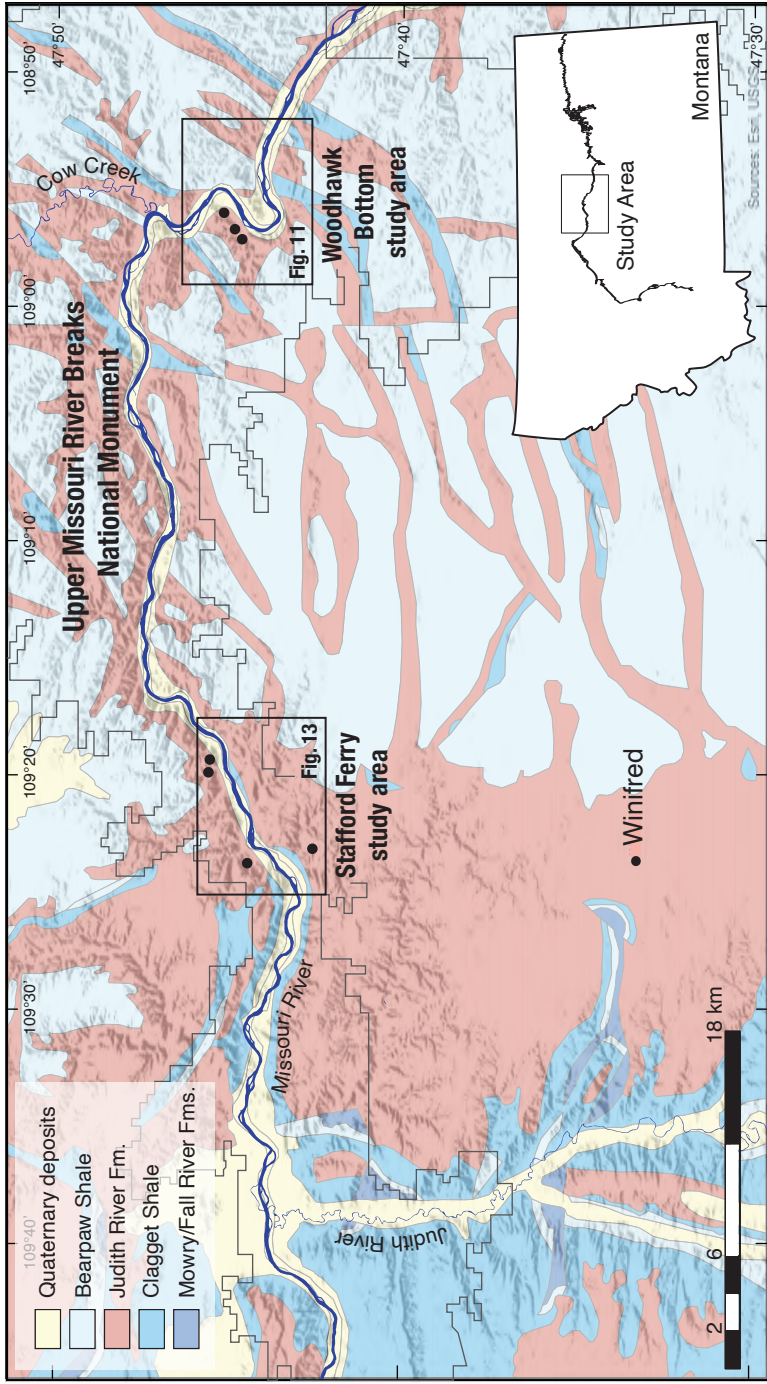


Figure 5. Example species-response curve for an organism. The probability of occurrence for a given species is a function of the position along an environmental gradient. Figure adapted from Holland (1995).

Figure 6. Map of study area in north-central Montana. The Judith River Formation is well exposed in the Missouri River valley within the Upper Missouri River Breaks National Monument (UMRBNM). Black dots indicate locations of seven measured columns in the Stafford Ferry and Woodhawk Bottom study areas.



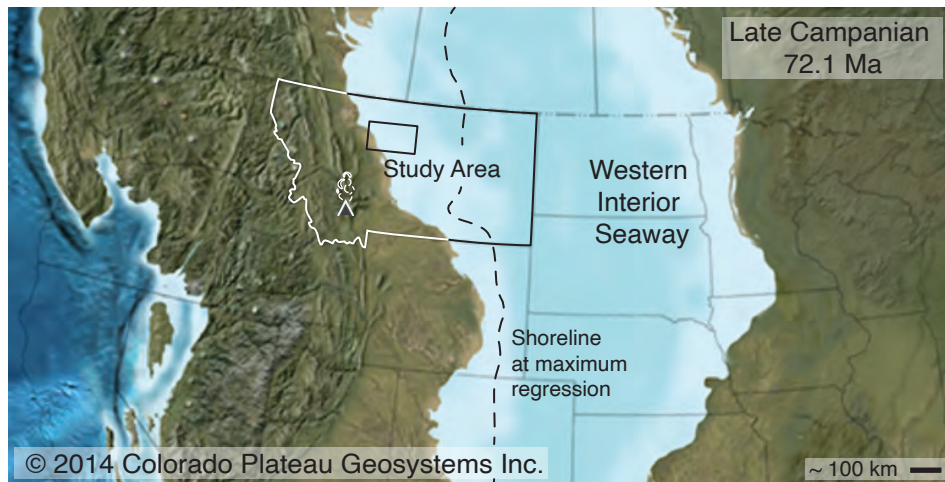


Figure 7. Paleogeographic map of the Western Interior Seaway, adapted from Blakey (2014). The Judith River Formation is slightly older than the time portrayed on this map and the shoreline was up to 100 km east of what is shown. The dashed line approximates the position of the shoreline at the time of maximum regression (*Baculites gregoryensis* Zone; Gill and Cobban, 1973).

Figure 8. Regional stratigraphic framework of the Judith River Formation. UMRBNM: Upper Missouri River Breaks National Monument. Modified from Rogers et al. (2016).

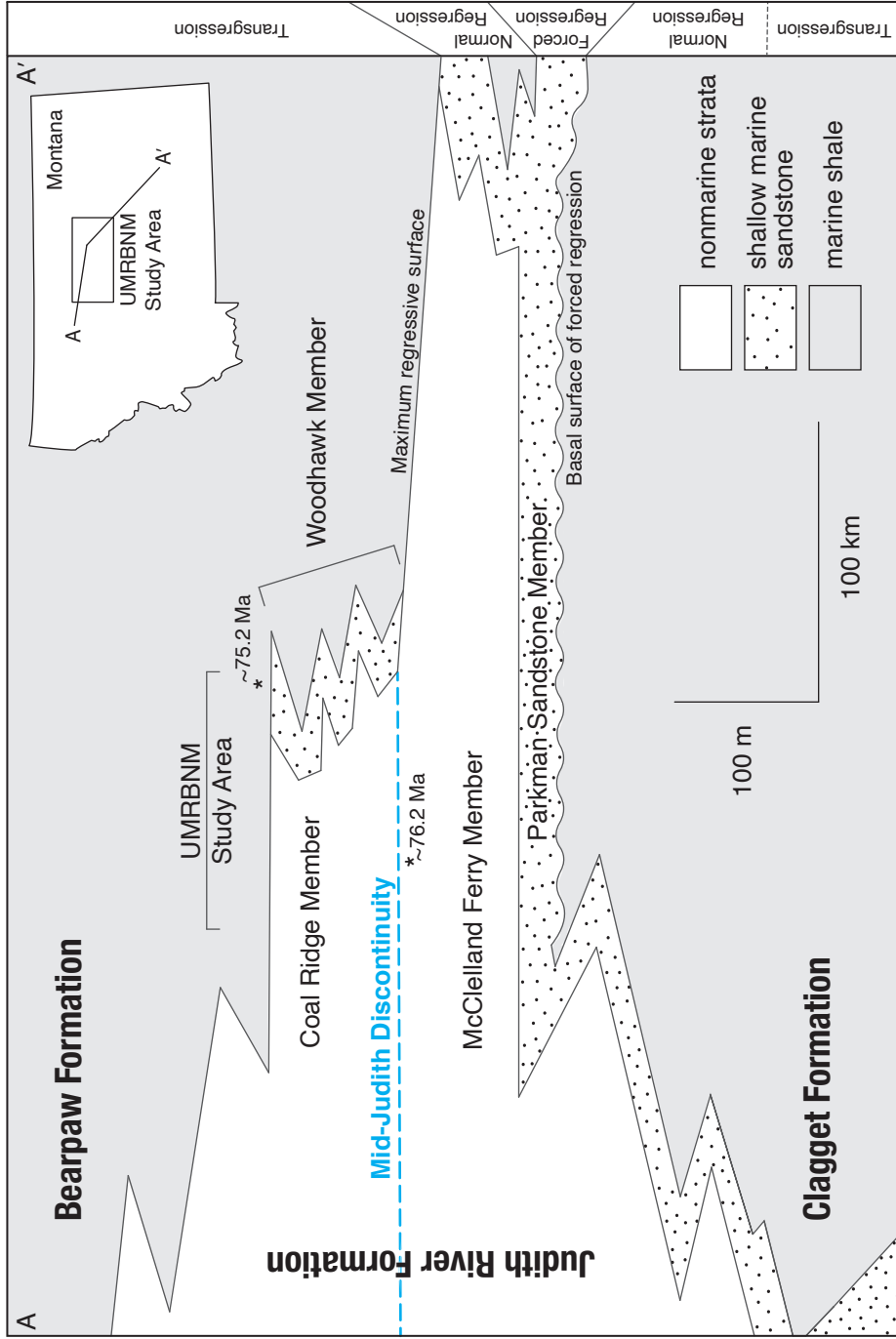


Figure 9. Floodplain facies associations. A) Mire facies with well-indurated, blocky bedding. B) Mire facies with fissile bedding. C) Pond/lake facies with abundant gastropods, bivalves, and indeterminate shell hash. Carbonaceous debris and plant fossils are rare. D) Typical pond/lake facies with carbonized wood, woody fragments, amber, and abundant carbonaceous debris. E) Pond/lake facies identified solely off the presence of invertebrate fossils. F) Floodplain mud facies displaying blocky bedding and dark grey coloration. G) Floodplain mud facies with lighter coloration and root traces. Notice the lack of carbonaceous material in G and F as compared to D (the pond/lake facies). H) Well-cemented interval of floodplain sand facies. A: amber. B: bivalve. CD: carbonaceous debris. G: gastropod. W: wood.

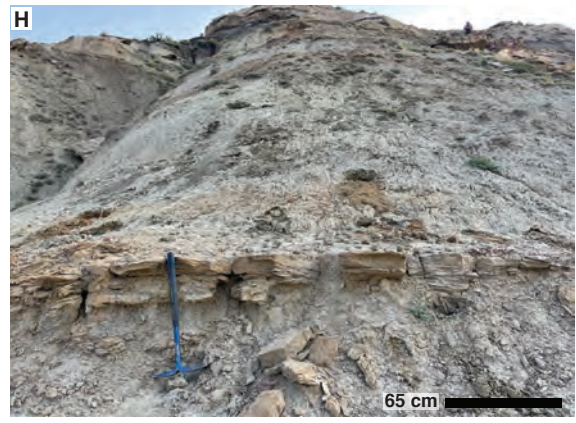
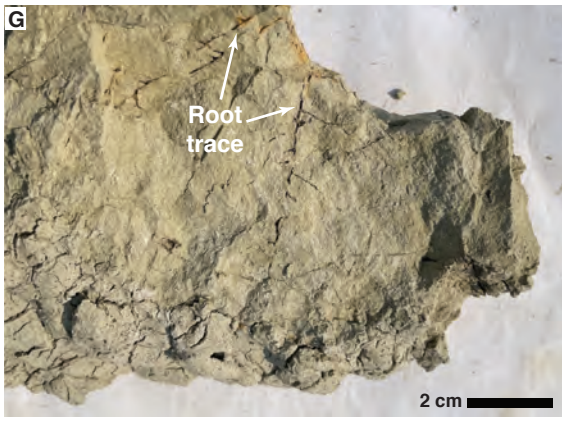
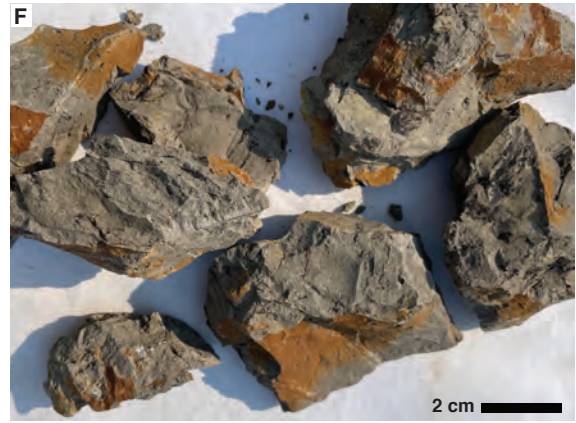
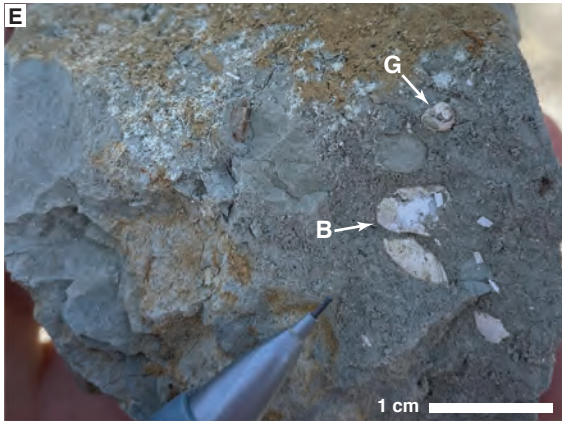
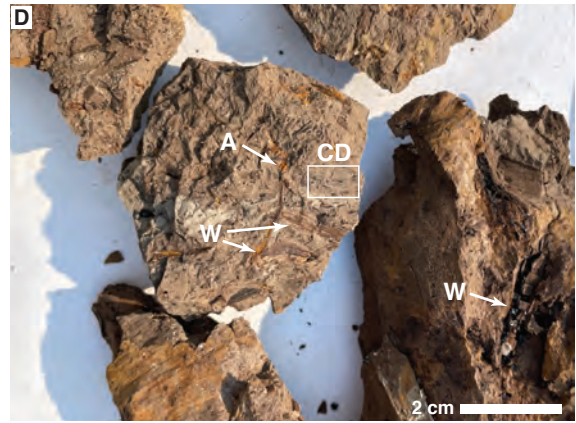
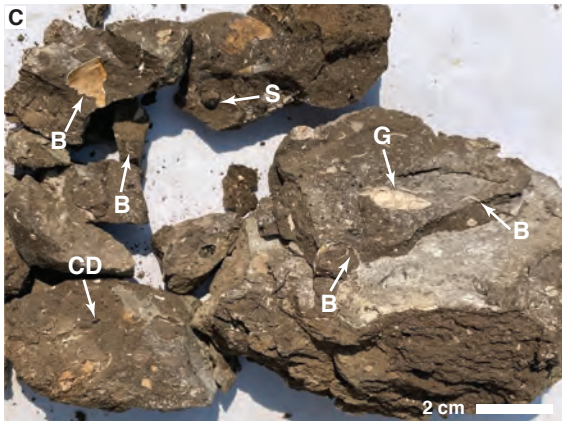
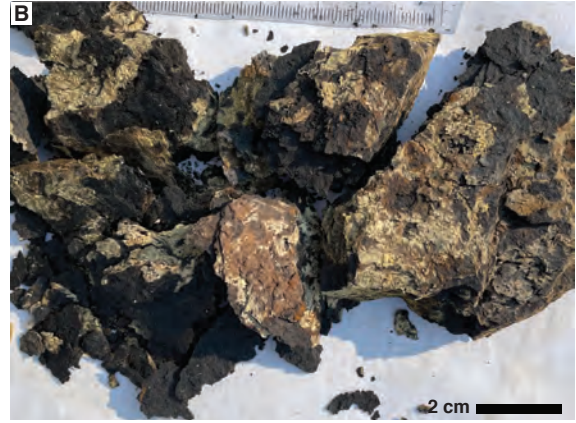


Figure 10. Channel facies associations. A) Fluvial channel lag facies in indurated sandstone with gravel to cobble sized clasts of cemented sand. B) Fluvial channel lag facies in non-indurated sandstone with weathered mud clasts. Arrows point to a few of the weathered clasts. C) Large-scale trough cross beds in the fluvial channel bar facies. D) Stacked fluvial channel bars. Person holding 1.5m Jacob's staff circled for scale. E) Large-scale trough cross beds with organic drapes in the tidally influenced channel bar facies. F) Upward thinning alternating beds of sand (light) and mud (dark; inclined heterolithic strata) in the tidally influenced channel bar facies. Arrows point to organic-draped foresets.



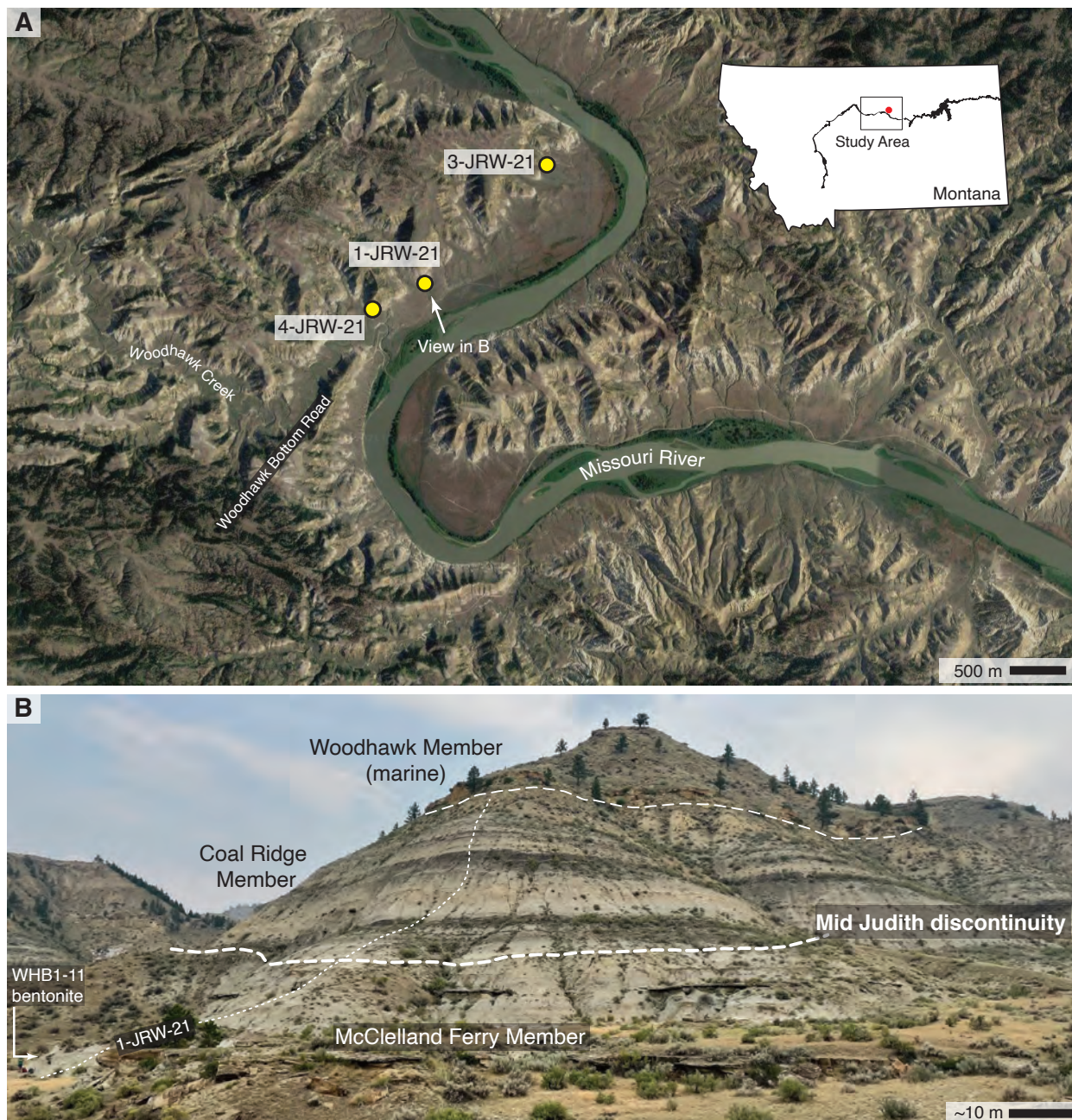
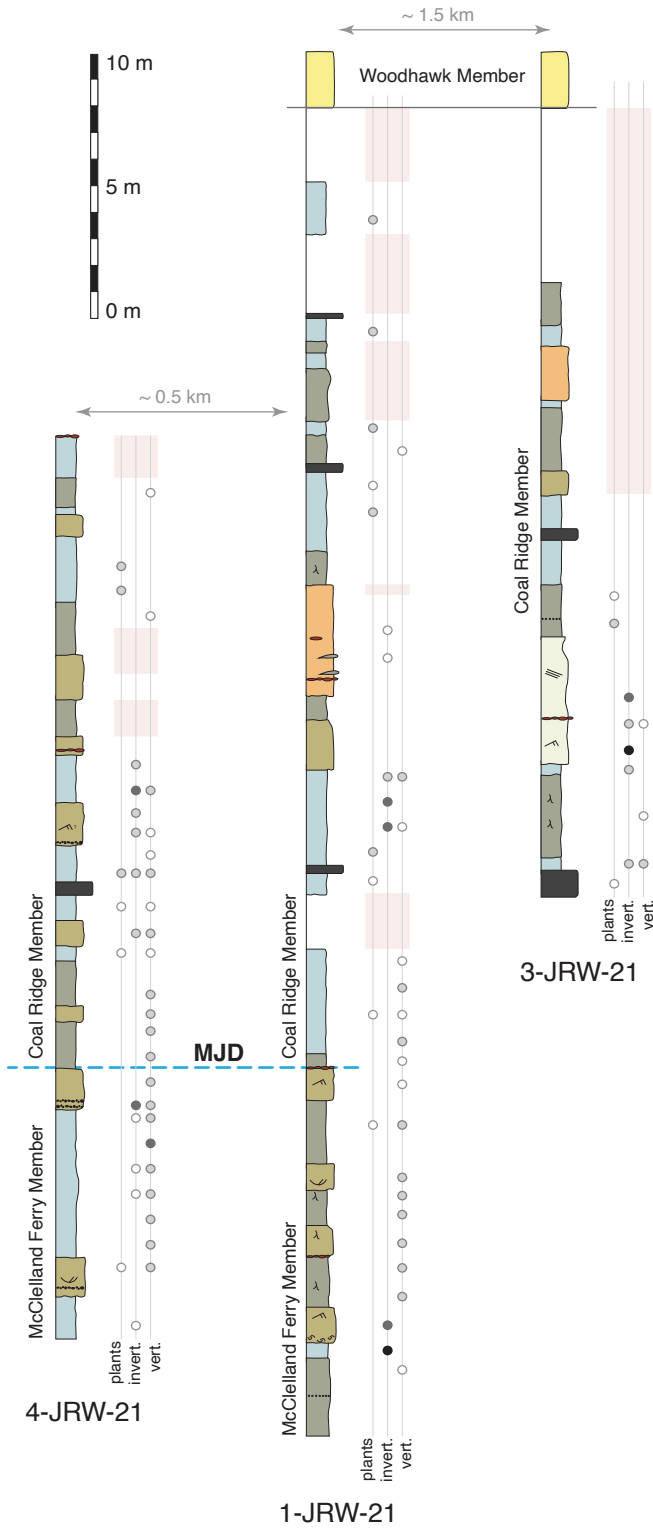


Figure 11. A) Map of the Woodhawk Bottom study area showing the locations of measured columns. B) Stratigraphy at the Woodhawk Bottom study area showing the McClelland Ferry, Coal Ridge, and Woodhawk members of the Judith River Formation with the path of column 1-JRW-21 dotted. The WHB1-11 bentonite has been dated to 76.17 Ma, roughly equivalent to the STI-03 bentonite at Stafford Ferry (Rogers et al., 2016).

Figure 12. Measured columns from the Woodhawk Bottom study area. Columns are vertically aligned by the base of the marine Woodhawk Member and the mid-Judith discontinuity. An area was deemed unsuitable for searching if it was too steep, narrow, vegetated, or weathered. MJD: mid-Judith discontinuity.



Facies Associations

- Mire
- Pond / Lake
- Floodplain mud
- Floodplain sand
- Fluvial channel bar
- Tidally influenced channel bar
- Marine sand
- Marine shale

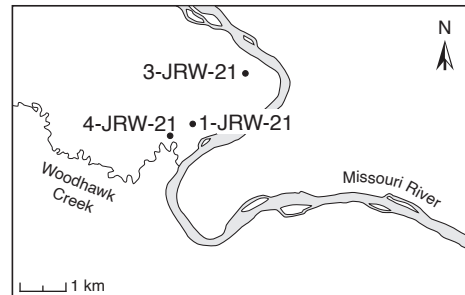
Symbols

- Small-scale ripple
- Large-scale trough
- Large-scale trough with organic drapes
- Root traces
- Shell bed
- Intraclast
- Soft-sediment deformation
- Inclined heterolithic strata
- Bentonite
- Lag
- Iron cemented

Fossils

- Abundant / Very abundant (300–1000+)
- Frequent / Common (30–300)
- Rare / Occasional (3–30)
- Very rare (1–3)
- Unsuitable search area

Woodhawk Bottom study area



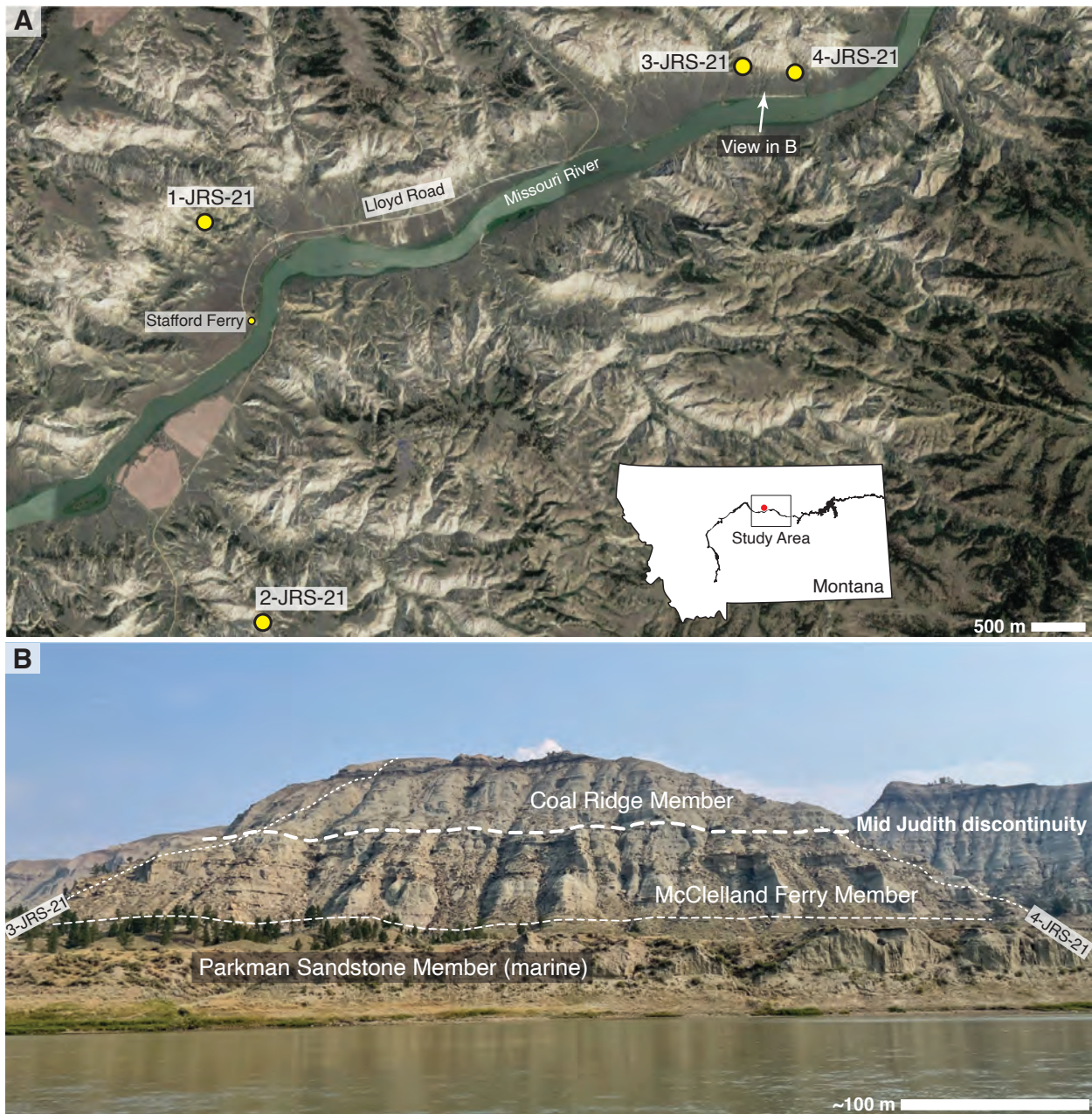


Figure 13. A) Map of the Stafford Ferry study area showing locations of measured columns. B) Stratigraphy at Stafford Ferry showing the Parkman Sandstone, McClelland Ferry, and Coal Ridge members of the Judith River Formation with paths of columns 3-JRS-21 and 4-JRS-21.

Figure 14. Measured columns from the Stafford Ferry study area. Columns are not vertically aligned. Columns 1-JRS-21 and 2-JRS-21 lie on depositional strike while columns 1-JRS-21, 3-JRS-21, and 4-JRS-21 lie on depositional dip. Column 3-JRS-21 is split into three consecutive pieces. Symbols, fossils, and facies colors follow key used in Figure 12. MFM: McClelland Ferry Member. CRM: Coal Ridge Member. MJD: mid-Judith discontinuity.

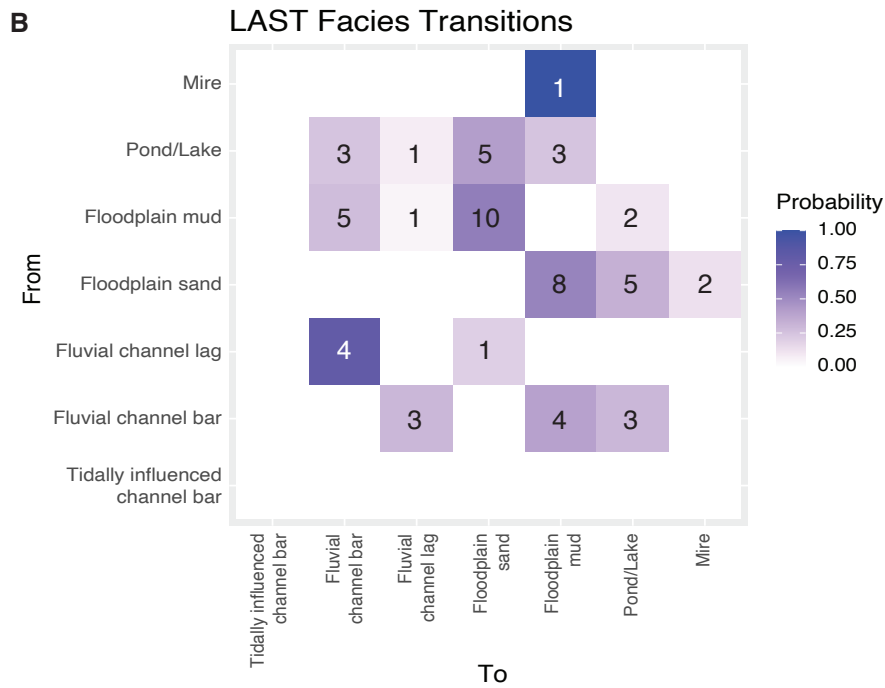
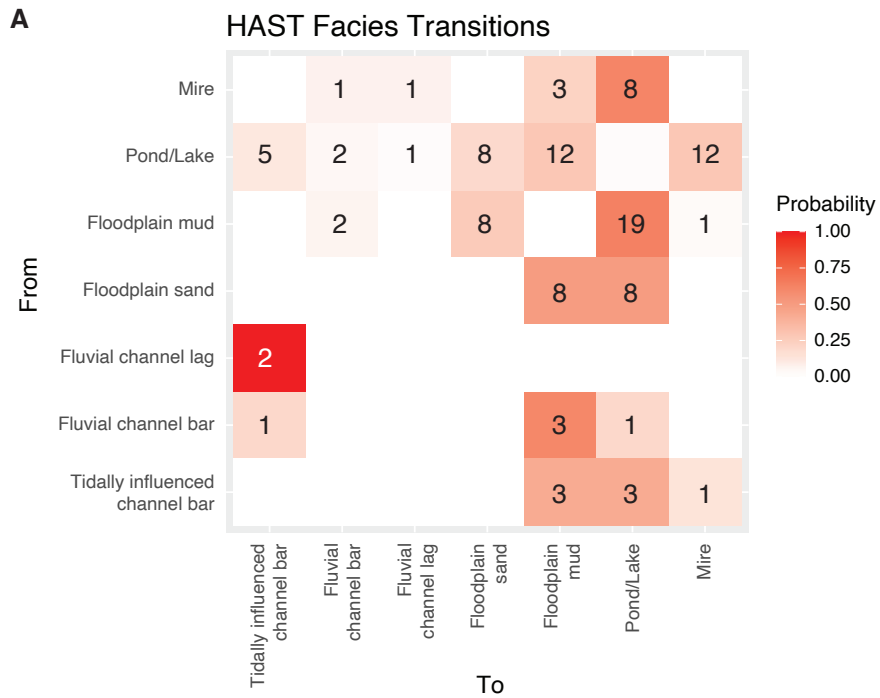


Figure 15. A) Heat map of HAST facies transitions (Table E1 in Appendix E). B) Heat map of LAST facies transitions (Table E2 in Appendix E). Values displayed in A and B are the total number of observed transitions to that facies.

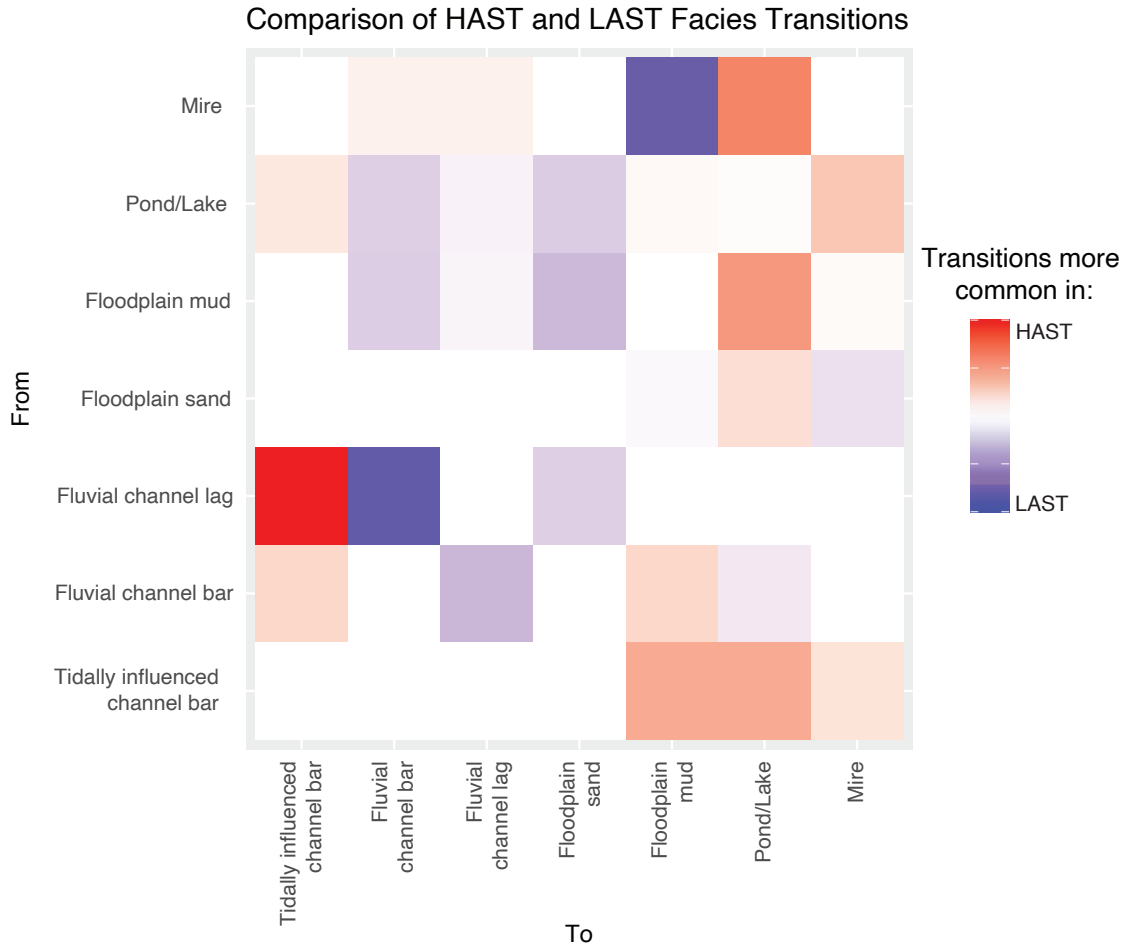


Figure 16. Transition matrix heat map comparing facies transitions in the HAST and LAST. Values are calculated by subtracting the LAST transition probabilities from the HAST transition probabilities (Table E3 in Appendix E).

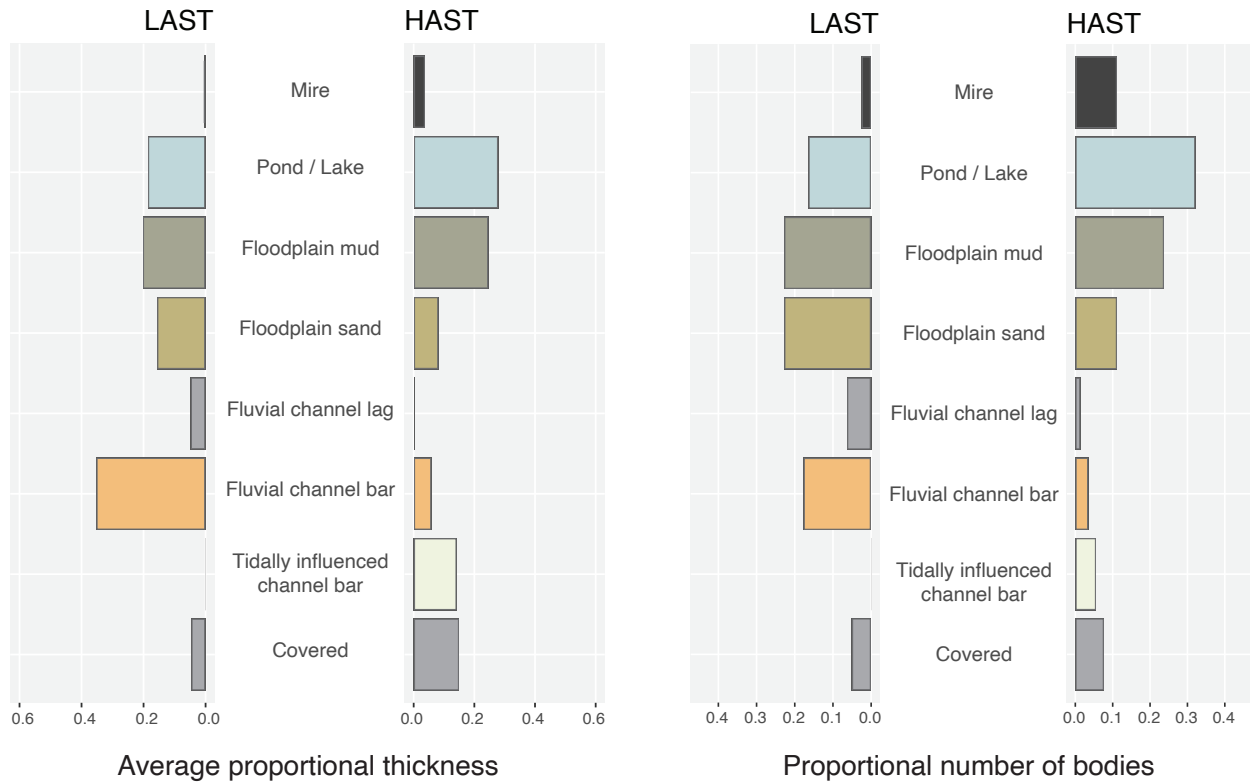


Figure 17. Numerical comparison of thickness and frequency of HAST and LAST facies. A) Average proportional thickness is the thickness of each facies in a column divided by the thickness of the measured column, averaged over all measured columns (Table F1 in Appendix F). B) The proportional number of bodies is the total number of times a facies occurred divided by the total number of facies in the measured columns (Table F2 in Appendix F). Each calculation is done with respect to systems tracts.

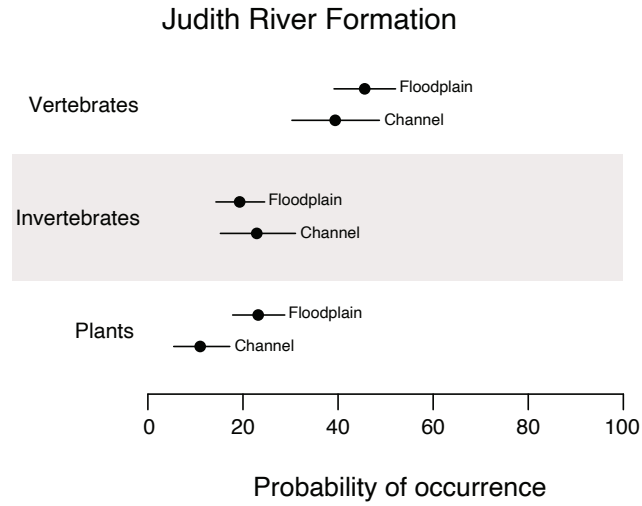


Figure 18. Comparison of probabilities of occurrence for taxa in the Judith River Formation floodplain and channel facies. Bars show 95% confidence intervals on the estimate (Table G1 in Appendix G).

Judith River Formation

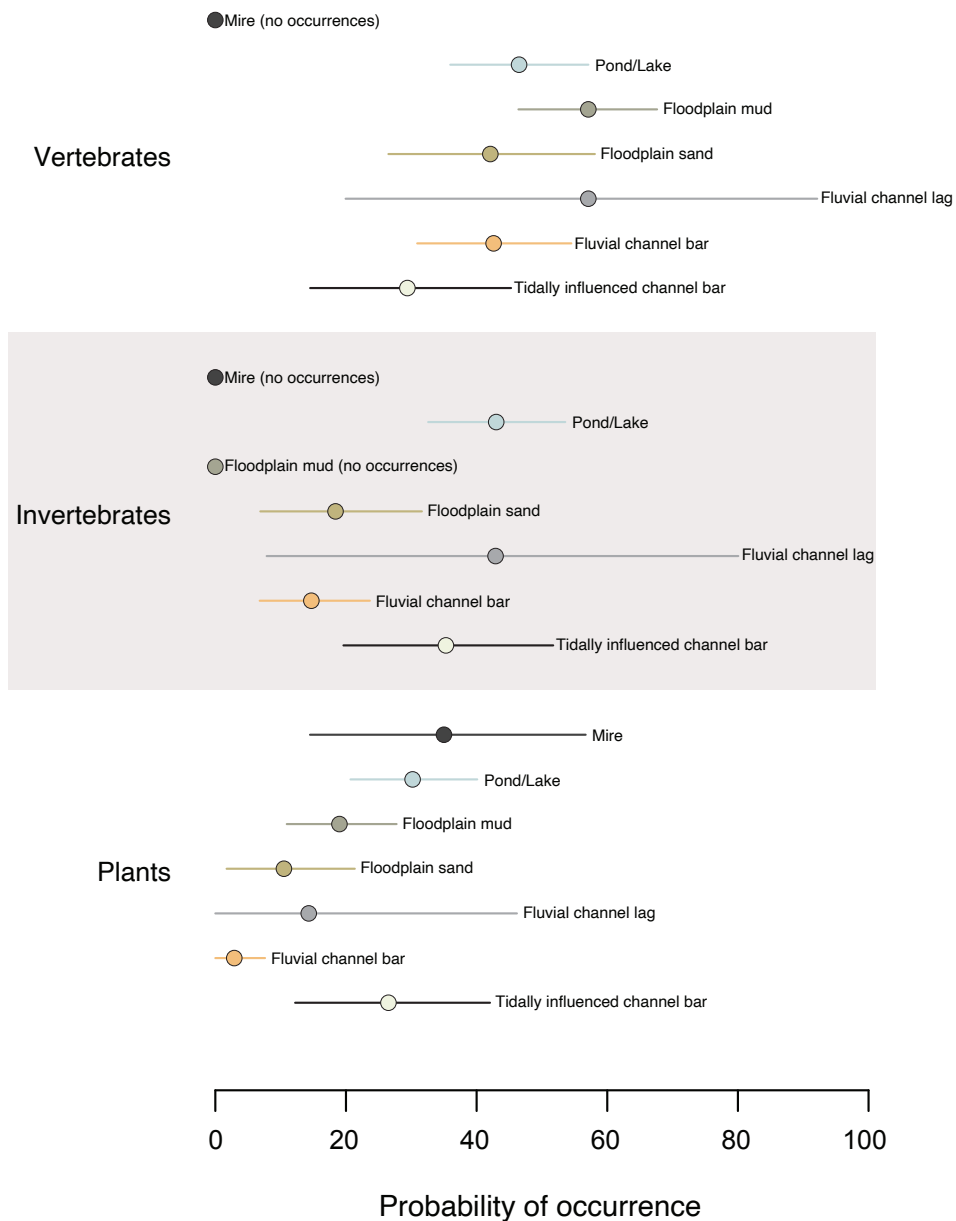


Figure 19. Comparison of probabilities of occurrence for taxa in the Judith River Formation per individual facies associations. Bars show 95% confidence intervals on the estimate (Table G2 in Appendix G).

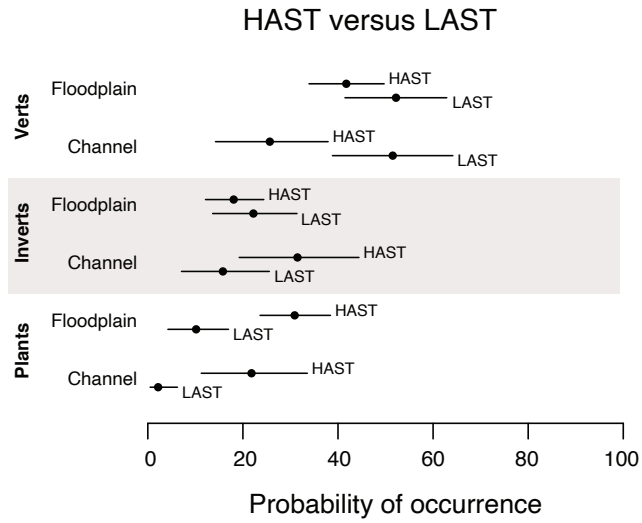


Figure 20. Comparison of probabilities of occurrence between floodplain and channel facies in the HAST (Coal Ridge Member) versus the LAST (McClelland Ferry Member). Bars show 95% confidence intervals on the estimate (Table G3 in Appendix G).

HAST versus LAST

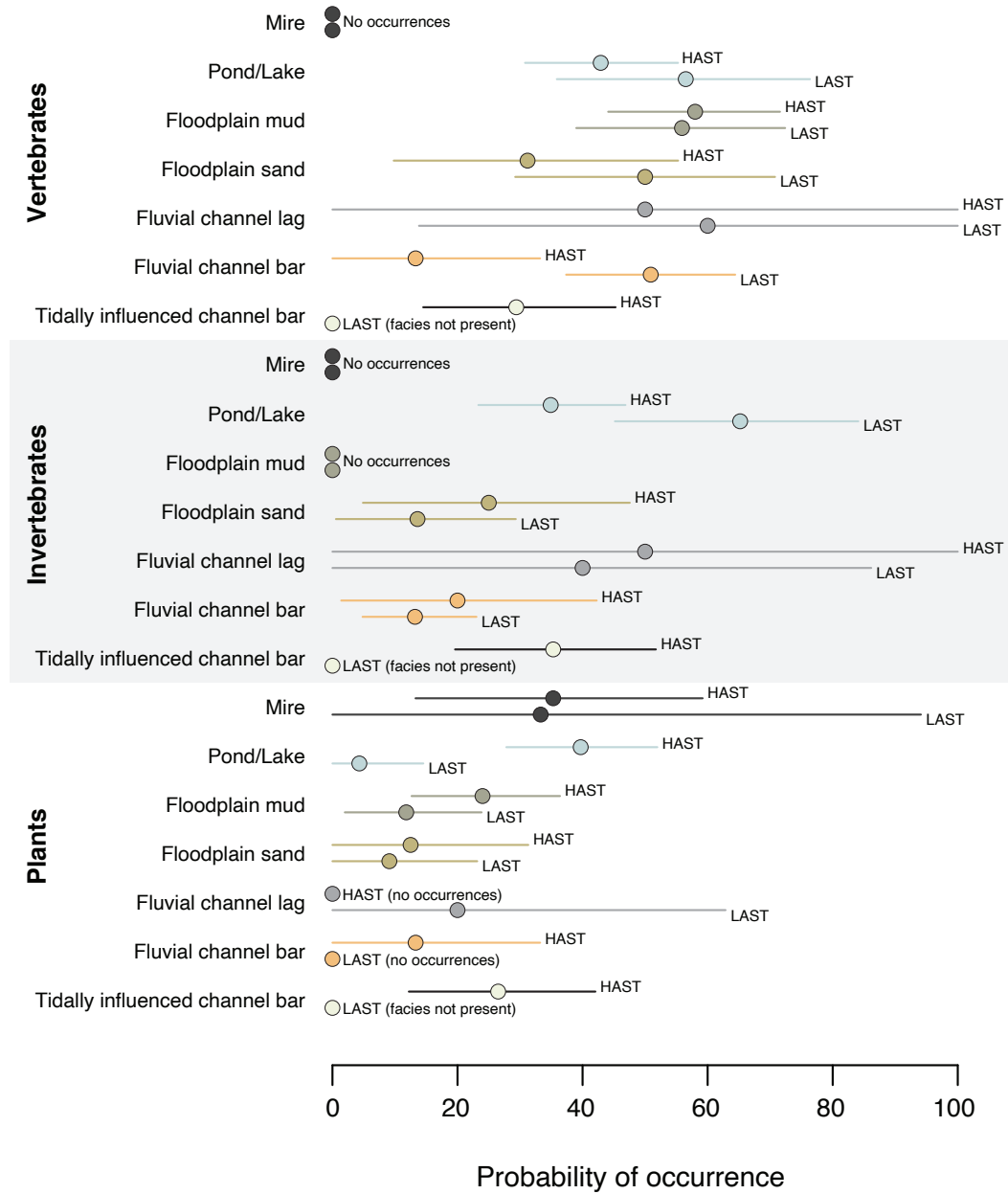


Figure 21. Comparison of probabilities of occurrence for taxa in HAST (Coal Ridge Member) and LAST (McClelland Ferry Member) facies associations. Bars show 95% confidence intervals on the estimate (Table G4 in Appendix G).

Updip HAST versus Downdip HAST

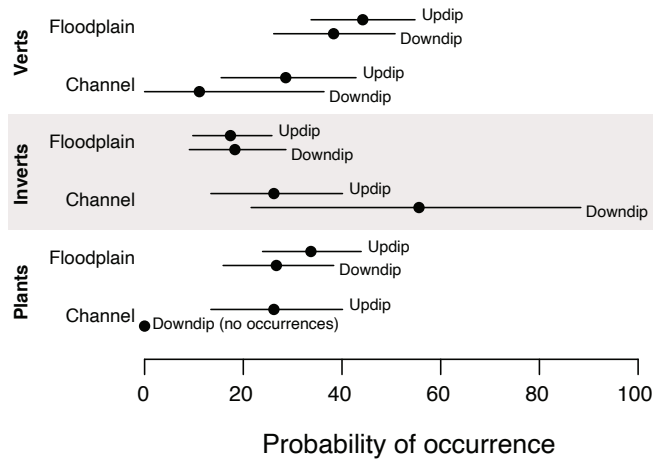


Figure 22. Comparison of probabilities of occurrence between floodplain and channel facies in the HAST updip (Stafford Ferry) and the HAST downdip (Woodhawk Bottom). Bars show 95% confidence intervals on the estimate (Table G5 in Appendix G).

Updip HAST versus Downdip HAST

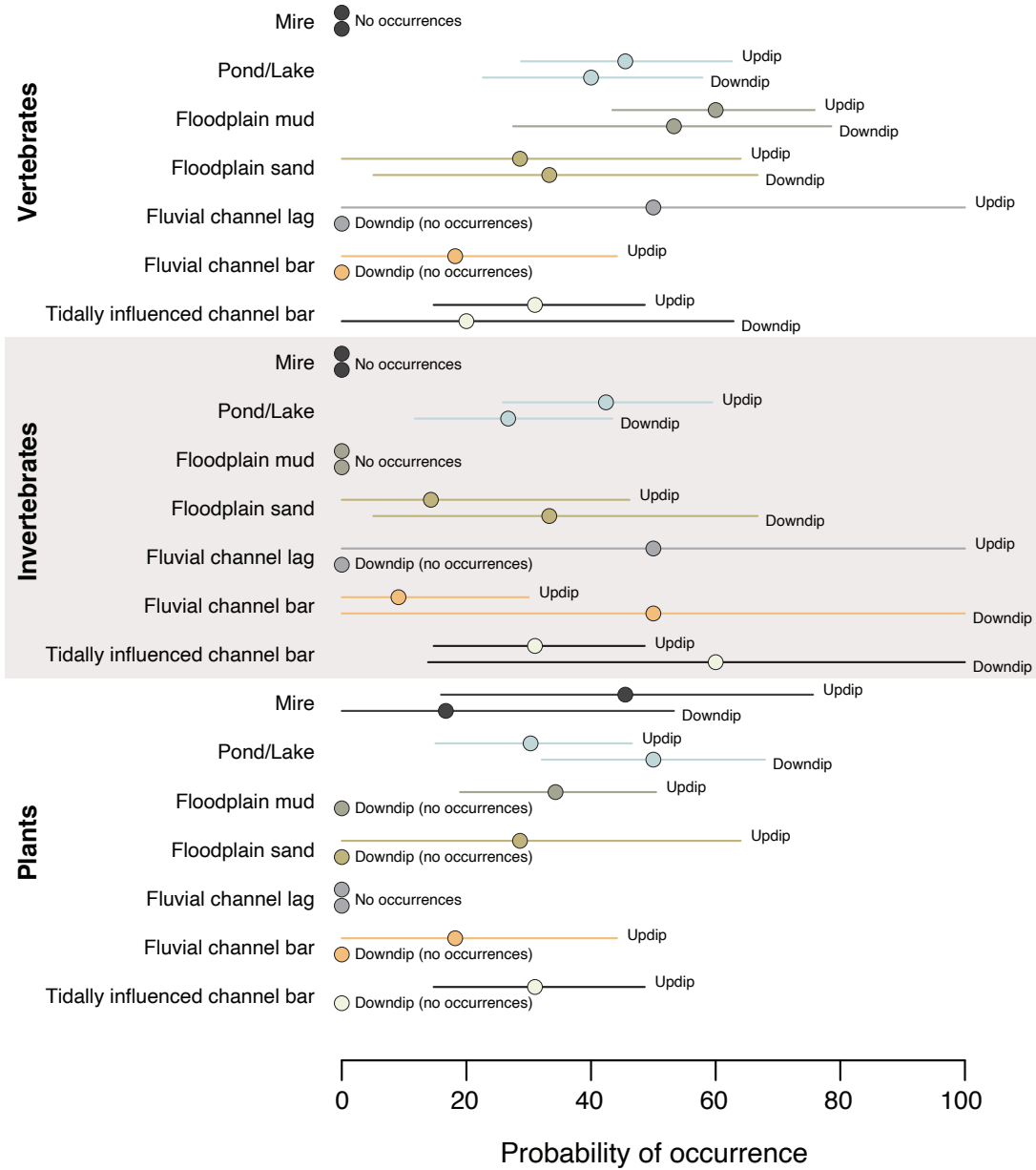


Figure 23. Comparison of probabilities of occurrence for taxa in the HAST updip (Stafford Ferry) versus the HAST downdip (Woodhawk Bottom) per individual facies associations. Bars show 95% confidence intervals on the estimate (Table G6 in Appendix G).

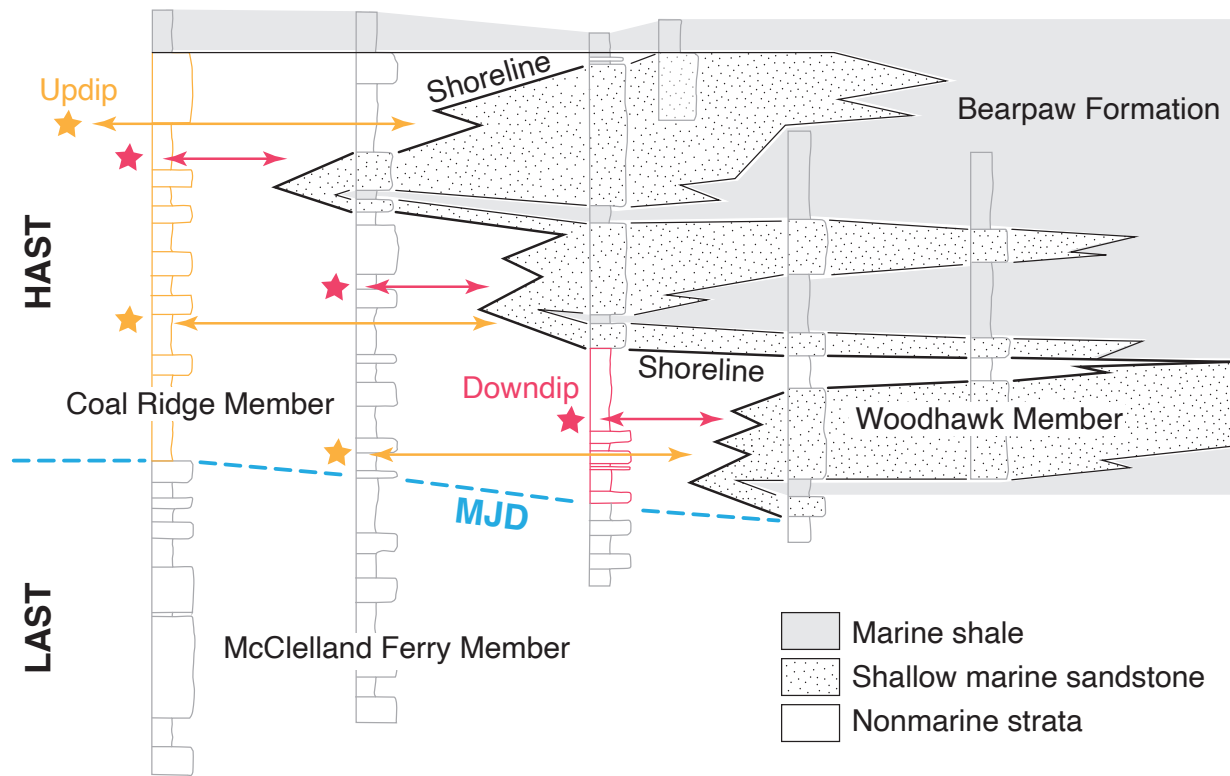
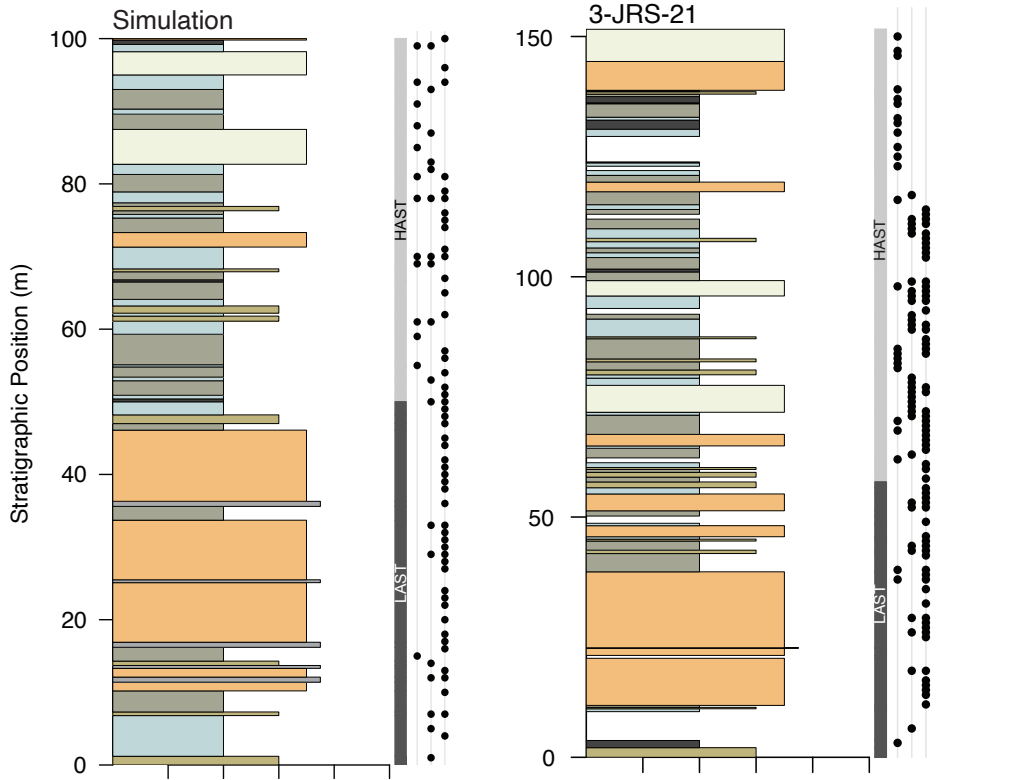


Figure 24. Sampling method to compare updip and downdip probabilities of occurrence. One strategy is to compare all samples from updip columns (shaded in orange) to downdip columns (shaded in red), as done in this study. A better strategy is to compare updip samples (orange stars) to downdip samples (red stars), while maintaining a constant distance from the shoreline. MJD: mid-Judith discontinuity. HAST: high-accommodation systems tract. LAST: low-accommodation systems tract. Modified from Rogers et al. (2016).

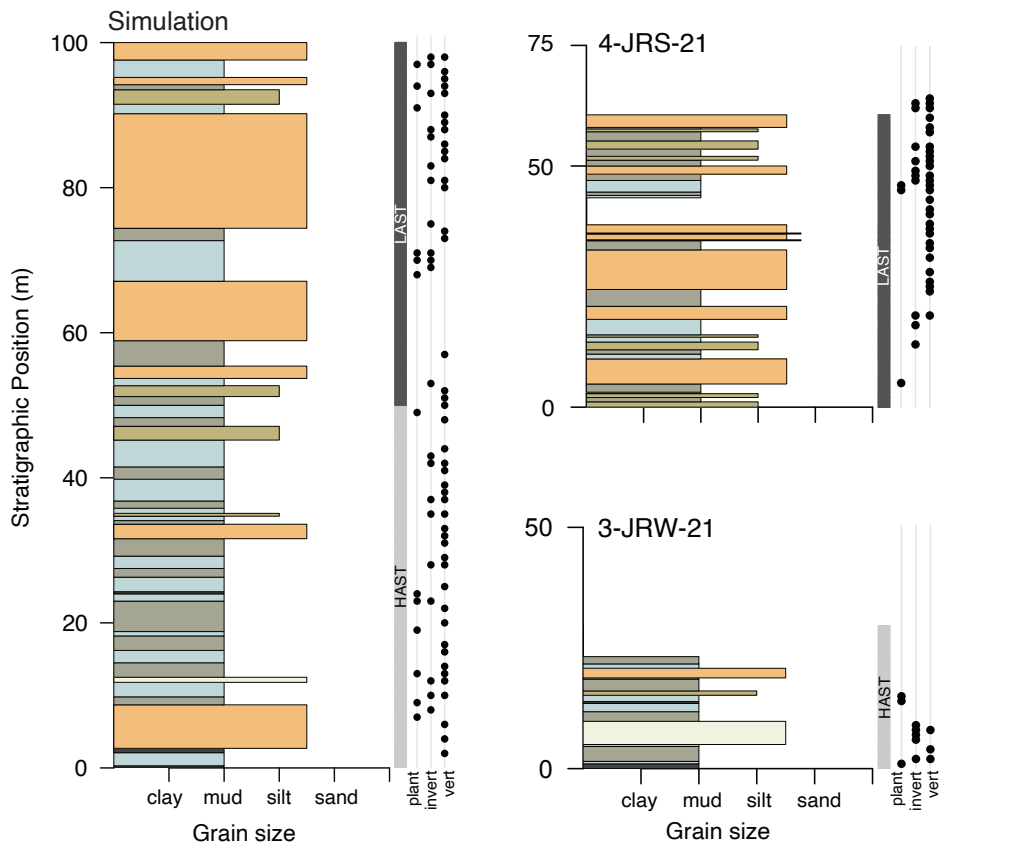
Figure 25. Comparison of simulated columns (left) and measured columns (right). A) Comparison of an expansion surface. B) Comparison of a sequence boundary. Facies colors follow conventions from Figure 12.

Expansion Surface



A

Sequence Boundary



B

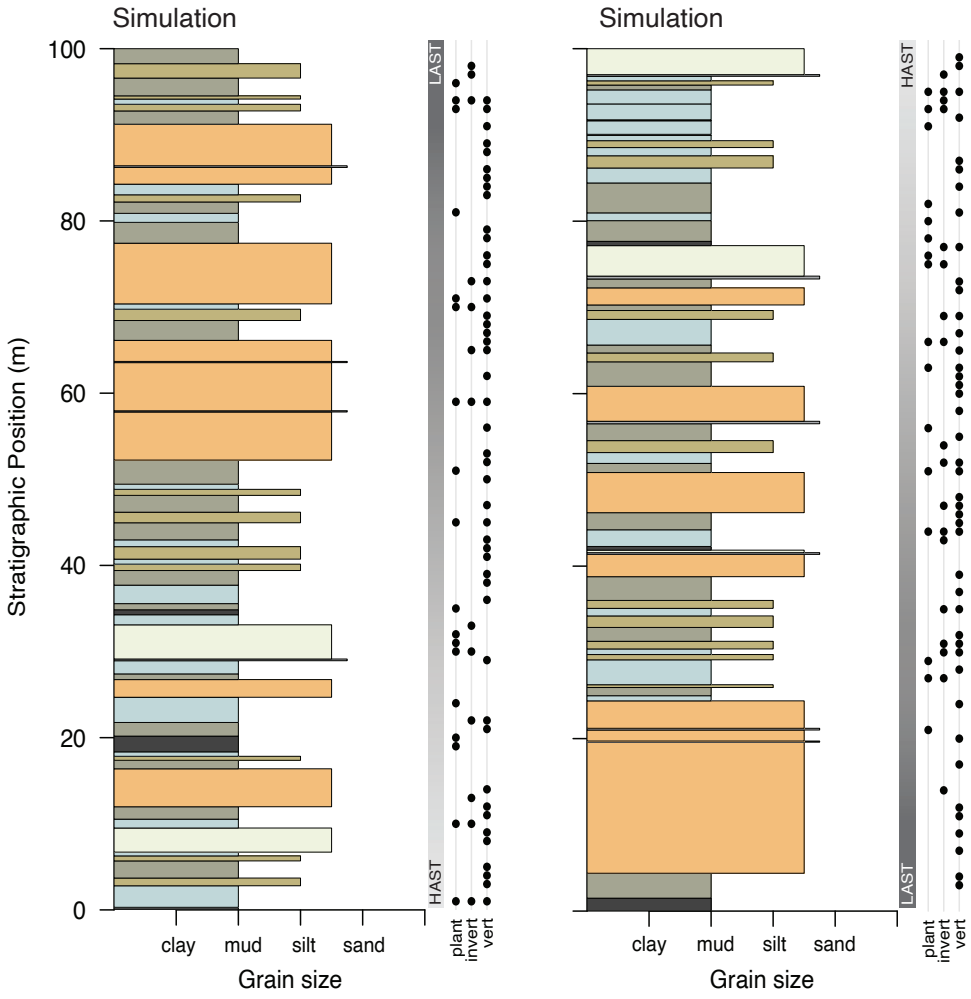


Figure 26. Simulations of the Judith River Formation with a gradual transition from HAST to LAST and vice versa. Facies colors follow conventions from Figure 12.

APPENDIX A

LOCALITIES OF MEASURED COLUMNS AND FOSSIL COLLECTIONS

Table A1. Location of measured columns

Name	Latitude	Longitude	Area	Notes
1-JRS-21	47.74676	-109.39894	Stafford Ferry	North of Stafford Ferry campground
2-JRS-21	47.71179	-109.39087	Stafford Ferry	Water catcher site on south side of Missouri
3-JRS-21	47.75972	-109.33079	Stafford Ferry	Reference section from Rogers et al. (2016)
4-JRS-21	47.75924	-109.32425	Stafford Ferry	Downriver of fence on same butte as reference section
1-JRW-21	47.74916	-108.94517	Woodhawk Bottom	Half mile from Woodhawk Bottom camp on road, on left bank of drainage
3-JRW-21	47.75810	-108.93061	Woodhawk Bottom	Near the end of Woodhawk Bottom Road
4-JRW-21	47.74732	-108.95164	Woodhawk Bottom	Butte on the left bank of Woodhawk Creek

Table A2. Location of fossil collections

Locality	Latitude	Longitude	Member	Facies	Date	Fossil Notes
2-JRS-21- LOC1	47.71157	-109.39051	Coal Ridge	Tidally influenced channel bar	7/7/21	Large amber chunk
3-JRS-21- LOC2	47.75977	-109.33074	McClelland Ferry	Fluvial channel bar	7/11/21	Hadrosaur teeth, gar scales, theropod tooth, theropod toe, unidentifiable material
3-JRS-21- LOC3	47.76026	-109.32999	McClelland Ferry	Pond/lake	7/12/21	Small theropod tooth
1-JRS-21- LOC4	47.74674	-109.39892	McClelland Ferry	Fluvial channel lag	7/16/21	Large freshwater clams, small bivalves and gastropods, wood fragments and bone fragments
UC-913 extension	47.74734	-108.95150	McClelland Ferry	Fluvial channel lag	7/21/21	Not collected- but rich in vertebrates and invertebrates
3-JRS-21- LOC2 extension	47.75990	-109.33090	McClelland Ferry	Fluvial channel bar	7/25/21	Ceratopsian jaw collected. Ribs and theropod teeth weathering out
2-JRS-21- LOC5	47.71111	-109.38974	Coal Ridge	Tidally influenced channel bar	7/26/21	Ironstone with wood and leaf impressions

APPENDIX B

STRATIGRAPHIC COLUMNS

Three input tables need to be supplied to the model: stratigraphic measurements, fossil counts (Appendix C), and a table that provides information for plotting (Appendix D). This appendix presents data from the measured columns ('stratColumn.csv' in R code inputs). 'section', 'unit', 'facies', 'top', and 'systemTract' are the only columns of this file used in the model to calculate the transition matrices and the distribution of facies thicknesses. Facies codes are as follows: Mire: mire. PL: pond/lake. Fp: floodplain mud. FpSand: floodplain sand. Lag: fluvial channel lag. Ch: fluvial channel bar. TiCh: tidally influenced channel bar. Base: indicates the beginning of each measured column. 'top' is measured in meters. Munsell 1–4 are the color codes from the Munsell Soil Color Book.

```
section,unit,facies,top,systemTract,munsell1,munsell2,munsell3,munsell4,photo
1,photo2,photo3,photo4,photo5,date,notes,collection
2JRS21,1,base,0,HAST,,,,,,,,,
2JRS21,2,PL,0.9,HAST,5YR2.5/1,,,,,9:02,,,,,7/7/21,,
2JRS21,3,Lag,1.1,HAST,,,,,9:02,,,,,
2JRS21,4,TiCh,4.2,HAST,,,,,9:22,9:15,,,,,
2JRS21,5,Mire,4.5,HAST,5YR3/1,,,,,10:03,,,,,
2JRS21,6,PL,7,HAST,,,,,10:36,,,,,
2JRS21,7,TiCh,10,HAST,,,,,11:00,11:14,,,,,2-JRS-21-LOC1
2JRS21,8,Fp,12.1,HAST,2.5Y5/2,5Y6/3,10YR6/4,,,,,,,
2JRS21,9,PL,12.5,HAST,,,,,,,bentonite,
2JRS21,10,Fp,12.9,HAST,2.5Y6/6,,,,,,,7/10/21,,
2JRS21,11,FpSand,13.3,HAST,,,,,,,
2JRS21,12,PL,13.5,HAST,,,,,1:19,1:20,,,,,
2JRS21,13,TiCh,14.2,HAST,,,,,,,
2JRS21,14,PL,15,HAST,,,,,1:36,,,,,
2JRS21,15,Mire,15.6,HAST,,,,,2:05,2:06,,,,,
2JRS21,16,PL,16,HAST,,,,,,,
2JRS21,17,Mire,16.1,HAST,,,,,,,
2JRS21,18,Lag,16.3,HAST,,,,,2:25,,,,,
```

2JRS21,19,TiCh,22.6,HAST,,,,,2:50,2:59,3:03,,,,,2-JRS-21-LOC5
 2JRS21,20,PL,23.3,HAST,,,,,3:14,3:17,3:18,,,,,
 2JRS21,21,Fp,24.4,HAST,,,,,3:34,3:36,,,,,
 2JRS21,22,Covered,24.9,HAST,,,,,
 2JRS21,23,Mire,25.2,HAST,,,,,
 2JRS21,24,PL,26.6,HAST,,,,,
 2JRS21,25,Mire,27.2,HAST,,,,,
 2JRS21,26,Covered,34,HAST,,,,,
 2JRS21,27,Msh,34.7,HAST,,,,,
 3JRS21,1,base,0, LAST,,,,,
 3JRS21,2,FpSand,2, LAST,5Y3/1,5Y4/1,2.5Y7/1,,11:01,,,,,7/13/21,,
 3JRS21,3,Mire,3.5, LAST,7.5YR2.5/1,,,,,
 3JRS21,4,Covered,9.5, LAST,,,,,
 3JRS21,5,PLi,10.1, LAST,2.5Y5/1,,,,,8:48,8:49,8:50,,7/11/21,,
 3JRS21,6,FpSand,10.4, LAST,,,,,
 3JRS21,7,Fp,10.8, LAST,,,,,9:00,8:24,,,,,
 3JRS21,8,Ch,20.6, LAST,2.5YR2.5/2,,,,,11:09,11:11,11:26,11:57,3:34,,purple
 facies,3-JRS-21-LOC2
 3JRS21,9,Covered,21.2, LAST,,,,,
 3JRS21,10,Ch,22.7, LAST,,,,,
 3JRS21,11,Lag,22.8, LAST,,,,,
 3JRS21,12,Ch,38.6, LAST,,,,,1:04,,,,,7/12/21,purple facies,
 3JRS21,13,Fp,42.4, LAST,2.5Y4/1,2.5Y6/2,,8:11,8:12,8:32,8:41,,,,,
 3JRS21,14,FpSand,43.1, LAST,,,,,8:45,8:47,,,,,
 3JRS21,15,Fp,45, LAST,,,,,9:05,,,,,
 3JRS21,16,FpSand,45.4, LAST,,,,,
 3JRS21,17,PL,45.9, LAST,5Y4/1,,,,,9:39,9:40,9:41,,,,,
 3JRS21,18,Ch,48.2, LAST,,,,,9:28,10:05,,,,,
 3JRS21,19,PL,48.7, LAST,7.5YR3/2,,,,,
 3JRS21,20,Covered,50.2, LAST,,,,,
 3JRS21,21,Fp,51.3, LAST,5Y7/1,,,,,10:52,,,,,
 3JRS21,22,Ch,54.8, LAST,,,,,10:52,11:24,11:25,11:26,,bentonite,
 3JRS21,23,PLi,56.1, LAST,,,,,11:46,11:59,,,,,
 3JRS21,24,FpSand,57.3, LAST,2.5Y7/1,5Y5/2,,,,,
 3JRS21,25,Fp,58.3, HAST,,,,,12:44AJ,,,,,
 3JRS21,26,FpSand,59.3, HAST,,,,,
 3JRS21,27,Fp,59.9, HAST,5Y6/1,,,,,
 3JRS21,28,FpSand,60.3, HAST,,,,,
 3JRS21,29,PL,61.3, HAST,2.5Y3/1,,,,,1:56,,,,,
 3JRS21,30,Covered,62.3, HAST,,,,,
 3JRS21,31,Fp,64.3, HAST,2.5Y3/2,5Y6/1,,2:19,,,,,
 3JRS21,32,PL,64.8, HAST,,,,,2:41,2:42,,,,,
 3JRS21,33,Ch,67.2, HAST,,,,,
 3JRS21,34,Fp,71.2, HAST,2.5Y5/2,5Y5/2,5Y6/2,,3:26,3:27,3:28,3:40,3:59,,
 3JRS21,35,PL,71.8, HAST,,,,,
 3JRS21,36,TiCh,77.4, HAST,,,,,4:36,4:24,,,,,
 3JRS21,37,PLi,78.9, HAST,5Y7/3,2.5Y6/1,,,,,7/13/21,,
 3JRS21,38,PL,79.6, HAST,,,,,8:15,8:16,8:17,,,,,
 3JRS21,39,FpSand,80.6, HAST,,,,,8:21,,,,,
 3JRS21,40,Fp,82.3, HAST,,,,,8:43,,,,,

3JRS21,41,FpSand,82.9,HAST,,,,,,,,,,,,,
3JRS21,42,Fp,87.1,HAST,2.5Y6/2,5Y5/1,,,9:15,,,,,,,,,
3JRS21,43,FpSand,87.5,HAST,,,,,,,,,,,,,
3JRS21,44,PLi,91.2,HAST,10YR3/1,2.5Y4/1,,,,,,,,,,,,,
3JRS21,45,Fp,92.2,HAST,5Y6/1,5Y5/2,,,,,,,,,,,,,
3JRS21,46,Covered,93.4,HAST,,,,,,,,,,,,,
3JRS21,47,PL,96,HAST,,,,,1:26,1:27,1:25,,,,,
3JRS21,48,TiCh,99.2,HAST,,,,,1:29,1:33,1:35,,,,,
3JRS21,49,Fp,101,HAST,10YR3/2,2.5Y5/1,,,,,,,,,,,,,
3JRS21,50,Mire,101.6,HAST,10YR3/1,,,,,,,,,,,,,7/14/21,,
3JRS21,51,Fp,104,HAST,2.5Y6/1,,,,,,,,,,,,,
3JRS21,52,PL,105,HAST,,,,,9:32,,,,,,,,,
3JRS21,53,Fp,106,HAST,5Y4/3,5Y4/1,,,,,,,,,,,,,
3JRS21,54,PLi,107.3,HAST,,,,,,,,,,,,,
3JRS21,55,FpSand,108,HAST,,,,,10:18,10:20,,,,,check facies,
3JRS21,56,PLi,110,HAST,10YR4/4,,,,,10:53,10:43,11:10,11:12,,,,,
3JRS21,57,Fp,112,HAST,,,,,,,,,,,,,
3JRS21,58,Covered,113,HAST,,,,,,,,,,,,,
3JRS21,59,Fp,114,HAST,,,,,,,,,,,,,
3JRS21,60,PLi,115,HAST,,,,,,,,,,,,,
3JRS21,61,Fp,117.7,HAST,,,,,,,,,,,,,
3JRS21,62,Ch,119.7,HAST,,,,,12:15,12:16,1:11,1:15,1:16,,,
3JRS21,63,Fp,121.1,HAST,2.5Y4/2,,,,,,,,,,,,,7/15/21,,
3JRS21,64,PL,122.1,HAST,,,,,8:16,8:17,8:18,8:23,,,,,
3JRS21,65,Covered,123,HAST,,,,,,,,,,,,,
3JRS21,66,PL,123.7,HAST,,,,,,,,,,,,,
3JRS21,67,Mire,123.9,HAST,,,,,,,,,,,,,
3JRS21,68,Covered,129.2,HAST,,,,,,,,,,,,,
3JRS21,69,PL,130.7,HAST,,,,,9:29,9:28,,,,,
3JRS21,70,Mire,132.6,HAST,,,,,9:37,,,,,,,,,
3JRS21,71,PL,133.2,HAST,,,,,,,,,,,,,
3JRS21,72,Fp,136,HAST,2.5Y6/2,,,,,10:07AJ,,,,,,,,,
3JRS21,73,PL,136.2,HAST,10YR5/2,,,,,10:30,,,,,,,,,
3JRS21,74,Mire,137.5,HAST,,,,,10:33,,,,,,,,,
3JRS21,75,Fp,138,HAST,2.5Y6/1,,,,,10:56,,,,,,,,,
3JRS21,76,FpSand,138.5,HAST,,,,,11:04,,,,,,,,,
3JRS21,77,PL,138.7,HAST,,,,,,,,,,,,,
3JRS21,78,Mire,138.8,HAST,7.5YR4/3,,,,,11:07,11:15,,,,,,,,,
3JRS21,79,Ch,144.8,HAST,,,,,12:06,12:07,,,,,,,,,
3JRS21,80,TiCh,151.5,HAST,,,,,12:16,12:20,12:21,12:24,12:44,,,
3JRS21,81,Msh,152.3,HAST,,,,,,,,,,,,,
1JRW21,1,base,0, LAST,,,,,,,,,,,,,
1JRW21,2,Fp,2.9, LAST,5Y7/2,5Y6/3,2.5Y7/2,,9:19,,,,,7/18/21,bentonite,
1JRW21,3,PLi,3.5, LAST,5Y5/2,,,,,10:12,,,,,,,,,
1JRW21,4,FpSand,4.8, LAST,,,,,10:13,10:14,10:19,10:43,,,,,
1JRW21,5,Fp,6.8, LAST,,,,,,,,,,,,,
1JRW21,6,FpSand,7.8, LAST,5Y6/3,5Y5/3,,11:16,11:17,11:35,,,,,
1JRW21,7,Fp,9.3, LAST,,,,,,,,,,,,,
1JRW21,8,FpSand,10.3, LAST,,,,,,,,,,,,,
1JRW21,9,Fp,12.7, LAST,5Y3/1,,,,,,,,,,,,,

1JRW21,10,FpSand,13.9,LAST,,,,,,,,,,,,,
1JRW21,11,Fp,14.4,HAST,5Y7/2,,,,,2:18,,,,,,
1JRW21,12,PL,18.4,HAST,2.5Y4/2,2.5Y3/1,,,,,2:10,2:58,3:00,,,,,
1JRW21,13,Covered,20.5,HAST,,,,,,,,,,,,,
1JRW21,14,PL,21.3,HAST,,,,,,,,,,,,,
1JRW21,15,Mire,21.6,HAST,,,,,7:14,7:33,7:34,,,,,7/19/21,,
1JRW21,16,PL,25.2,HAST,2.5Y5/2,2.5Y3/1,,,,,7:22,,,,,,
1JRW21,17,FpSand,27.1,HAST,,,,,8:24,,,,,,
1JRW21,18,Fp,28,HAST,,,,,,,,,,,,,
1JRW21,19,Ch,32.3,HAST,,,,,9:57,,,,,,
1JRW21,20,Fp,33.5,HAST,,,,,,,,,,,,,
1JRW21,21,PL,36.5,HAST,,,,,,,,,,,,,
1JRW21,22,Mire,36.8,HAST,,,,,,,,,,,,,
1JRW21,23,Fp,38,HAST,2.5Y4/1,,,,,,,,,,,,,
1JRW21,24,PL,38.4,HAST,,,,,,,,,,,,,
1JRW21,25,Fp,40.4,HAST,,,,,,,,,,,,,
1JRW21,26,PL,40.9,HAST,,,,,,,,,,,,,
1JRW21,27,Fp,41.4,HAST,,,,,,,,,,,,,
1JRW21,28,PL,42.3,HAST,,,,,,,,,,,,,
1JRW21,29,Mire,42.5,HAST,,,,,,,,,,,,,
1JRW21,30,Covered,45.5,HAST,,,,,,,,,,,,,
1JRW21,31,PL,47.5,HAST,,,,,,,,,,,,,
1JRW21,32,Covered,50.5,HAST,,,,,,,,,,,,,
1JRS21,1,base,0,LAST,,,,,,,,,,,,,
1JRS21,2,Ch,1,LAST,,,,,,,,,7/16/21,,1-JRS-21-LOC4
1JRS21,3,Lag,1.7,LAST,,,,,8:49,9:30,,,,,,
1JRS21,4,Ch,3.6,LAST,,,,,,,,,,,,,
3JRW21,1,base,0,HAST,,,,,,,,,,,,,
3JRW21,2,Mire,1,HAST,,,,,10:42,,,,,7/20/21,,
3JRW21,3,PLi,1.5,HAST,5Y3/2,5Y6/1,,,,,11:10,,,,,,
3JRW21,4,Fp,4.6,HAST,,,,,,,,,,,,,
3JRW21,5,PLi,5,HAST,,,,,,,,,,,,,
3JRW21,6,TiCh,9.8,HAST,,,,,,,,,,,,,
3JRW21,7,Fp,11.8,HAST,5Y5/1,5Y4/3,,,,,,bentonite weathering,
3JRW21,8,PL,13.5,HAST,,,,,,,,,,,,,
3JRW21,9,Mire,13.9,HAST,,,,,,,,,,,,,
3JRW21,10,PL,15.2,HAST,,,,,,,,,,,,,
3JRW21,11,FpSand,16.1,HAST,,,,,,,,,,,,,
3JRW21,12,Fp,18.5,HAST,,,,,,,,,,,,,
3JRW21,13,PL,18.8,HAST,,,,,,,,,,,,,
3JRW21,14,Ch,20.8,HAST,,,,,,,,,,,,,
3JRW21,15,PL,21.7,HAST,,,,,,,,,,,,,
3JRW21,16,Fp,23.2,HAST,,,,,,,,,,,,,
3JRW21,17,Covered,29.6,HAST,,,,,,,,,,,,,
4JRW21,1,base,0,LAST,,,,,,,,,,,,,
4JRW21,2,PLi,1.6,LAST,,,,,7:17,,,,,7/21/21,,
4JRW21,3,FpSand,3.1,LAST,,,,,7:13,,,,,7/20/21,,
4JRW21,4,PLi,8.7,LAST,10Y5GY4/2,2.5Y4/1,5Y3/2,5Y4/2,7:08,7:28,7:31,7:32,7:34,
7/21/21,,
4JRW21,5,Lag,9.1,LAST,,,,,7:48,8:14,8:15,,,,,

4JRW21,6,FpSand,10.3,LAST,,,,,,,,,,,,,
 4JRW21,7,Fp,12,HAST,5Y3/1,,,,,8:49,,,,,
 4JRW21,8,FpSand,12.6,HAST,,,,,9:02,,,,,
 4JRW21,9,Fp,14.3,HAST,5Y4/1,2.5Y2.5/1,,,,,
 4JRW21,10,PL,14.8,HAST,,,,,9:40,,,,,
 4JRW21,11,FpSand,15.8,HAST,,,,,
 4JRW21,12,PL,16.8,HAST,,,,,
 4JRW21,13,Mire,17.3,HAST,,,,,9:48,,,,,
 4JRW21,14,PL,18.7,HAST,,,,,
 4JRW21,15,FpSand,20.3,HAST,,,,,
 4JRW21,16,PLi,22.1,HAST,,,,,
 4JRW21,17,FpSand,22.8,HAST,,,,,
 4JRW21,18,Fp,24.2,HAST,,,,,
 4JRW21,19,FpSand,25.9,HAST,,,,,
 4JRW21,20,Fp,27.9,HAST,,,,,
 4JRW21,21,PL,30.4,HAST,,,,,
 4JRW21,22,FpSand,31.2,HAST,,,,,
 4JRW21,23,PL,31.5,HAST,,,,,
 4JRW21,24,Fp,32.6,HAST,,,,,
 4JRW21,25,PL,34.2,HAST,,,,,
 4JRS21,1,base,0, LAST,,,,,
 4JRS21,2,FpSand,1.1, LAST,,,,,8:02,,,,,7/24/21,,
 4JRS21,3,Fp,2, LAST,5Y5/1,,,,,8:12,,,,,
 4JRS21,4,FpSand,2.8, LAST,,,,,
 4JRS21,5,Mire,3.1, LAST,5YR2.5/2,,,,,8:35,8:36,,,,,
 4JRS21,6,Fp,4.8, LAST,,,,,8:51,,,,,
 4JRS21,7,Ch,10, LAST,,,,,9:05,9:06,9:07,9:08,9:09,,,
 4JRS21,8,PLi,11, LAST,5Y6/1,,,,,10:23,,,,,
 4JRS21,9,Fp,11.9, LAST,,,,,10:30,,,,,
 4JRS21,10,FpSand,13.5, LAST,,,,,
 4JRS21,11,PLi,14.5, LAST,,,,,11:10,,,,,
 4JRS21,12,FpSand,15, LAST,,,,,
 4JRS21,13,PLi,18.2, LAST,,,,,
 4JRS21,14,Ch,20.9, LAST,,,,,12:57,12:58,,,,,
 4JRS21,15,Fp,24.4, LAST,,,,,1:37,1:38,,,,,
 4JRS21,16,Ch,32.6, LAST,,,,,
 4JRS21,17,Fp,34.5, LAST,,,,,
 4JRS21,18,Lag,34.7, LAST,,,,,
 4JRS21,19,Ch,35.9, LAST,,,,,7:59,8:00,,,,,7/25/21,,
 4JRS21,20,Lag,36.1, LAST,,,,,
 4JRS21,21,Ch,37.8, LAST,,,,,
 4JRS21,22,Covered,43.4, LAST,,,,,
 4JRS21,23,PL,43.9, LAST,,,,,8:56,8:57,,,,,
 4JRS21,24,Fp,44.6, LAST,5Y5/3,,,,,9:23,,,,,
 4JRS21,25,PL,47, LAST,2.5Y5/3,5Y4/3,,,9:34,9:36,9:41,9:53,9:55,,,
 4JRS21,26,Fp,48.3, LAST,2.5Y3/1,,,,,10:00,,,,,
 4JRS21,27,Ch,50, LAST,,,,,10:22,10:24,,,,,
 4JRS21,28,Fp,51.2, LAST,,,,,
 4JRS21,29,FpSand,52, LAST,,,,,
 4JRS21,30,Fp,53.5, LAST,,,,,

4JRS21,31,FpSand,55.2,LAST,,,,,,,,,
4JRS21,32,Fp,57.1,LAST,,,,,11:43,,,,,
4JRS21,33,FpSand,57.7,LAST,,,,,,,,,
4JRS21,34,PL,58,LAST,,,,,12:24,,,,,
4JRS21,35,Ch,60.6,LAST,,,,,,,,,

APPENDIX C

FOSSIL COUNTS

Fossil counts used to calculate probabilities of occurrence ('fossilCounts.csv' in R code inputs). 'section' is the measured column. Facies codes are as follows: Mire: mire. PL: pond/lake. Fp: floodplain mud. FpSand: floodplain sand. Lag: fluvial channel lag. Ch: fluvial channel bar. TiCh: tidally influenced channel bar. 'samplingUnit' is the interval that was searched for 5 minutes. 'SystemTract' is the nonmarine systems tract. Columns 5–21 are the categories of fossils scored for abundance. Codes beginning with 'P' correspond to plant fossils. Codes beginning with 'I' correspond with invertebrate fossils. Codes beginning with 'V' correspond to vertebrate fossils. 'Pcd': carbonaceous debris. 'Pa': amber. 'Pcw': carbonized wood. 'Pw': silicified wood. 'Ps': seed. 'Pim': leaf or wood impression. 'Ii': indeterminant shell hash. 'Ib': bivalve. 'Ig': gastropod. 'If': operculum. 'Vi': indeterminant vertebrate bone. 'Vt': tooth. 'Vgar': gar scale. 'Vturt': turtle shell. 'Vot': ossified tendon. 'Vcroc': crocodile scute. 'Vfish': fish vertebrae. The fossil abundance scale (from -1–3) is described in Table 1.

```
section, facies, samplingUnit, SystemTract, Pcd, Pa, Pcw, Pw, Ps, Pim, Ii, Ib, Ig, If, Vi, Vt, Vgar, Vturt, Vot, Vcroc, Vfish
2JRS21, PL, 1, HAST, 3, -1, -1, -1, -1, -1, -1, -1, -1, -1, 0, -1, 0, -1, -1, -1, -1
2JRS21, Lag, 2, HAST, -1, -1, 1, -1, -1, -1, 2.5, -1, -1, -1, -1, -1, -1, -1, -1, -1, -1
2JRS21, TiCh, 3, HAST, -1, -1, -1, -1, -1, -1, -1, -1, -1, -1, -1, -1, -1, -1, -1, -1, -1
2JRS21, TiCh, 4, HAST, -1, -1, -1, -1, -1, -1, -1, -1, -1, -1, -1, -1, -1, -1, -1, -1, -1
2JRS21, TiCh, 5, HAST, -1, -1, -1, -1, -1, -1, -1, -1, -1, -1, -1, -1, -1, -1, -1, -1, -1
2JRS21, Mire, 6, HAST, 3, -1, -1, -1, 0, -1, -1, -1, -1, -1, -1, -1, -1, -1, -1, -1, -1
2JRS21, PL, 7, HAST, NS, NS, NS, NS, NS, NS, -1, NS, NS, NS, NS, NS, NS, NS, NS, NS, NS
2JRS21, PL, 8, HAST, NS, NS, NS, NS, NS, NS, -1, NS, NS, NS, NS, NS, NS, NS, NS, NS, NS
2JRS21, PL, 9, HAST, 3, 0.5, -1, -1, -1, -1, -1, -1, -1, -1, -1, -1, -1, -1, -1, -1, -1
```

2JRS21, TiCh, 10, HAST, -1, -1, -1, -1, -1, -1, -1, -1, -1, -1, -1, -1, -1, -1, -1, -1, -1, -1
2JRS21, TiCh, 11, HAST, -1, 0, -1, 0, -1, -1, 0.5, -1, -1, -1, 0, -1, -1, 0, 0, -1, -1
2JRS21, TiCh, 12, HAST, -1, -1, -1, -1, -1, -1, 0, -1, -1, -1, 0, -1, -1, -1, -1, -1, -1
2JRS21, Fp, 13, HAST, 3, -1, -1, -1, -1, -1, -1, -1, -1, -1, 0, -1, -1, -1, -1, -1, -1
2JRS21, Fp, 14, HAST, 2.5, 0.5, -1, -1, -1, -1, -1, -1, -1, -1, -1, -1, -1, -1, -1, -1, -1
2JRS21, PL, 15, HAST, 3, -1, -1, -1, 0, -1, -1, -1, -1, -1, -1, -1, -1, -1, -1, -1, -1
2JRS21, Fp, 16, HAST, -1, -1, -1, 1.5, -1, -1, -1, -1, -1, -1, 0, -1, -1, -1, -1, -1, -1
2JRS21, FpSand, 17, HAST, 1.5, -1, -1, 1.5, -1, -1, -1, -1, -1, -1, 0, -1, -1, -1, -1, -1, -1
2JRS21, PL, 18, HAST, 3, -1, 1.5, 1, -1, -1, -1, -1, -1, -1, -1, -1, -1, -1, -1, -1, -1
2JRS21, TiCh, 19, HAST, 3, -1, -1, 0.5, -1, -1, -1, -1, -1, -1, 0.5, -1, -1, -1, -1, -1, -1
2JRS21, PL, 20, HAST, 3, -1, -1, -1, -1, -1, -1, -1, -1, -1, 0, -1, -1, -1, -1, -1, -1
2JRS21, Mire, 21, HAST, 3, 0.5, 0.5, -1, 0, -1, -1, -1, -1, -1, -1, -1, -1, -1, -1, -1, -1
2JRS21, PL, 22, HAST, 3, 0.5, 1, -1, -1, -1, -1, -1, -1, -1, -1, -1, -1, -1, -1, -1, -1
2JRS21, Mire, 23, HAST, 3, -1, 3, -1, -1, -1, -1, -1, -1, -1, -1, -1, -1, -1, -1, -1, -1
2JRS21, Lag, 24, HAST, -1, -1, 1.5, -1, -1, -1, -1, -1, -1, -1, 1.5, 0.5, -1, -1, -1, 0, -1
2JRS21, TiCh, 25, HAST, 3, -1, 2, -1, -1, -1, -1, -1, -1, -1, -1, -1, -1, -1, -1, -1, -1
2JRS21, TiCh, 26, HAST, 3, 0.5, -1, -1, -1, -1, -1, -1, -1, -1, -1, -1, -1, -1, -1, -1, -1
2JRS21, TiCh, 27, HAST, 3, 0, 0.5, -1, -1, 0.5, -1, -1, -1, -1, -1, -1, -1, -1, -1, -1, -1
2JRS21, TiCh, 28, HAST, 3, 0.5, -1, -1, -1, -1, -1, -1, -1, -1, -1, -1, -1, -1, -1, -1, -1
2JRS21, TiCh, 29, HAST, 3, 0, -1, 0, -1, -1, -1, -1, -1, -1, 0, -1, -1, -1, -1, -1, -1
2JRS21, TiCh, 30, HAST, 3, -1, -1, 0.5, -1, -1, -1, -1, -1, -1, -1, -1, -1, -1, -1, -1, -1
2JRS21, PL, 31, HAST, 3, -1, 0.5, 1.5, -1, -1, -1, -1, -1, -1, 1, -1, -1, -1, -1, 0, -1
2JRS21, Fp, 32, HAST, 2, -1, -1, 0.5, -1, -1, -1, -1, -1, -1, -1, -1, -1, -1, -1, -1, -1
2JRS21, Covered, 33, HAST, NS, NS, NS, NS, NS, NS, NS, NS, NS, NS, NS, NS, NS, NS, NS, NS
2JRS21, Mire, 34, HAST, 3, -1, -1, -1, -1, -1, -1, -1, -1, -1, -1, -1, -1, -1, -1, -1, -1
2JRS21, PL, 35, HAST, 3, -1, 0, -1, -1, -1, -1, -1, -1, -1, -1, -1, -1, -1, -1, -1, -1
2JRS21, PL, 36, HAST, NS, NS, NS, NS, NS, NS, NS, NS, NS, NS, NS, NS, NS, NS, NS, NS
2JRS21, Mire, 36, HAST, 3, -1, 3, -1, -1, -1, -1, -1, -1, -1, -1, -1, -1, -1, -1, -1, -1
2JRS21, Covered, 37, HAST, NS, NS, NS, NS, NS, NS, NS, NS, NS, NS, NS, NS, NS, NS, NS, NS
2JRS21, Msh, 38, HAST, -1, -1, -1, -1, -1, -1, -1, 3, -1, -1, -1, -1, -1, -1, -1, -1, -1
3JRS21, FpSand, 1, LAST, 0, -1, -1, -1, -1, -1, -1, -1, -1, -1, -1, -1, -1, -1, -1, -1
3JRS21, FpSand, 2, LAST, 2, -1, -1, -1, -1, -1, -1, -1, -1, -1, -1, -1, -1, -1, -1, -1
3JRS21, Mire, 3, LAST, 3, -1, -1, -1, 0, -1, -1, -1, -1, -1, -1, -1, -1, -1, -1, -1
3JRS21, Mire, 4, LAST, 3, -1, -1, -1, -1, -1, -1, -1, -1, -1, -1, -1, -1, -1, -1, -1
3JRS21, Covered, 5, LAST, NS, NS, NS, NS, NS, NS, NS, NS, NS, NS, NS, NS, NS, NS, NS, NS
3JRS21, PLi, 6, LAST, 2, -1, -1, -1, -1, -1, -1, 1, -1, -1, -1, -1, -1, -1, -1, -1
3JRS21, FpSand, 7, LAST, -1, -1, -1, -1, -1, -1, -1, -1, -1, -1, -1, -1, -1, -1, -1, -1
3JRS21, Fp, 8, LAST, 1, -1, -1, -1, -1, -1, -1, -1, -1, -1, -1, -1, -1, -1, -1, -1
3JRS21, Ch, 9, LAST, -1, -1, -1, -1, -1, -1, -1, -1, -1, -1, -1, -1, -1, -1, -1, -1
3JRS21, Ch, 10, LAST, NS, NS, NS, NS, NS, NS, NS, NS, NS, NS, NS, NS, NS, NS, NS, NS
3JRS21, Ch, 11, LAST, -1, -1, -1, -1, -1, -1, -1, -1, -1, -1, 0, -1, -1, -1, -1, -1
3JRS21, Ch, 12, LAST, -1, -1, -1, -1, -1, -1, -1, -1, -1, -1, -1, -1, -1, -1, -1, -1
3JRS21, Ch, 13, LAST, -1, -1, -1, -1, -1, -1, -1, -1, -1, -1, 0, -1, -1, -1, -1, -1
3JRS21, Ch, 14, LAST, -1, -1, -1, -1, -1, -1, -1, -1, -1, -1, 0.5, 0, 0, -1, -1, -1, -1
3JRS21, Ch, 15, LAST, -1, -1, -1, -1, -1, -1, -1, -1, -1, -1, 1, -1, -1, -1, -1, -1
3JRS21, Ch, 16, LAST, -1, -1, -1, -1, -1, -1, -1, -1, -1, -1, 1, -1, -1, -1, -1, -1
3JRS21, Ch, 17, LAST, -1, -1, -1, -1, -1, -1, -1, -1, -1, -1, -1, -1, -1, -1, -1, -1
3JRS21, Ch, 18, LAST, 2, -1, -1, -1, -1, -1, 2, -1, -1, -1, 1.5, 0, -1, -1, -1, -1
3JRS21, Covered, 19, LAST, NS, NS, NS, NS, NS, NS, NS, NS, NS, NS, NS, NS, NS, NS, NS, NS
3JRS21, Ch, 20, LAST, -1, -1, -1, -1, -1, -1, -1, -1, -1, -1, -1, -1, -1, -1, -1, -1

3JRS21, TiCh, 71, HAST, -1, -1, -1, -1, -1, -1, 1.5, -1, -1, -1, 0.5, -1, -1, -1, -1, -1, -1
3JRS21, TiCh, 72, HAST, 3, -1, -1, -1, -1, -1, 1, -1, 0, -1, 0, 0, -1, -1, -1, -1, -1
3JRS21, TiCh, 73, HAST, 3, -1, -1, -1, -1, -1, 1, -1, -1, -1, -1, -1, -1, -1, -1, -1
3JRS21, TiCh, 74, HAST, 0, -1, -1, -1, -1, -1, 0.5, -1, -1, -1, -1, -1, -1, -1, -1, -1
3JRS21, TiCh, 75, HAST, 0.5, -1, -1, -1, -1, -1, 0, -1, -1, -1, -1, -1, -1, -1, -1, -1
3JRS21, TiCh, 76, HAST, -1, -1, -1, -1, -1, -1, 1, -1, -1, -1, 0.5, -1, -1, -1, -1, -1
3JRS21, PLi, 77, HAST, 1, -1, -1, -1, -1, -1, 1.5, -1, -1, -1, 0, -1, -1, -1, -1, -1
3JRS21, PLi, 78, HAST, 1, -1, -1, -1, -1, -1, 1.5, -1, -1, -1, -1, -1, -1, -1, -1, -1
3JRS21, PL, 79, HAST, 2.5, -1, -1, -1, -1, -1, 2.5, -1, -1, -1, -1, -1, -1, -1, -1, -1
3JRS21, FpSand, 80, HAST, NS, NS, NS, NS, NS, NS, NS, NS, NS, NS, NS, NS, NS, NS, NS, NS
3JRS21, Fp, 81, HAST, 2, -1, -1, 0.5, -1, -1, -1, -1, -1, -1, -1, -1, -1, -1, -1, -1
3JRS21, Fp, 82, HAST, 2, -1, -1, 0.5, -1, -1, -1, -1, -1, -1, -1, -1, -1, -1, -1, -1
3JRS21, FpSand, 83, HAST, -1, -1, -1, 0.5, -1, -1, -1, -1, -1, -1, -1, -1, -1, -1, -1, -1
3JRS21, Fp, 84, HAST, -1, -1, -1, 0.5, -1, -1, -1, -1, -1, -1, 0, -1, -1, -1, -1, -1
3JRS21, Fp, 85, HAST, -1, -1, -1, 0, -1, -1, -1, -1, -1, -1, 0.5, -1, -1, 0, -1, -1, -1
3JRS21, Fp, 86, HAST, -1, -1, -1, -1, -1, -1, -1, -1, -1, -1, 0, -1, -1, -1, -1, -1
3JRS21, Fp, 87, HAST, 1.5, -1, -1, -1, -1, -1, -1, -1, -1, -1, 0.5, -1, -1, -1, -1, -1
3JRS21, FpSand, 88, HAST, -1, -1, -1, -1, -1, -1, -1, -1, -1, -1, -1, -1, -1, -1, -1, -1
3JRS21, PLi, 89, HAST, -1, -1, -1, -1, -1, -1, 1, -1, -1, -1, 0, -1, -1, -1, -1, -1
3JRS21, PLi, 90, HAST, 2.5, -1, -1, -1, -1, -1, 1, -1, -1, -1, 0.5, -1, -1, -1, -1, -1
3JRS21, PLi, 91, HAST, -1, -1, -1, -1, -1, -1, 1, -1, -1, -1, -1, -1, -1, -1, -1, -1
3JRS21, PLi, 92, HAST, 1.5, -1, -1, -1, -1, -1, 2, -1, -1, -1, -1, -1, -1, -1, -1, -1
3JRS21, Fp, 93, HAST, 2, -1, -1, -1, -1, -1, -1, -1, -1, -1, 0.5, 0, -1, -1, -1, -1, -1
3JRS21, Covered, 94, HAST, NS, NS, NS, NS, NS, NS, NS, NS, NS, NS, NS, NS, NS, NS, NS, NS
3JRS21, PL, 95, HAST, 2.5, -1, 0, -1, -1, -1, 1.5, -1, -1, -1, 0, -1, -1, -1, -1, -1, -1
3JRS21, PL, 96, HAST, 1.5, -1, 0.5, -1, -1, -1, 0.5, -1, -1, -1, 0, -1, -1, -1, -1, -1, -1
3JRS21, PLi, 97, HAST, 1, -1, -1, -1, -1, -1, 0, -1, -1, -1, 0.5, -1, -1, -1, -1, -1, -1
3JRS21, TiCh, 98, HAST, 3, -1, -1, 0.5, -1, -1, -1, -1, -1, -1, 0.5, 0, -1, -1, -1, -1, -1
3JRS21, TiCh, 99, HAST, 3, -1, -1, -1, -1, -1, 0, -1, -1, -1, 0.5, -1, -1, -1, -1, 0, -1
3JRS21, TiCh, 100, HAST, -1, -1, -1, -1, -1, -1, -1, -1, -1, -1, -1, -1, -1, -1, -1, -1
3JRS21, Fp, 101, HAST, 2.5, -1, -1, -1, -1, -1, -1, -1, -1, -1, -1, -1, -1, -1, -1, -1
3JRS21, Fp, 102, HAST, 0.5, -1, -1, -1, -1, -1, -1, -1, -1, -1, -1, -1, -1, -1, -1, -1
3JRS21, Mire, 103, HAST, 2.5, -1, -1, -1, -1, -1, -1, -1, -1, -1, -1, -1, -1, -1, -1, -1
3JRS21, Fp, 104, HAST, 0.5, -1, 0, -1, -1, -1, -1, -1, -1, -1, 0, -1, -1, -1, -1, -1, -1
3JRS21, Fp, 105, HAST, 1, -1, -1, -1, -1, -1, -1, -1, -1, -1, 0.5, -1, -1, -1, -1, 0, -1
3JRS21, Fp, 106, HAST, 0.5, -1, -1, -1, -1, -1, -1, -1, -1, -1, 0, -1, -1, -1, -1, -1, -1
3JRS21, PL, 107, HAST, 2.5, -1, -1, -1, -1, -1, -1, -1, -1, -1, 0, -1, -1, -1, -1, -1, -1
3JRS21, Fp, 108, HAST, -1, -1, -1, -1, -1, -1, -1, -1, -1, -1, 0.5, -1, -1, -1, -1, -1, -1
3JRS21, PLi, 109, HAST, 1.5, -1, -1, -1, -1, -1, 0.5, -1, -1, -1, 0.5, -1, -1, -1, -1, -1, -1
3JRS21, FpSand, 110, HAST, -1, -1, -1, -1, -1, -1, -1, 3, -1, -1, -1, -1, -1, -1, -1, -1, -1
3JRS21, PLi, 111, HAST, 0.5, -1, -1, -1, -1, -1, -1, 1, -1, -1, 0.5, 0, -1, 0, -1, -1, -1, -1
3JRS21, PLi, 112, HAST, 0.5, -1, -1, -1, -1, -1, 0, -1, -1, -1, 0.5, 0, -1, -1, -1, -1, -1
3JRS21, Fp, 113, HAST, 1.5, -1, -1, -1, -1, -1, -1, -1, -1, -1, 0.5, 0, -1, -1, -1, -1, -1
3JRS21, Fp, 114, HAST, 0.5, -1, -1, -1, -1, -1, -1, -1, -1, -1, 0, -1, -1, -1, -1, -1, -1
3JRS21, Covered, 115, HAST, NS, NS, NS, NS, NS, NS, NS, NS, NS, NS, NS, NS, NS, NS, NS, NS
3JRS21, Fp, 116, HAST, 2, 0, -1, -1, -1, -1, -1, -1, -1, -1, -1, -1, -1, -1, -1, -1, -1
3JRS21, PLi, 117, HAST, 0.5, -1, 0.5, -1, -1, -1, 0.5, -1, -1, -1, -1, -1, -1, -1, -1, -1, -1
3JRS21, Fp, 118, HAST, -1, -1, -1, -1, -1, -1, -1, -1, -1, -1, -1, -1, -1, -1, -1, -1, -1
3JRS21, Fp, 119, HAST, NS, NS, NS, NS, NS, NS, NS, NS, NS, NS, NS, NS, NS, NS, NS, NS
3JRS21, Fp, 120, HAST, NS, NS, NS, NS, NS, NS, NS, NS, NS, NS, NS, NS, NS, NS, NS, NS

3JRS21,Ch,121,HAST,-1,-1,-1,-1,-1,-1,-1,-1,-1,-1,-1,-1,-1,-1,-1,-1,-1,-1
3JRS21,Ch,122,HAST,-1,-1,-1,-1,-1,-1,-1,-1,-1,-1,-1,-1,-1,-1,-1,-1,-1,-1
3JRS21,Fp,123,HAST,-1,-1,-1,0,-1,-1,-1,-1,-1,-1,-1,-1,-1,-1,-1,-1,-1,-1
3JRS21,Fp,124,HAST,-1,-1,-1,-1,-1,-1,-1,-1,-1,-1,-1,-1,-1,-1,-1,-1,-1,-1
3JRS21,PL,125,HAST,2.5,-1,-1,-1,0,-1,-1,-1,-1,-1,-1,-1,-1,-1,-1,-1,-1,-1
3JRS21,Covered,126,HAST,NS,NS,NS,NS,NS,NS,NS,NS,NS,NS,NS,NS,NS,NS,NS,NS,NS
3JRS21,PL,127,HAST,3,1,1,-1,-1,-1,-1,-1,-1,-1,-1,-1,-1,-1,-1,-1,-1,-1
3JRS21,Mire,128,HAST,3,-1,1.5,-1,-1,-1,-1,-1,-1,-1,-1,-1,-1,-1,-1,-1,-1
3JRS21,Covered,129,HAST,NS,NS,NS,NS,NS,NS,NS,NS,NS,NS,NS,NS,NS,NS,NS,NS,NS
3JRS21,PL,130,HAST,3,1,0,-1,-1,-1,-1,-1,-1,-1,-1,-1,-1,-1,-1,-1,-1,-1
3JRS21,PL,131,HAST,2.5,-1,-1,-1,-1,-1,-1,-1,-1,-1,-1,-1,-1,-1,-1,-1,-1,-1
3JRS21,Mire,132,HAST,3,1,3,-1,-1,-1,-1,-1,-1,-1,-1,-1,-1,-1,-1,-1,-1,-1
3JRS21,Mire,133,HAST,3,0.5,3,0,-1,-1,-1,-1,-1,-1,-1,-1,-1,-1,-1,-1,-1,-1
3JRS21,PL,134,HAST,3,-1,-1,-1,-1,-1,-1,-1,-1,-1,-1,-1,-1,-1,-1,-1,-1,-1
3JRS21,Fp,135,HAST,0.5,-1,-1,-1,-1,-1,-1,-1,-1,-1,-1,-1,-1,-1,-1,-1,-1,-1
3JRS21,Fp,136,HAST,1.5,-1,-1,0,-1,-1,-1,-1,-1,-1,-1,-1,-1,-1,-1,-1,-1,-1
3JRS21,Fp,137,HAST,1.5,-1,-1,0,-1,-1,-1,-1,-1,-1,-1,-1,-1,-1,-1,-1,-1,-1
3JRS21,PL,138,HAST,3,-1,-1,-1,-1,-1,-1,-1,-1,-1,-1,-1,-1,-1,-1,-1,-1,-1
3JRS21,Mire,139,HAST,3,-1,3,0,-1,-1,-1,-1,-1,-1,-1,-1,-1,-1,-1,-1,-1,-1
3JRS21,Fp,140,HAST,2,-1,-1,-1,-1,-1,-1,-1,-1,-1,-1,-1,-1,-1,-1,-1,-1,-1
3JRS21,FpSand,141,HAST,3,-1,-1,-1,-1,-1,-1,-1,-1,-1,-1,-1,-1,-1,-1,-1,-1,-1
3JRS21,PL,142,HAST,3,-1,-1,-1,-1,-1,-1,-1,-1,-1,-1,-1,-1,-1,-1,-1,-1,-1
3JRS21,Mire,143,HAST,3,-1,-1,-1,-1,-1,-1,-1,-1,-1,-1,-1,-1,-1,-1,-1,-1,-1
3JRS21,Ch,144,HAST,-1,-1,-1,-1,-1,-1,-1,-1,-1,-1,-1,-1,-1,-1,-1,-1,-1,-1
3JRS21,Ch,145,HAST,-1,-1,-1,-1,-1,-1,-1,-1,-1,-1,-1,-1,-1,-1,-1,-1,-1,-1
3JRS21,Ch,146,HAST,-1,-1,-1,0,-1,-1,-1,-1,-1,-1,-1,-1,-1,-1,-1,-1,-1,-1
3JRS21,Ch,147,HAST,-1,-1,-1,0,-1,-1,-1,-1,-1,-1,-1,-1,-1,-1,-1,-1,-1,-1
3JRS21,Ch,148,HAST,-1,-1,-1,-1,-1,-1,-1,-1,-1,-1,-1,-1,-1,-1,-1,-1,-1,-1
3JRS21,Ch,149,HAST,-1,-1,-1,-1,-1,-1,-1,-1,-1,-1,-1,-1,-1,-1,-1,-1,-1,-1
3JRS21,TiCh,150,HAST,-1,-1,-1,0,-1,-1,-1,-1,-1,-1,-1,-1,-1,-1,-1,-1,-1,-1
3JRS21,TiCh,151,HAST,-1,-1,-1,-1,-1,-1,-1,-1,-1,-1,-1,-1,-1,-1,-1,-1,-1,-1
3JRS21,TiCh,152,HAST,3,-1,-1,-1,-1,-1,-1,-1,-1,-1,-1,-1,-1,-1,-1,-1,-1,-1
3JRS21,TiCh,153,HAST,-1,-1,-1,-1,-1,-1,-1,-1,-1,-1,-1,-1,-1,-1,-1,-1,-1,-1
3JRS21,TiCh,154,HAST,3,-1,-1,-1,-1,-1,-1,-1,-1,-1,-1,-1,-1,-1,-1,-1,-1,-1
3JRS21,TiCh,155,HAST,-1,-1,-1,-1,-1,-1,-1,-1,-1,-1,-1,-1,-1,-1,-1,-1,-1,-1
3JRS21,TiCh,156,HAST,-1,-1,-1,-1,-1,-1,-1,-1,-1,-1,-1,-1,-1,-1,-1,-1,-1,-1
3JRS21,Msh,157,HAST,-1,-1,-1,-1,-1,-1,-1,-1,3,-1,-1,-1,-1,-1,-1,-1,-1,-1
1JRW21,Fp,1,LAST,-1,-1,-1,-1,-1,-1,-1,-1,-1,-1,-1,-1,-1,-1,-1,-1,-1,-1
1JRW21,Fp,2,LAST,-1,-1,-1,-1,-1,-1,-1,-1,-1,-1,-1,-1,-1,-1,-1,-1,-1,-1
1JRW21,Fp,3,LAST,0.5,-1,-1,-1,-1,-1,-1,-1,-1,-1,0,-1,-1,-1,-1,-1,-1,-1
1JRW21,PLi,4,LAST,2,-1,-1,-1,-1,-1,3,-1,-1,-1,-1,-1,-1,-1,-1,-1,-1,-1
1JRW21,FpSand,5,LAST,0,-1,-1,-1,-1,-1,2,-1,-1,-1,-1,-1,-1,-1,-1,-1,-1,-1
1JRW21,Fp,6,LAST,-1,-1,-1,-1,-1,-1,-1,-1,-1,-1,1,0,-1,0,-1,-1,-1,-1
1JRW21,Fp,7,LAST,1,-1,-1,-1,-1,-1,-1,-1,-1,-1,1,-1,-1,-1,-1,-1,-1,-1
1JRW21,FpSand,8,LAST,1,-1,0,-1,-1,-1,-1,-1,-1,-1,1,-1,-1,-1,-1,-1,-1,-1
1JRW21,Fp,9,LAST,1.5,-1,-1,-1,-1,-1,-1,-1,-1,-1,0.5,-1,-1,-1,-1,-1,-1,-1
1JRW21,Fp,10,LAST,1,-1,-1,-1,-1,-1,-1,-1,-1,-1,1,-1,-1,-1,-1,-1,-1,-1
1JRW21,FpSand,11,LAST,0.5,-1,-1,-1,-1,-1,-1,-1,-1,-1,0.5,0,-1,-1,-1,-1,0
1JRW21,Fp,12,LAST,1.5,-1,1,-1,-1,-1,-1,-1,-1,-1,-1,-1,-1,-1,-1,-1,-1
1JRW21,Fp,13,LAST,1,0,-1,-1,-1,-1,-1,-1,-1,-1,0.5,-1,-1,-1,-1,-1,-1,-1

1JRW21, Fp, 14, LAST, 0.5, -1, -1, -1, -1, -1, -1, -1, -1, -1, -1, -1, -1, -1, -1, -1, -1, -1
1JRW21, FpSand, 15, LAST, -1, -1, -1, -1, -1, -1, -1, -1, -1, -1, -1, 0, -1, -1, -1, -1, -1, -1
1JRW21, Fp, 16, HAST, 1, -1, -1, -1, -1, -1, -1, -1, -1, -1, 0, -1, -1, -1, -1, -1, -1
1JRW21, PL, 17, HAST, 2.5, -1, -1, -1, -1, -1, -1, -1, -1, -1, 0.5, -1, -1, -1, -1, -1, -1
1JRW21, PL, 18, HAST, 1, 0, 0, 0, -1, -1, -1, -1, -1, -1, 0, -1, -1, -1, -1, -1, -1
1JRW21, PL, 19, HAST, 2, -1, 0, -1, -1, -1, -1, -1, -1, -1, 0.5, -1, -1, -1, -1, -1, -1
1JRW21, PL, 20, HAST, -1, -1, -1, -1, -1, -1, -1, -1, -1, -1, 0, -1, -1, -1, -1, -1, -1
1JRW21, Covered, 21, HAST, NS, NS, NS, NS, NS, NS, NS, NS, NS, NS, NS, NS, NS, NS, NS, NS, NS
1JRW21, PL, 22, HAST, 3, 0, 1, -1, -1, -1, -1, -1, -1, -1, -1, -1, -1, -1, -1, -1, -1
1JRW21, Mire, 23, HAST, 3, -1, 3, -1, -1, -1, -1, -1, -1, -1, -1, -1, -1, -1, -1, -1, -1
1JRW21, PL, 24, HAST, 3, 1, 3, -1, -1, -1, -1, -1, -1, -1, -1, -1, -1, -1, -1, -1, -1
1JRW21, PL, 25, HAST, 3, -1, 1, -1, -1, -1, 2, -1, -1, -1, -1, -1, -1, -1, -1, 0, -1
1JRW21, PL, 26, HAST, 0.5, -1, -1, -1, -1, -1, 1.5, -1, -1, -1, -1, -1, -1, -1, -1, -1, -1
1JRW21, PL, 27, HAST, -1, -1, -1, -1, -1, -1, 1, -1, -1, -1, 0.5, -1, -1, -1, -1, -1, -1
1JRW21, FpSand, 28, HAST, -1, -1, -1, -1, -1, -1, -1, -1, -1, -1, -1, -1, -1, -1, -1, -1, -1
1JRW21, FpSand, 29, HAST, -1, -1, -1, -1, -1, -1, -1, -1, -1, -1, -1, -1, -1, -1, -1, -1, -1
1JRW21, Fp, 30, HAST, -1, -1, -1, -1, -1, -1, -1, -1, -1, -1, -1, -1, -1, -1, -1, -1, -1
1JRW21, Ch, 31, HAST, -1, -1, -1, -1, -1, -1, -1, -1, -1, -1, -1, -1, -1, -1, -1, -1, -1
1JRW21, Ch, 32, HAST, -1, -1, 0, -1, -1, -1, 0, -1, -1, -1, -1, -1, -1, -1, -1, -1, -1
1JRW21, Ch, 33, HAST, -1, -1, -1, -1, -1, -1, 0, -1, -1, -1, -1, -1, -1, -1, -1, -1, -1
1JRW21, Ch, 34, HAST, -1, -1, -1, -1, -1, -1, -1, -1, -1, -1, -1, -1, -1, -1, -1, -1, -1
1JRW21, Ch, 35, HAST, NS, NS, NS, NS, NS, NS, NS, NS, NS, NS, NS, NS, NS, NS, NS, NS, NS
1JRW21, Fp, 36, HAST, -1, -1, 0, -1, -1, -1, -1, -1, -1, -1, -1, -1, -1, -1, -1, -1, -1
1JRW21, PL, 37, HAST, 2.5, -1, -1, -1, -1, -1, -1, -1, -1, -1, -1, -1, -1, -1, -1, -1, -1
1JRW21, PL, 38, HAST, 3, 0.5, 0.5, -1, -1, -1, -1, -1, -1, -1, -1, -1, -1, -1, -1, -1, -1
1JRW21, PL, 39, HAST, 3, 0, 1, -1, -1, -1, -1, -1, -1, -1, -1, -1, -1, -1, -1, -1, -1
1JRW21, Mire, 40, HAST, 3, -1, 3, -1, -1, -1, -1, -1, -1, -1, -1, -1, -1, -1, -1, -1, -1
1JRW21, Fp, 41, HAST, 2, -1, -1, -1, -1, -1, -1, -1, -1, -1, 0, -1, -1, -1, -1, -1, -1
1JRW21, PL, 42, HAST, 3, 1, 2, -1, -1, -1, -1, -1, -1, -1, -1, -1, -1, -1, -1, -1, -1
1JRW21, Fp, 43, HAST, NS, NS, NS, NS, NS, NS, NS, NS, NS, NS, NS, NS, NS, NS, NS, NS, NS
1JRW21, Fp, 44, HAST, NS, NS, NS, NS, NS, NS, NS, NS, NS, NS, NS, NS, NS, NS, NS, NS, NS
1JRW21, PL, 45, HAST, NS, NS, NS, NS, NS, NS, NS, NS, NS, NS, NS, NS, NS, NS, NS, NS, NS
1JRW21, Fp, 46, HAST, NS, NS, NS, NS, NS, NS, NS, NS, NS, NS, NS, NS, NS, NS, NS, NS, NS
1JRW21, PL, 47, HAST, 3, 0.5, -1, -1, -1, -1, -1, -1, -1, -1, -1, -1, -1, -1, -1, -1, -1
1JRW21, Mire, 48, HAST, 3, -1, 3, -1, -1, -1, -1, -1, -1, -1, -1, -1, -1, -1, -1, -1, -1
1JRW21, Covered, 49, HAST, NS, NS, NS, NS, NS, NS, NS, NS, NS, NS, NS, NS, NS, NS, NS, NS, NS
1JRW21, PL, 50, HAST, 3, 0.5, -1, -1, -1, -1, -1, -1, -1, -1, -1, -1, -1, -1, -1, -1, -1
1JRW21, PL, 51, HAST, NS, NS, NS, NS, NS, NS, NS, NS, NS, NS, NS, NS, NS, NS, NS, NS, NS
1JRW21, Covered, 52, HAST, NS, NS, NS, NS, NS, NS, NS, NS, NS, NS, NS, NS, NS, NS, NS, NS, NS
1JRS21, Ch, 1, LAST, 0.5, -1, -1, -1, -1, -1, 3, -1, -1, -1, 0, 0, -1, -1, -1, -1, -1
1JRS21, Lag, 2, LAST, -1, -1, -1, 0.5, -1, -1, -1, 3, 3, -1, 0, -1, -1, -1, -1, -1, -1
1JRS21, Ch, 3, LAST, -1, -1, -1, -1, -1, -1, -1, -1, -1, -1, -1, -1, -1, -1, -1, -1, -1
1JRS21, Ch, 4, LAST, -1, -1, -1, -1, -1, -1, -1, -1, -1, -1, -1, -1, -1, -1, -1, -1, -1
3JRW21, Mire, 1, HAST, 3, -1, 3, -1, 0, -1, -1, -1, -1, -1, -1, -1, -1, -1, -1, -1, -1
3JRW21, PLi, 2, HAST, 1, -1, -1, -1, -1, -1, -1, 1, -1, -1, 0.5, -1, -1, -1, -1, -1, -1
3JRW21, Fp, 3, HAST, 1, -1, -1, -1, -1, -1, -1, -1, -1, -1, -1, -1, -1, -1, -1, -1, -1
3JRW21, Fp, 4, HAST, -1, -1, -1, -1, -1, -1, -1, -1, -1, -1, 0, -1, -1, -1, -1, -1, -1
3JRW21, Fp, 5, HAST, -1, -1, -1, -1, -1, -1, -1, -1, -1, -1, -1, -1, -1, -1, -1, -1, -1
3JRW21, PLi, 6, HAST, 1, -1, 0, -1, -1, -1, -1, 1, -1, -1, -1, -1, -1, -1, -1, -1, -1
3JRW21, TiCh, 7, HAST, 2, -1, -1, -1, -1, -1, 3, 1, -1, -1, -1, -1, -1, -1, -1, -1, -1

3JRW21,TiCh,8,HAST,-1,-1,-1,-1,-1,-1,0.5,-1,-1,-1,0,-1,-1,-1,-1,-1,-1
3JRW21,TiCh,9,HAST,-1,-1,-1,-1,-1,-1,1.5,-1,-1,-1,-1,-1,-1,-1,-1,-1,-1
3JRW21,TiCh,10,HAST,-1,-1,-1,-1,-1,-1,-1,-1,-1,-1,-1,-1,-1,-1,-1,-1
3JRW21,TiCh,11,HAST,-1,-1,-1,-1,-1,-1,-1,-1,-1,-1,-1,-1,-1,-1,-1,-1
3JRW21,Fp,12,HAST,1.5,-1,-1,-1,-1,-1,-1,-1,-1,-1,-1,-1,-1,-1,-1,-1
3JRW21,Fp,13,HAST,-1,-1,-1,-1,-1,-1,-1,-1,-1,-1,-1,-1,-1,-1,-1,-1
3JRW21,PL,14,HAST,3,1,0.5,-1,-1,-1,-1,-1,-1,-1,-1,-1,-1,-1,-1,-1
3JRW21,PL,15,HAST,3,0,-1,-1,-1,-1,-1,-1,-1,-1,-1,-1,-1,-1,-1,-1
3JRW21,Mire,16,HAST,3,-1,3,-1,-1,-1,-1,-1,-1,-1,-1,-1,-1,-1,-1,-1
3JRW21,PL,17,HAST,3,-1,0.5,-1,-1,-1,-1,-1,-1,-1,-1,-1,-1,-1,-1,-1
4JRW21,PLi,1,LAST,-1,-1,-1,-1,-1,-1,-1,-1,-1,-1,0,-1,-1,-1,-1,-1,-1
4JRW21,PLi,2,LAST,-1,-1,-1,-1,-1,-1,-1,-1,-1,-1,-1,-1,-1,-1,-1,-1
4JRW21,FpSand,3,LAST,-1,-1,-1,-1,-1,-1,-1,-1,-1,-1,-1,-1,-1,-1,-1,-1
4JRW21,FpSand,4,LAST,-1,-1,-1,0,-1,-1,-1,-1,-1,-1,1,0,0,-1,-1,-1,0
4JRW21,PLi,5,LAST,1,-1,-1,-1,-1,-1,-1,-1,-1,-1,1,0,0,-1,-1,-1,-1
4JRW21,PLi,6,LAST,-1,-1,-1,-1,-1,-1,-1,-1,-1,-1,1,0,-1,-1,-1,-1,-1
4JRW21,PLi,7,LAST,-1,-1,-1,-1,-1,-1,-1,-1,-1,-1,0,1,-1,0.5,-1,-1,-1,-1
4JRW21,PLi,8,LAST,-1,-1,-1,-1,-1,-1,-1,-1,-1,-1,0,1,-1,0,-1,-1,-1,-1
4JRW21,PLi,9,LAST,0,-1,-1,-1,-1,-1,-1,-1,-1,-1,1.5,0.5,1,-1,-1,-1,-1
4JRW21,PLi,10,LAST,-1,-1,-1,-1,-1,-1,-1,-1,-1,0,1,-1,1,-1,-1,-1,0
4JRW21,Lag,11,LAST,2.5,-1,-1,-1,-1,-1,2,1.5,-1,-1,0.5,-1,0.5,-1,-1,-1,0
4JRW21,FpSand,12,LAST,-1,-1,-1,-1,-1,-1,-1,-1,-1,-1,0.5,-1,-1,-1,-1,-1,-1
4JRW21,Fp,13,HAST,1,-1,-1,-1,-1,-1,-1,-1,-1,-1,0.5,-1,-1,-1,-1,-1,-1
4JRW21,Fp,14,HAST,0.5,-1,-1,-1,-1,-1,-1,-1,-1,-1,1,-1,-1,-1,-1,-1,-1
4JRW21,FpSand,15,HAST,1.5,-1,-1,-1,-1,-1,-1,-1,-1,-1,0.5,-1,-1,-1,-1,-1,-1
4JRW21,Fp,16,HAST,1,-1,-1,-1,-1,-1,-1,-1,-1,-1,0.5,-1,-1,-1,-1,-1,-1
4JRW21,Fp,17,HAST,1,-1,-1,-1,-1,-1,-1,-1,-1,-1,-1,-1,-1,-1,-1,-1
4JRW21,PL,18,HAST,3,-1,0.5,0,-1,-1,-1,-1,-1,-1,0,0,0,-1,-1,-1,-1
4JRW21,FpSand,19,HAST,-1,-1,-1,-1,-1,-1,0.5,-1,-1,-1,0.5,-1,-1,-1,-1,-1,-1
4JRW21,PL,20,HAST,3,0,1,-1,-1,-1,-1,-1,-1,-1,0,-1,-1,-1,-1,-1,-1
4JRW21,Mire,21,HAST,3,-1,3,-1,-1,-1,-1,-1,-1,-1,-1,-1,-1,-1,-1,-1
4JRW21,PL,22,HAST,3,0.5,1,-1,-1,-1,0.5,-1,-1,-1,0.5,-1,-1,-1,-1,-1,-1
4JRW21,PL,23,HAST,3,-1,-1,-1,-1,-1,-1,-1,-1,-1,0,-1,-1,-1,-1,-1,-1
4JRW21,FpSand,24,HAST,2,-1,-1,-1,-1,-1,-1,0.5,-1,-1,0,-1,-1,-1,-1,-1,-1
4JRW21,FpSand,25,HAST,-1,-1,-1,-1,-1,-1,1,-1,-1,-1,-1,-1,-1,-1,-1,-1
4JRW21,PLi,26,HAST,1.5,-1,-1,-1,-1,-1,1.5,-1,-1,-1,0.5,-1,-1,-1,-1,-1,-1
4JRW21,PLi,27,HAST,1.5,-1,-1,-1,-1,-1,1,-1,0,-1,-1,-1,-1,-1,-1,-1
4JRW21,FpSand,28,HAST,-1,-1,-1,-1,-1,-1,-1,-1,-1,-1,-1,-1,-1,-1,-1,-1
4JRW21,Fp,29,HAST,NS,NS,NS,NS,NS,NS,NS,NS,NS,NS,NS,NS,NS,NS,NS,NS
4JRW21,FpSand,30,HAST,-1,-1,-1,-1,-1,-1,-1,-1,-1,-1,-1,-1,-1,-1,-1,-1
4JRW21,FpSand,31,HAST,NS,NS,NS,NS,NS,NS,NS,NS,NS,NS,NS,NS,NS,NS,NS,NS
4JRW21,Fp,32,HAST,NS,NS,NS,NS,NS,NS,NS,NS,NS,NS,NS,NS,NS,NS,NS,NS
4JRW21,Fp,33,HAST,1,-1,-1,-1,-1,-1,-1,-1,-1,-1,0,-1,-1,-1,-1,-1,-1
4JRW21,PL,34,HAST,3,0.5,-1,-1,-1,-1,-1,-1,-1,-1,-1,-1,-1,-1,-1,-1
4JRW21,PL,35,HAST,3,0.5,-1,-1,-1,-1,-1,-1,-1,-1,-1,-1,-1,-1,-1,-1
4JRW21,PL,36,HAST,3,-1,0,-1,-1,-1,-1,-1,-1,-1,-1,-1,-1,-1,-1,-1
4JRW21,FpSand,37,HAST,3,-1,-1,-1,-1,-1,-1,-1,-1,-1,-1,-1,-1,-1,-1,-1
4JRW21,PL,38,HAST,3,-1,-1,-1,-1,-1,-1,-1,-1,-1,-1,-1,-1,-1,-1,-1
4JRW21,Fp,39,HAST,-1,-1,-1,-1,-1,-1,-1,-1,-1,-1,0,-1,-1,-1,-1,-1,-1
4JRW21,PL,40,HAST,NS,NS,NS,NS,NS,NS,NS,NS,NS,NS,NS,NS,NS,NS,NS,NS

4JRS21, Fp, 50, LAST, -1, -1, -1, -1, -1, -1, -1, -1, -1, -1, -1, 0, -1, -1, -1, -1, -1, -1
4JRS21, Ch, 51, LAST, -1, -1, -1, -1, -1, -1, 2, -1, -1, -1, 0.5, -1, -1, -1, -1, -1, -1
4JRS21, Ch, 52, LAST, -1, -1, -1, -1, -1, -1, -1, -1, -1, -1, -1, 0, -1, -1, -1, -1, -1, -1
4JRS21, Fp, 53, LAST, 0.5, -1, -1, -1, -1, -1, -1, -1, -1, -1, -1, 0.5, -1, -1, -1, -1, -1, -1
4JRS21, FpSand, 54, LAST, -1, -1, -1, -1, -1, -1, 2, -1, -1, -1, 0.5, -1, -1, -1, -1, -1, -1
4JRS21, Fp, 55, LAST, 1.5, -1, -1, -1, -1, -1, -1, -1, -1, -1, -1, -1, -1, -1, -1, -1, -1
4JRS21, Fp, 56, LAST, 1.5, -1, -1, -1, -1, -1, -1, -1, -1, -1, -1, -1, -1, -1, -1, -1, -1
4JRS21, FpSand, 57, LAST, -1, -1, -1, -1, -1, -1, -1, -1, -1, -1, -1, 0, -1, -1, -1, -1, -1, -1
4JRS21, FpSand, 58, LAST, -1, -1, -1, -1, -1, -1, -1, -1, -1, -1, -1, 0.5, -1, -1, -1, -1, -1, -1
4JRS21, Fp, 59, LAST, NS, NS, NS, NS, NS, NS, NS, NS, NS, NS, NS, NS, NS, NS, NS, NS, NS
4JRS21, Fp, 60, LAST, -1, -1, -1, -1, -1, -1, -1, -1, -1, -1, -1, 0.5, -1, -1, -1, -1, -1, -1
4JRS21, FpSand, 61, LAST, -1, -1, -1, -1, -1, -1, -1, -1, -1, -1, -1, -1, -1, -1, -1, -1, -1, -1
4JRS21, PL, 62, LAST, 2, -1, -1, -1, -1, -1, -1, 2.5, 2.5, -1, 0.5, -1, -1, -1, -1, -1, -1, -1
4JRS21, Ch, 63, LAST, -1, -1, -1, -1, -1, -1, 0, -1, -1, -1, 1.5, -1, -1, -1, -1, -1, -1, -1
4JRS21, Ch, 64, LAST, -1, -1, -1, -1, -1, -1, -1, -1, -1, -1, -1, 0.5, -1, -1, -1, -1, -1, -1
4JRS21, Ch, 65, LAST, -1, -1, -1, -1, -1, -1, -1, -1, -1, -1, -1, -1, -1, -1, -1, -1, -1, -1

APPENDIX D

COLUMN KEY

One final input file for the model contains a mapping mechanism to connect the facies codes, names, grain size, and color (expressed as hex RGB values) for plotting and other calculations ('JRFcolors.txt' in R code inputs). 'code' reflects the facies codes used when measuring columns. 'name' is the full name of the facies. 'grainSize' is an arbitrary value used to plot the width of rectangles in the simulated columns. 'isSurface' designates if the facies is a significant stratigraphic surface (i.e., sequence boundary). 'legendOrder' specifies the layout of the facies in the legend.

```
code,name,grainSize,color,isSurface,legendOrder
PL,Pond/Lake,2,"#C0D6D8",FALSE,2
FpSand,Floodplain sand,3,"#C1B47E",FALSE,4
Fp,Floodplain mud,2,"#A4A591",FALSE,3
Mire,Mire,2,"#434343",FALSE,1
Ch,Fluvial channel bar,3.5,"#F2BE7D",FALSE,6
TiCh,Tidally influenced channel bar,3.5,"#EEF2DF",FALSE,7
Lag,Fluvial channel lag,3.75,"#A7A9AC",FALSE,5
```

APPENDIX E

TRANSITION MATRICES

Transition matrices for the HAST (Table E1), LAST (Table E2), and comparison of HAST and LAST (Table E3). Calculations are based on data in Appendix B. Values correspond to the heat map figures 15 and 16. Tables referred to as ‘faciesTransitions’ in R code. Facies codes are as follows: Mire: mire. PL: pond/lake. Fp: floodplain mud. FpSand: floodplain sand. Lag: fluvial channel lag. Ch: fluvial channel bar. TiCh: tidally influenced channel bar.

Table E1. Transition probabilities for the HAST

	Ch	Fp	FpSand	Lag	Mire	PL	TiCh
Ch	0	0.6	0	0	0	0.2	0.2
Fp	0.067	0	0.267	0	0.033	0.633	0
FpSand	0	0.5	0	0	0	0.5	0
Lag	0	0	0	0	0	0	1
Mire	0.077	0.231	0	0.077	0	0.615	0
PL	0.049	0.293	0.195	0.024	0.293	0.024	0.122
TiCh	0	0.429	0	0	0.143	0.429	0

Table E2. Transition probabilities for the LAST

	Ch	Fp	FpSand	Lag	Mire	PL	TiCh
Ch	0	0.4	0	0.3	0	0.3	0
Fp	0.278	0	0.556	0.056	0	0.111	0
FpSand	0	0.533	0	0	0.133	0.333	0
Lag	0.8	0	0.2	0	0	0	0
Mire	0	1	0	0	0	0	0
PL	0.25	0.25	0.417	0.083	0	0	0
TiCh	0	0	0	0	0	0	0

Table E3. Transition probabilities for the HAST minus the LAST. Negative values indicate transitions are more common in the LAST. Positive values indicate transitions are more common in the HAST.

	Ch	Fp	FpSand	Lag	Mire	PL	TiCh
Ch	0	0.2	0	-0.3	0	-0.1	0.2
Fp	-0.211	0	-0.289	-0.056	0.033	0.522	0
FpSand	0	-0.033	0	0	-0.133	0.167	0
Lag	-0.8	0	-0.2	0	0	0	1
Mire	0.077	-0.769	0	0.077	0	0.615	0
PL	-0.201	0.043	-0.222	-0.059	0.293	0.024	0.122
TiCh	0	0.429	0	0	0.143	0.429	0

APPENDIX F

PROPORTIONAL FACIES THICKNESS AND FREQUENCIES

Tables summarizing the proportional facies thickness and frequencies used in Figure 15.

Table F1: ‘sampling unit’ defines all the units that fall under a unique systems tract and column combination (i.e., all the units in the HAST of column 3-JRS-21 are a sampling unit). ‘column’ is the measured column name. ‘systems tract’ is the nonmarine systems tract. ‘%Fp’ is the percent of the sampling unit that is floodplain facies. ‘%Ch’ is the percent of the sampling unit that is channel facies. ‘%Cov’ is the percent of the sampling unit that is covered by vegetation or too weathered to determine a facies. Columns 7–14 (‘Fp’–‘Cov’) are the total thicknesses of each facies in the sampling unit divided by the total thickness of the sampling unit (proportional thickness). Facies codes are defined as follows. Fp: floodplain mud. Mire: mire. PL: pond/lake. FpSand: floodplain sand. Ch: fluvial channel bar. Lag: fluvial channel lag. TiCh: tidally influenced channel bar. Cov: covered interval.

Table F2 and F3: facies follow codes conventions in Table F1. n: proportional number of bodies.

Table F1. Summary of facies percent and proportional thickness. Table referred to as ‘metrics’ in R code.

sampling unit	column	systems tract	%Fp	%Ch	%Cov	Fp	Mire	PL	FpSand	Ch	Lag	TiCh	Cov
1	2JRS21	HAST	38.8	39.7	21.5	0.106	0.056	0.215	0.012	0	0.012	0.385	0.215
2	3JRS21	LAST	28.3	57.6	14.1	0.126	0.026	0.051	0.08	0.574	0.002	0	0.141
3	3JRS21	HAST	62.5	27.5	10	0.32	0.044	0.213	0.049	0.110	0	0.165	0.1
4	1JRW21	LAST	100	0	0	0.633	0	0.043	0.324	0	0	0	0
5	1JRW21	HAST	66.1	11.7	22.1	0.172	0.022	0.415	0.052	0.117	0	0	0.221
6	1JRS21	LAST	0	1	0	0	0	0	0	0.806	0.194	0	0
7	3JRW21	HAST	55.4	23	21.6	0.304	0.047	0.172	0.03	0.068	0	0.162	0.216
8	4JRW21	LAST	96.1	3.9	0	0	0	0.699	0.262	0	0.039	0	0
9	4JRW21	HAST	1	0	0	0.331	0.021	0.381	0.268	0	0	0	0
10	4JRS21	LAST	51.7	39.1	9.2	0.256	0.005	0.139	0.117	0.384	0.007	0	0.092

Table F2. Proportional
facies count in the HAST.
Table referred to as
'HASTfacies' in R code.

facies	n
Ch	0.036
Covered	0.079
Fp	0.246
FpSand	0.116
Lag	0.014
Mire	0.116
PL	0.333
TiCh	0.058

Table F3. Proportional facies
count in the LAST. Table
referred to as 'LASTfacies'
in R code.

facies	n
Ch	0.189
Covered	0.054
Fp	0.243
FpSand	0.243
Lag	0.068
Mire	0.027
PL	0.176
TiCh	0

APPENDIX G

PROBABILITIES OF OCCURRENCE

The following tables report the values for the probabilities of occurrence and 95% confidence intervals shown in figures 18–23. Facies codes are defined as follows. Ch: fluvial channel bar. Fp: floodplain mud. FpSand: floodplain sand. Lag: fluvial channel lag. Mire: mire. PL: pond/lake. TiCh: tidally influenced channel bar.

Table G1. Probabilities of occurrence for channel and floodplain facies. Values correspond with Figure 18.

facies	fossil type	probability of occurrence	lower confidence interval	upper confidence interval	sample size
channel	plants	11	5.433	17.223	109
floodplain	plants	23.2	17.832	28.789	228
channel	invertebrates	22.9	15.251	31.04	109
floodplain	invertebrates	19.3	14.307	24.558	228
channel	vertebrates	39.4	30.296	48.687	109
floodplain	vertebrates	45.6	39.15	52.087	228

Table G2. Probabilities of occurrence for individual facies associations. Values correspond with Figure 19.

facies	fossil type	probability of occurrence	lower confidence interval	upper confidence interval	sample size
Ch	plants	2.9	0	7.608	68
Fp	plants	19	10.936	27.749	84
FpSand	plants	10.5	1.725	21.349	38
Lag	plants	14.3	0	46.167	7
Mire	plants	35	14.497	56.693	20
PL	plants	30.2	20.68	40.095	86
TiCh	plants	26.5	12.21	42.046	34

facies	fossil type	probability of occurrence	lower confidence interval	upper confidence interval	sample size
Ch	invertebrates	14.7	6.789	23.65	68
Fp	invertebrates	0	NA	NA	84
FpSand	invertebrates	18.4	6.889	31.619	38
Lag	invertebrates	42.9	7.858	80.057	7
Mire	invertebrates	0	NA	NA	20
PL	invertebrates	43	32.581	53.572	86
TiCh	invertebrates	35.3	19.611	51.722	34
Ch	vertebrates	42.6	30.904	54.502	68
Fp	vertebrates	57.1	46.402	67.626	84
FpSand	vertebrates	42.1	26.496	58.103	38
Lag	vertebrates	57.1	19.943	92.142	7
Mire	vertebrates	0	NA	NA	20
PL	vertebrates	46.5	35.965	57.11	86
TiCh	vertebrates	29.4	14.516	45.274	34

Table G3. Probabilities of occurrence for channel and floodplain facies among the HAST and LAST. Values correspond with Figure 20.

facies	fossil type	probability of occurrence	lower confidence interval	upper confidence interval	sample size	systems tract
channel	plants	1.7	0	5.804	58	LAST
floodplain	plants	9.8	3.786	16.697	82	LAST
channel	invertebrates	15.5	6.677	25.389	58	LAST
floodplain	invertebrates	22	13.318	31.286	82	LAST
channel	vertebrates	51.7	38.849	64.516	58	LAST
floodplain	vertebrates	52.4	41.53	63.207	82	LAST
channel	plants	21.6	10.889	33.492	51	HAST
floodplain	plants	30.8	23.427	38.427	146	HAST
channel	invertebrates	31.4	18.985	44.494	51	HAST
floodplain	invertebrates	17.8	11.796	24.214	146	HAST
channel	vertebrates	25.5	13.925	37.928	51	HAST
floodplain	vertebrates	41.8	33.86	49.863	146	HAST

Table G4. Probabilities of occurrence for individual facies associations in the HAST and LAST. Values correspond with Figure 21.

facies	fossil type	probability of occurrence	lower confidence interval	upper confidence interval	sample size	systems tract
Ch	plants	0	NA	NA	53	LAST
Fp	plants	11.8	1.979	23.84	34	LAST
FpSand	plants	9.1	0	23.148	22	LAST
Lag	plants	20	0	62.859	5	LAST
Mire	plants	33.3	0	94.099	3	LAST
PL	plants	4.3	0	14.527	23	LAST
TiCh	plants	0	NA	NA	0	LAST
Ch	invertebrates	13.2	4.818	23.025	53	LAST
Fp	invertebrates	0	NA	NA	34	LAST
FpSand	invertebrates	13.6	0.56	29.315	22	LAST
Lag	invertebrates	40	0	86.156	5	LAST
Mire	invertebrates	0	NA	NA	3	LAST
PL	invertebrates	65.2	45.171	84.09	23	LAST
TiCh	invertebrates	0	NA	NA	0	LAST
Ch	vertebrates	50.9	37.372	64.405	53	LAST
Fp	vertebrates	55.9	38.998	72.393	34	LAST
FpSand	vertebrates	50	29.229	70.771	22	LAST
Lag	vertebrates	60	13.844	100	5	LAST
Mire	vertebrates	0	NA	NA	3	LAST
PL	vertebrates	56.5	35.885	76.363	23	LAST
TiCh	vertebrates	0	NA	NA	0	LAST
Ch	plants	13.3	0	33.209	15	HAST
Fp	plants	24	12.658	36.389	50	HAST
FpSand	plants	12.5	0	31.315	16	HAST
Lag	plants	0	NA	NA	2	HAST
Mire	plants	35.3	13.285	59.198	17	HAST
PL	plants	39.7	27.813	51.955	63	HAST
TiCh	plants	26.5	12.218	42.046	34	HAST
Ch	invertebrates	20	1.404	42.257	15	HAST
Fp	invertebrates	0	NA	NA	50	HAST
FpSand	invertebrates	25	4.876	47.552	16	HAST
Lag	invertebrates	50	0	100	2	HAST
Mire	invertebrates	0	NA	NA	17	HAST
PL	invertebrates	34.9	23.336	46.85	63	HAST
TiCh	invertebrates	35.3	19.611	51.722	34	HAST

facies	fossil type	probability of occurrence	lower confidence interval	upper confidence interval	sample size	systems tract
Ch	vertebrates	13.3	0	33.209	15	HAST
Fp	vertebrates	58	44.099	71.57	50	HAST
FpSand	vertebrates	31.2	9.797	55.275	16	HAST
Lag	vertebrates	50	0	100	2	HAST
Mire	vertebrates	0	NA	NA	17	HAST
PL	vertebrates	42.9	30.802	55.262	63	HAST
TiCh	vertebrates	29.4	14.516	45.274	34	HAST

Table G5. Probabilities of occurrence for channel and floodplain facies in the HAST updip and downdip. Values correspond with Figure 22.

facies	fossil type	probability of occurrence	lower confidence interval	upper confidence interval	sample size	location along dip
channel	plants	0	NA	NA	9	Downdip
floodplain	plants	26.7	15.914	38.317	60	Downdip
channel	invertebrates	55.6	21.589	88.379	9	Downdip
floodplain	invertebrates	18.3	9.072	28.632	60	Downdip
channel	vertebrates	11.1	0	36.35	9	Downdip
floodplain	vertebrates	38.3	26.162	50.756	60	Downdip
channel	plants	26.2	13.433	40.101	42	Updip
floodplain	plants	33.7	23.906	43.882	86	Updip
channel	invertebrates	26.2	13.43	40.101	42	Updip
floodplain	invertebrates	17.4	15.512	25.798	86	Updip
channel	vertebrates	28.6	15.512	42.842	42	Updip
floodplain	vertebrates	44.2	33.735	54.79	86	Updip

Table G6. Probabilities of occurrence for individual facies associations in the HAST updip and downdip. Values correspond with Figure 23.

facies	fossil type	probability of occurrence	lower confidence interval	upper confidence interval	sample size	location along dip
Ch	plants	0	NA	NA	4	Downdip
Fp	plants	0	NA	NA	15	Downdip
FpSand	plants	0	NA	NA	9	Downdip
Lag	plants	0	NA	NA	0	Downdip

facies	fossil type	probability of occurrence	lower confidence interval	upper confidence interval	sample size	location along dip
Mire	plants	16.7	0	53.308	6	Downdip
PL	plants	50	32.097	67.903	30	Downdip
TiCh	plants	0	NA	NA	5	Downdip
Ch	invertebrates	50	0	100	4	Downdip
Fp	invertebrates	0	NA	NA	15	Downdip
FpSand	invertebrates	33.3	5.075	66.74	9	Downdip
Lag	invertebrates	0	NA	NA	0	Downdip
Mire	invertebrates	0	NA	NA	6	Downdip
PL	invertebrates	26.7	11.754	43.421	30	Downdip
TiCh	invertebrates	60	13.844	100	5	Downdip
Ch	vertebrates	0	NA	NA	4	Downdip
Fp	vertebrates	53.3	27.507	78.556	15	Downdip
FpSand	vertebrates	33.3	5.075	66.74	9	Downdip
Lag	vertebrates	0	NA	NA	0	Downdip
Mire	vertebrates	0	NA	NA	6	Downdip
PL	vertebrates	40	22.656	57.867	30	Downdip
TiCh	vertebrates	20	0	62.859	5	Downdip
Ch	plants	18.2	0	44.16	11	Updip
Fp	plants	34.3	18.983	50.449	35	Updip
FpSand	plants	28.6	0	64.014	7	Updip
Lag	plants	0	NA	NA	2	Updip
Mire	plants	45.5	15.927	75.625	11	Updip
PL	plants	30.3	15.036	46.556	33	Updip
TiCh	plants	31	14.746	48.613	29	Updip
Ch	invertebrates	9.1	0	30	11	Updip
Fp	invertebrates	0	NA	NA	35	Updip
FpSand	invertebrates	14.3	0	46.167	7	Updip
Lag	invertebrates	50	0	100	2	Updip
Mire	invertebrates	0	NA	NA	11	Updip
PL	invertebrates	42.4	25.85	59.453	33	Updip
TiCh	invertebrates	31	14.746	48.613	29	Updip
Ch	vertebrates	18.2	0	44.16	11	Updip
Fp	vertebrates	60	43.427	75.887	35	Updip
FpSand	vertebrates	28.6	0	64.014	7	Updip
Lag	vertebrates	50	0	100	2	Updip
Mire	vertebrates	0	NA	NA	11	Updip
PL	vertebrates	45.5	28.756	62.625	33	Updip

facies	fossil type	probability of occurrence	lower confidence interval	upper confidence interval	sample size	location along dip
TiCh	vertebrates	31	14.746	48.613	29	Updip

APPENDIX H

R CODE FOR MODEL, CALCULATIONS, AND FIGURES

R code workflow used for all calculations, model simulations, and figures. See Appendix I for helper functions ('markovModelFunctions.R'). File inputs for the model are given in preceding appendices. 'stratColumns.csv' is presented in Appendix B. 'fossilCounts.csv' is presented in Appendix C. 'JRFcolors.txt' is presented in Appendix D.

```
#setup
source("markovModelFunctions.R")
source("binomialErrorBars.R") #available from Steven M. Holland
library(tidyverse)
require(gridExtra)

#-----
#input variables
rawData <- read.table("stratColumns.csv", header=TRUE, sep=",",
stringsAsFactors=TRUE) #Appendix B
rawData <- rawData[ ,1:5]
columnKey <- read.table("JRFcolors.txt", header=TRUE, sep=",", as.is=TRUE)
#Appendix D
taxa <- read.table("fossilCounts.csv", header=TRUE, sep=",") #Appendix C

baseCode <- "base"
coveredCode <- "Covered"
stratSurfaceThickness <- 0.015
thicknessCutoff <- 0
simulatedColThickness <- 50
fossilSampleInterval <- 1
allFossilCategories <- c("Pcd", "Pa", "Pcw", "Pw", "Ps", "Pim", "Ii", "Ib", "Ig",
"If", "Vi", "Vt", "Vgar", "Vturt", "Vot", "Vcroc", "Vfish")
compressedFossilCat <- c("plants", "invertebrates", "vertebrates")

#-----
#cleaning and exploring the taxa probabilities
taxa$facies <- as.factor(taxa$facies)
taxa$SystemTract <- as.factor(taxa$SystemTract)
systemTracts <- levels(taxa$SystemTract)

nrow(taxa)
taxa <- taxa[!grepl("NS", taxa$Pcd), ] #getting rid of NS in dataframe
nrow(taxa)

taxa$facies[taxa$facies == 'PLi'] <- 'PL' #combining the PL and PLi facies
```

```

taxa <- taxa[taxa$facies != 'Msh', ] #getting rid of the marine facies
taxa$facies <- droplevels(taxa$facies)

nrow(taxa)

hastTaxa <- taxa[taxa$SystemTract == "HAST", ]
lastTaxa <- taxa[taxa$SystemTract == "LAST", ]

nrow(hastTaxa)
nrow(lastTaxa)

facies <- levels(taxa$facies)
sapply(facies, function(x) sum(lastTaxa$facies == x)) #counting the number of
searched intervals
sapply(facies, function(x) sum(hastTaxa$facies == x))

#-----
#adding new columns for broader categories of plants, invertebrates, and vertebrates

plantCol <- taxa[,c(6,8:10)]
plants <- apply(plantCol, MARGIN=1, FUN=max)

invertCol <- taxa[,11:14]
invertebrates <- apply(invertCol, MARGIN=1, FUN=max)

vertCol <- taxa[,15:21]
vertebrates <- apply(vertCol, MARGIN=1, FUN=max)

#checking for any vertebrate bins that need to be bumped up
moreThan3 <- apply(vertCol, MARGIN=1, function(x) sum(x == 0))
bumped <- moreThan3[moreThan3 >= 3]
vertebrates[names(bumped)]
vertebrates[c("11", "287")] <- c("0.5", "0.5") #bumping up to a higher bin

taxa <- cbind(taxa, plants, invertebrates, vertebrates)

#-----
#converting taxa counts to probabilities

#no separation of HAST and LAST for all categories

taxaProbability <- obsToProbs(taxa, categories=allFossilCategories, cutoff=-1)

#separation of HAST and LAST for all categories

taxaProbSysTracts <- lapply(systemTracts, FUN=obsToProbs, observations=taxa,
categories=allFossilCategories, cutoff=-1)
names(taxaProbSysTracts) <- systemTracts

HASTtaxaProbability <- taxaProbSysTracts$HAST
LASTtaxaProbability <- taxaProbSysTracts$LAST

#no separation of HAST and LAST for combined categories

combTaxaProbability <- obsToProbs(taxa, categories=compressedFossilCat, cutoff=-1)

```

```

#separation of HAST and LAST for combined categories

combTaxaProbSysTracts <- lapply(systemTracts, FUN=obsToProbs, observations=taxa,
categories=compressedFossilCat, cutoff=-1)
names(combTaxaProbSysTracts) <- systemTracts

combHASTtaxaProb <- combTaxaProbSysTracts$HAST
combLASTtaxaProb <- combTaxaProbSysTracts$LAST

#calculating probabilities for updip and downdip HAST
hastTaxa <- taxa[taxa$SystemTract == "HAST", ]
#lastTaxa <- taxa[taxa$SystemTract == "LAST", ]
stafford <- hastTaxa[grepl("JRS", hastTaxa$section), ]
woodhawk <- hastTaxa[grepl("JRW", hastTaxa$section), ]

#all categories updip (stafford ferry)

staffordProbabilities <- obsToProbs(stafford, categories=allFossilCategories,
cutoff=-1)

#all categories downdip (woodhawk bottom)

woodhawkProbabilities <- obsToProbs(woodhawk, categories=allFossilCategories,
cutoff=-1)

#combined categories updip

combStaffordProbs <- obsToProbs(stafford, categories=compressedFossilCat, cutoff=-1)

#combined categories downdip

combWoodhawkProbs <- obsToProbs(woodhawk, categories=compressedFossilCat, cutoff=-1)

#-----
#calculating confidence intervals on the probability of occurrence

CItaxaProbAll <- probabilityConfInt(taxaProbability, allFossilCategories)
CIhastTaxaProbAll <- probabilityConfInt(HASTtaxaProbability, allFossilCategories)
CIlastTaxaProbAll <- probabilityConfInt(LASTtaxaProbability, allFossilCategories)

CItaxaProbComb <- probabilityConfInt(combTaxaProbability, compressedFossilCat)
CIhastTaxaProbComb <- probabilityConfInt(combHASTtaxaProb, compressedFossilCat)
CIlastTaxaProbComb <- probabilityConfInt(combLASTtaxaProb, compressedFossilCat)

CIstaffordAll <- probabilityConfInt(staffordProbabilities, allFossilCategories)
CIwoodhawkAll <- probabilityConfInt(woodhawkProbabilities, allFossilCategories)

CIstaffordComb <- probabilityConfInt(combStaffordProbs, compressedFossilCat)
CIwoodhawkComb <- probabilityConfInt(combWoodhawkProbs, compressedFossilCat)

#-----
#creating new data set with compressed facies categories (floodplain and channel)

```

```

taxaFpCh <- taxa

taxaFpCh$facies[taxaFpCh$facies == 'PL' | taxaFpCh$facies == 'Mire' | taxaFpCh$facies
== 'FpSand'] <- 'Fp' #combining the floodplain facies into 1 Fp category

taxaFpCh$facies[taxaFpCh$facies == 'TiCh' | taxaFpCh$facies == 'Lag'] <- 'Ch'
      #combining the channel facies into 1 Ch category

#-----
#calculating probability of occurrence for compressed facies categories (floodplain
and channel)

#no separation of HAST and LAST for combined categories

combChFpTaxaProb <- obsToProbs(taxaFpCh, categories=compressedFossilCat, cutoff=-1)
combChFpTaxaProb <- combChFpTaxaProb[1:2, ]

#separation of HAST and LAST for combined categories

combChFpTaxaProbSysTracts <- lapply(systemTracts, FUN=obsToProbs,
observations=taxaFpCh, categories=compressedFossilCat, cutoff=-1)
names(combChFpTaxaProbSysTracts) <- systemTracts

ChFpHASTtaxaProb <- combChFpTaxaProbSysTracts$HAST
ChFpHASTtaxaProb <- ChFpHASTtaxaProb[1:2, ]
ChFpLASTtaxaProb <- combChFpTaxaProbSysTracts$LAST
ChFpLASTtaxaProb <- ChFpLASTtaxaProb[1:2, ]

#separating updip and downdip for channel and floodplain
hastTaxaComb <- taxaFpCh[taxaFpCh$SystemTract == "HAST", ]
staffordComb <- hastTaxaComb[grep("JRS", hastTaxaComb$section), ]
woodhawkComb <- hastTaxaComb[grep("JRW", hastTaxaComb$section), ]

#calculating updip and downdip probabilities for channel and floodplain
combChFpStaffordProbs <- obsToProbs(staffordComb, categories=compressedFossilCat,
cutoff=-1)
combChFpStaffordProbs <- combChFpStaffordProbs[1:2, ]
combChFpWoodhawkProbs <- obsToProbs(woodhawkComb, categories=compressedFossilCat,
cutoff=-1)
combChFpWoodhawkProbs <- combChFpWoodhawkProbs[1:2, ]

#calculating confidence intervals for floodplain and channel groups

CICHfPComb <- probabilityConfInt(combChFpTaxaProb, compressedFossilCat)
CICHfPHAST <- probabilityConfInt(ChFpHASTtaxaProb, compressedFossilCat)
CICHfPLAST <- probabilityConfInt(ChFpLASTtaxaProb, compressedFossilCat)
CICHfPUpdip <- probabilityConfInt(combChFpStaffordProbs, compressedFossilCat)
CICHfPDowndip <- probabilityConfInt(combChFpWoodhawkProbs, compressedFossilCat)

#-----
#data error checking

sysTractList <- levels(rawData$systemTract)
surfacesToDelete <- c(baseCode, coveredCode)

```

```

rawData$facies[rawData$facies == 'PLi'] <- 'PL' #combining the PL and PLi facies
rawData <- rawData[rawData$facies != 'Msh', ] #getting rid of marine rows of data
rawData$facies <- droplevels(rawData$facies)

stratSurfaces <- columnKey$code[columnKey$isSurface == TRUE]
checkData(rawData, columnKey, taxaProbability, stratSurfaces, surfacesToDelete,
stratSurfaceThickness)

#-----
#adding sampling units to dataframe to help with metric calculations

allColumns <- addSamplingUnits(rawData, "systemTract", "section")
str(allColumns)

#-----
#adding transitions between HAST and LAST

allColumns <- addBase(allColumns, baseCode)

#-----
#calculate a thickness column from tops of measured sections

allColumns <- thickness(allColumns)
head(allColumns)

#-----
#split data into separate HAST and LAST dataframes

sysTractData <- splitData(allColumns, sysTractList)
head(sysTractData$HAST)
head(sysTractData$LAST)

#-----
#calculate HAST and LAST facies transition matrix

faciesTransitions <- lapply(X=sysTractData, FUN=transitionMatrix,
del=surfacesToDelete)
faciesThickDist$LAST$TiCh <- 0 #manually adding a tidally influenced channel of 0
thickness to ease simulation

#-----
#calculate facies distribution for HAST and LAST dataframes

faciesThickDist <- lapply(X=sysTractData, FUN=faciesThicknessDist,
del=surfacesToDelete)

#-----
#calculate system tract thickness distribution

sysTractThickDist <- lapply(X=sysTractList, FUN=sysTractThickness,
allColumns=allColumns, thicknessCutoff=thicknessCutoff)
names(sysTractThickDist) <- sysTractList

#-----
#calculate system tract transition matrix

```

```

baseRows <- allColumns[allColumns$facies == baseCode, ]

sysTractTransitions <- systemTractTransitionMatrix(baseRows)
sysTractTransitions

#-----
#simulate column with expansion surface (sharp)

columnGeneratorOutput_ES <- columnGenerator_systemTractSharp(faciesTransitions,
sysTractTransitions, faciesThickDist, sysTractThickDist,
maxHeight=simulatedColThickness, sysTractForce=c("LAST", "HAST"),
sysTractThickForce=c(50,50))

simulatedColumn_ES <- columnGeneratorOutput_ES$simulatedColumn
simulatedSysTractDF_ES <- columnGeneratorOutput_ES$sysTractDF

#-----
#draw column with expansion surface

columnPlotData_ES <- plottingStrata(simulatedColumn_ES, columnKey)
drawStrata(columnPlotData_ES, columnKey, yScale=100)

#-----
#plot HAST and LAST

sysTractColors <- data.frame(systemTract=sysTractList, barColor=c("grey80",
"grey32"))
plotSystemTract(columnPlotData_ES, sysTractColors)
text(x=5.2, y=25, labels="LAST", col="white", srt=90, cex=.7)
text(x=5.2, y=75, labels="HAST", col="black", srt=90, cex=.7)

#-----
#plot fossil occurrences

taxaProbsForPlot <- combTaxaProbability[ , -5]
occurrenceData_ES <- fossilGenerator(simulatedColumn_ES, taxaProbsForPlot,
fossilSampleInterval)

plotFossils(occurrenceData_ES, columnPlotData_ES, columnKey)

#-----
#simulate column with sequence boundary (sharp)

columnGeneratorOutput_SB <- columnGenerator_systemTractSharp(faciesTransitions,
sysTractTransitions, faciesThickDist, sysTractThickDist,
maxHeight=simulatedColThickness, sysTractForce=c("HAST", "LAST"),
sysTractThickForce=c(50,50))

simulatedColumn_SB <- columnGeneratorOutput_SB$simulatedColumn
simulatedSysTractDF_SB <- columnGeneratorOutput_SB$sysTractDF

#-----
#draw column with expansion surface

```

```

columnPlotData_SB <- plottingStrata(simulatedColumn_SB, columnKey)
drawStrata(columnPlotData_SB, columnKey, yScale=100)

#-----
#plot HAST and LAST

sysTractColors <- data.frame(systemTract=sysTractList, barColor=c("grey80",
"grey32"))
plotSystemTract(columnPlotData_SB, sysTractColors)
text(x=5.2, y=75, labels="LAST", col="white", srt=90, cex=.7)
text(x=5.2, y=25, labels="HAST", col="black", srt=90, cex=.7)

#-----
#plot fossil occurrences

occurrenceData_SB <- fossilGenerator(simulatedColumn_SB, taxaProbsForPlot,
fossilSampleInterval)

plotFossils(occurrenceData_SB, columnPlotData_SB, columnKey)

#-----
#simulate gradual transition from HAST to LAST

columnGeneratorOutput_GhastLast <-
columnGenerator_systemTractGradual(faciesTransitions=faciesTransitions,
faciesThickDist=faciesThickDist, startSysTract="HAST", endSysTract="LAST",
maxThick=100)

HASTLASTgradual <- columnGeneratorOutput_GhastLast$simulatedColumn

#-----
#Plot gradual transition from HAST to LAST

HastLastgradData <- plottingStrata(HASTLASTgradual, columnKey)
drawStrata(HastLastgradData, columnKey, yScale=100)
HLgradOccurrenceData <- fossilGenerator(HastLastgradData, taxaProbsForPlot,
fossilSampleInterval)
plotFossils(HLgradOccurrenceData, HastLastgradData, columnKey)

#-----
#simulate gradual transition from LAST to HAST

columnGeneratorOutput_GlastHast <-
columnGenerator_systemTractGradual(faciesTransitions=faciesTransitions,
faciesThickDist=faciesThickDist, startSysTract="LAST", endSysTract="HAST",
maxThick=100)

LASTHASTgradual <- columnGeneratorOutput_GlastHast$simulatedColumn

#-----
#Plot gradual transition from LAST to HAST

LastHastgradData <- plottingStrata(LASTHASTgradual, columnKey)
drawStrata(LastHastgradData, columnKey, yScale=100)

```

```

LHgradOccurrenceData <- fossilGenerator(LastHastgradData, taxaProbsForPlot,
fossilSampleInterval)
plotFossils(LHgradOccurrenceData, LastHastgradData, columnKey)

#-----
#Judith River Formation Columns with fossil occurrences

#getting and plotting 3-JRS-21 example of Expansion surface
JRS21_3 <- allColumns[allColumns$section == "3JRS21", ]
col3JRS21 <- plottingStrata(JRS21_3, columnKey)
drawStrata(col3JRS21, columnKey, main="3-JRS-21", yScale=155)
plotSystemTract(col3JRS21, sysTractColors)

#coercing occurrence data into the correct format for plotting
occurrenceData3JRS21 <- taxa[taxa$section == "3JRS21", c("samplingUnit", "plants",
"invertebrates", "vertebrates")]
colnames(occurrenceData3JRS21)[1] <- "stratPosition"
occurrenceData3JRS21[ ,2:4][occurrenceData3JRS21[ ,2:4] > -1] <- 1
occurrenceData3JRS21[ ,2:4][occurrenceData3JRS21[ ,2:4] == -1] <- 0

cols.num <- c("plants", "invertebrates", "vertebrates")
occurrenceData3JRS21[cols.num] <- sapply(occurrenceData3JRS21[cols.num], as.numeric)
plotFossils(occurrenceData3JRS21, col3JRS21, columnKey)

#getting and plotting 4-JRS-21 example of LAST
JRS21_4 <- allColumns[allColumns$section == "4JRS21", ]
col4JRS21 <- plottingStrata(JRS21_4, columnKey)
drawStrata(col4JRS21, columnKey, main="4-JRS-21", yScale=155)
plotSystemTract(col4JRS21, sysTractColors)

#coercing occurrence data into the correct format for plotting
occurrenceData4JRS21 <- taxa[taxa$section == "4JRS21", c("samplingUnit", "plants",
"invertebrates", "vertebrates")]
colnames(occurrenceData4JRS21)[1] <- "stratPosition"
occurrenceData4JRS21[ ,2:4][occurrenceData4JRS21[ ,2:4] > -1] <- 1
occurrenceData4JRS21[ ,2:4][occurrenceData4JRS21[ ,2:4] == -1] <- 0

occurrenceData4JRS21[cols.num] <- sapply(occurrenceData4JRS21[cols.num], as.numeric)
plotFossils(occurrenceData4JRS21, col4JRS21, columnKey)

#getting and plotting 3-JRW-21- example of HAST
JRW21_3 <- allColumns[allColumns$section == "3JRW21", ]
col3JRW21 <- plottingStrata(JRW21_3, columnKey)
drawStrata(col3JRW21, columnKey, main="3-JRW-21", yScale=155)
plotSystemTract(col3JRW21, sysTractColors)

#coercing occurrence data into the correct format for plotting
occurrenceData3JRW21 <- taxa[taxa$section == "3JRW21", c("samplingUnit", "plants",
"invertebrates", "vertebrates")]
colnames(occurrenceData3JRW21)[1] <- "stratPosition"
occurrenceData3JRW21[ ,2:4][occurrenceData3JRW21[ ,2:4] > -1] <- 1
occurrenceData3JRW21[ ,2:4][occurrenceData3JRW21[ ,2:4] == -1] <- 0

occurrenceData3JRW21[cols.num] <- sapply(occurrenceData3JRW21[cols.num], as.numeric)
plotFossils(occurrenceData3JRW21, col3JRW21, columnKey)

```

```

#-----
#calculate metrics

fpFacies <- c("Fp", "Mire", "PL", "FpSand")
chFacies <- c("Ch", "Lag", "TiCh")

percentFloodplain <- percentFaciesThick(allColumns, fpFacies)
percentChannel <- percentFaciesThick(allColumns, chFacies)
percentCovered <- percentFaciesThick(allColumns, coveredCode)

faciesList <- c(fpFacies, chFacies, coveredCode)
propAvgThick <- lapply(X=faciesList, FUN=propFaciesThickness, allColumns=allColumns)
names(propAvgThick) <- faciesList

#-----
#create new metrics dataframe and add desired metrics

metrics <- createMetricsTable(allColumns)

metrics$percentFloodplain <- percentFloodplain
metrics$percentChannel <- percentChannel
metrics$percentCovered <- percentCovered

avgThick <- as.data.frame(matrix(unlist(propAvgThick),
nrow=length(unlist(propAvgThick[1]))))
colnames(avgThick) <- faciesList
metrics <- cbind(metrics, avgThick)

#-----
#Plot bar plot comparing HAST/LAST proportional average thickness

plotTargetOrder <- c("Covered", "Tidally influenced channel bar", "Fluvial channel
bar", "Fluvial channel lag", "Floodplain sand", "Floodplain mud", "Pond/Lake",
"Mire")

metricsPlotHast <- metrics %>%
  select(systemTract, all_of(faciesList)) %>%
  filter(systemTract == "HAST") %>%
  summarise(across(all_of(faciesList), mean)) %>%
  gather("facies", "average") %>%
  mutate(systemTract="HAST") %>%
  mutate(facies_name=c("Floodplain mud", "Mire", "Pond/Lake", "Floodplain sand",
"Fluvial channel bar", "Fluvial channel lag", "Tidally influenced channel bar",
"Covered"))
metricsPlotHast$facies_name <- factor(metricsPlotHast$facies_name,
levels=plotTargetOrder)

metricsPlotLast <- metrics %>%
  select(systemTract, all_of(faciesList)) %>%
  filter(systemTract == "LAST") %>%
  summarise(across(all_of(faciesList), mean)) %>%
  gather("facies", "average") %>%
  mutate(systemTract="LAST") %>%

```

```

mutate(facies_name=c("Floodplain mud", "Mire", "Pond/Lake", "Floodplain sand",
"Fluvial channel bar", "Fluvial channel lag", "Tidally influenced channel bar",
"Covered"))
metricsPlotLast$facies_name <- factor(metricsPlotLast$facies_name,
levels=plotTargetOrder)

gg.HAST <- ggplot(metricsPlotHast, aes(x=facies_name, y=average)) +
  geom_bar(position=position_dodge(), stat="identity") +
  theme(axis.title.y=element_blank(), axis.ticks.y=element_blank(),
panel.grid.minor.x = element_blank(), panel.grid.minor.y = element_blank()) +
  theme(axis.text.y=element_text(size=9, hjust=0.5, vjust=0.2)) +
  coord_flip() +
  ylim(0, 0.6) +
  labs(title="HAST", y=" ")

gg.LAST <- ggplot(metricsPlotLast, aes(x=facies_name, y=average)) +
  geom_bar(position=position_dodge(), stat="identity") +
  theme(axis.title.y=element_blank(), axis.text.y=element_text(color="white"),
axis.ticks.y=element_blank(), panel.grid.minor.x = element_blank(),panel.grid.minor.y
= element_blank()) +
  coord_flip() +
  scale_y_continuous(limits=c(0.6, 0), trans="reverse") +
  labs(title="LAST", y=" ")

grid.arrange(gg.LAST, gg.HAST, ncol=2)

#-----
#bar plot comparing HAST LAST facies counts

nFacies <- lapply(X=sysTractData, FUN=proportionalFaciesCounts, del=baseCode)

HASTfacies <- nFacies$HAST %>%
  mutate(facies_name=c("Fluvial channel bar", "Covered", "Floodplain mud",
"Floodplain sand", "Fluvial channel lag", "Mire", "Pond/Lake", "Tidally influenced
channel bar"))
HASTfacies$facies_name <- factor(HASTfacies$facies_name, levels=plotTargetOrder)

LASTfacies <- nFacies$LAST %>%
  add_row(facies="TiCh", n=0) %>%
  mutate(facies_name=c("Fluvial channel bar", "Covered", "Floodplain mud",
"Floodplain sand", "Fluvial channel lag", "Mire", "Pond/Lake", "Tidally influenced
channel bar"))
LASTfacies$facies_name <- factor(LASTfacies$facies_name, levels=plotTargetOrder)

count.HAST <- ggplot(HASTfacies, aes(x=facies_name, y=n)) +
  geom_bar(position=position_dodge(), stat="identity") +
  theme(axis.title.y=element_blank(), axis.ticks.y=element_blank(),
panel.grid.minor.x = element_blank(),panel.grid.minor.y=element_blank()) +
  theme(axis.text.y=element_text(size=9, hjust=0.5,vjust=0.2)) +
  coord_flip() +
  ylim(0, 0.45) +
  labs(title="HAST", y= "Proportional number of bodies")

count.LAST <- ggplot(LASTfacies, aes(x=facies_name, y=n)) +
  geom_bar(position=position_dodge(), stat="identity") +

```

```

    theme(axis.title.y=element_blank(), axis.text.y=element_text(color="white"),
axis.ticks.y=element_blank(), panel.grid.minor.x = element_blank(),panel.grid.minor.y
= element_blank()) +
    coord_flip() +
    scale_y_continuous(limits=c(0.45, 0), trans="reverse") +
    labs(title="LAST", y="Proportional number of bodies")

grid.arrange(count.LAST, count.HAST, ncol=2)

#-----
#Creates the transition matrix heat maps

tmatrixNames <- c("Fluvial channel bar", "Floodplain mud", "Floodplain sand",
"Fluvial channel lag", "Mire", "Pond/Lake", "Tidally influenced channel bar")

hastTransitions <- faciesTransitions$HAST
lastTransitions <- faciesTransitions$LAST
hastMinusLast <- hastTransitions - lastTransitions

rownames(hastTransitions) <- tmatrixNames
colnames(hastTransitions) <- tmatrixNames

rownames(lastTransitions) <- tmatrixNames
colnames(lastTransitions) <- tmatrixNames

rownames(hastMinusLast) <- tmatrixNames
colnames(hastMinusLast) <- tmatrixNames

lastDF <- JRtMatrixFigure(lastTransitions)
lastDF$To <- factor(lastDF$To, levels=plotTargetOrder) #matching previous order
lastDF$From <- factor(lastDF$From, levels=plotTargetOrder)

hastDF <- JRtMatrixFigure(hastTransitions)
hastDF$To <- factor(hastDF$To, levels=plotTargetOrder)
hastDF$From <- factor(hastDF$From, levels=plotTargetOrder)

hastMinusLastDF <- JRtMatrixFigure(hastMinusLast)
hastMinusLastDF$To <- factor(hastMinusLastDF$To, levels=plotTargetOrder)
hastMinusLastDF$From <- factor(hastMinusLastDF$From, levels=plotTargetOrder)

dev.new()
ggplot(lastDF, aes(To, From, fill= Probability)) +
geom_tile() +
ggtitle("LAST Transitions") +
theme(axis.text.x = element_text(angle = 90, hjust=1)) +
scale_fill_gradient(low="white", high="blue", limits=c(0, 1)) #two colors

dev.new()
ggplot(hastDF, aes(To, From, fill= Probability)) +
geom_tile() +
ggtitle("HAST Transitions") +
theme(axis.text.x = element_text(angle = 90, hjust=1)) +
scale_fill_gradient(low="white", high="red", limits=c(0, 1)) #two colors

```

```

dev.new()
ggplot(hastMinusLastDF, aes(To, From, fill= Probability)) +
geom_tile() +
ggtitle("HAST Minus LAST Transitions") +
theme(axis.text.x = element_text(angle = 90, hjust=1)) +
scale_fill_gradientn(colours = c("blue", "white", "red"), limits=c(-1, 1)) #three
colors

#-----
#Probabilities of occurrence for floodplain and channel facies (all JRF)

CIChFpComb$facies <- c("Channel", "Floodplain", "Channel", "Floodplain", "Channel",
"Floodplain")
CIChFpComb$facies <- as.factor(CIChFpComb$facies)
CIChFpComb$fossilType <- as.factor(CIChFpComb$fossilType)
CIChFpComb$probCol <- as.numeric(CIChFpComb$probCol)
CIChFpComb$upperCI <- as.numeric(CIChFpComb$upperCI)
CIChFpComb$lowerCI <- as.numeric(CIChFpComb$lowerCI)

nTaxa <- length(levels(CIChFpComb$fossilType))
nFacies <- length(levels(CIChFpComb$facies))

yAxisLen <- (nTaxa + 1) * nFacies #calculates total length needed
yposition <- 1:yAxisLen
spaces <- seq(from=nFacies + 1, to=yAxisLen, by=3) #calculates space between
clusters
yposition <- yposition[-spaces] #creates a vector of positions for plotting means

par(mai=c(1, 1.5, .5, 1))
plot(0, 0, type="n", ylim=c(0, yAxisLen), xlim=c(0, 100), xlab="Probability of
occurrence", ylab="", yaxt="n", bty="n", main="Judith River Formation")

rect(ybottom=3, ytop=6, xleft=0, xright=100, col="snow2", border=NA)
points(CIChFpComb$probCol, yposition, pch=16)
segments(y0=yposition, x0=CIChFpComb$lowerCI, x1=CIChFpComb$upperCI)

text(y=yposition, x=CIChFpComb$upperCI + 1.5, labels=CIChFpComb$facies, cex=0.5,
adj=0.1)
mtext(text=c("Plants", "Invertebrates", "Vertebrates"), side=2, at=c(1.5, 4.5, 7.5),
cex=0.75, las=2)

#-----
#Probabilities of occurrence for LAST vs. HAST- combined channel and floodplain
facies

CIChFpHAST$systemTract <- "HAST"
CIChFpLAST$systemTract <- "LAST"

hastVlastCombFacies <- rbind(CIChFpLAST, CIChFpHAST)

plotFossilsFactorOrder <- c("plants", "invertebrates", "vertebrates")
plotFaciesFactorOrder <- c("Ch", "Fp")
faciesNames <- c("Channel", "Floodplain")

```

```

hastVlastCombFacies <- pocDataOrder(hastVlastCombFacies, plotFaciesFactorOrder,
faciesNames, plotFossilsFactorOrder)
hastVlastCombFacies$systemTract <- as.factor(hastVlastCombFacies$systemTract)

nSysTract <- length(levels(hastVlastCombFacies$systemTract))
nTaxa <- length(levels(hastVlastCombFacies$fossilType))
nFacies <- length(levels(hastVlastCombFacies$facies))

yAxisLen <- (nSysTract+1) * nTaxa * nFacies #calculates total length needed
yposition <- 1:yAxisLen
spaces <- seq(from=nTaxa, to=yAxisLen, by=3) #calculates space between clusters
yposition <- yposition[-spaces] #creates a vector of positions for plotting means

par(mai=c(1, 1.5, .5, 1))
plot(0, 0, type="n", ylim=c(0, yAxisLen), xlim=c(0, 100), xlab="Probability of
occurrence", ylab="", yaxt="n", bty="n", main="HAST versus LAST")
rect(ybottom=6, ytop=12, xleft=0, xright=100, col="snow2", border=NA)

points(hastVlastCombFacies$probCol, yposition, pch=16)
segments(y0=yposition, x0=hastVlastCombFacies$lowerCI,
x1=hastVlastCombFacies$upperCI)

text(y=yposition, x=hastVlastCombFacies$upperCI + 1.5,
labels=hastVlastCombFacies$systemTract, cex=0.5, adj=0.1)
mtext(text=plotFossilsFactorOrder, side=4, at=c(4, 10, 16), cex=0.75, las=2)
mtext(text=faciesNames, side=2, at=seq(from=1.5, to=16.5, by=3), cex=0.65, las=2)

#-----
#Probabilities of occurrence for updip vs. downdip HAST- combined channel and
floodplain facies

CIChFpUpdip$systemTract <- "Updip"
CIChFpDowndip$systemTract <- "Downdip"

upVdownCombFacies <- rbind(CIChFpDowndip, CIChFpUpdip)

upVdownCombFacies <- pocDataOrder(upVdownCombFacies, plotFaciesFactorOrder,
faciesNames, plotFossilsFactorOrder)
upVdownCombFacies$systemTract <- factor(upVdownCombFacies$systemTract,
levels=c("Updip", "Downdip"))

nSysTract <- length(levels(upVdownCombFacies$systemTract))
nTaxa <- length(levels(upVdownCombFacies$fossilType))
nFacies <- length(levels(upVdownCombFacies$facies))

yAxisLen <- (nSysTract+1) * nTaxa * nFacies #calculates total length needed
yposition <- 1:yAxisLen
spaces <- seq(from=nTaxa, to=yAxisLen, by=3) #calculates space between clusters
yposition <- yposition[-spaces] #creates a vector of positions for plotting means

par(mai=c(1, 1.5, .5, 1))
plot(0, 0, type="n", ylim=c(0, yAxisLen), xlim=c(0, 100), xlab="Probability of
occurrence", ylab="", yaxt="n", bty="n", main="Updip HAST versus Downdip HAST")
rect(ybottom=6, ytop=12, xleft=0, xright=100, col="snow2", border=NA)

```

```

points(upVdownCombFacies$probCol, yposition, pch=16)
segments(y0=yposition, x0=upVdownCombFacies$lowerCI, x1=upVdownCombFacies$upperCI)

text(y=yposition, x=upVdownCombFacies$upperCI + 1.5,
labels=upVdownCombFacies$systemTract, cex=0.5, adj=0.1)
mtext(text=plotFossilsFactorOrder, side=4, at=c(4, 10, 16), cex=0.75, las=2)
mtext(text=faciesNames, side=2, at=seq(from=1.5, to=16.5, by=3), cex=0.65, las=2)

#-----
#Comparison of probabilities of occurrence (Combined)

#objects that will be used for all following plots
plotFaciesFactorOrder <- c("TiCh", "Ch", "Lag", "FpSand", "Fp", "PL", "Mire")
plotFossilsFactorOrder <- c("plants", "invertebrates", "vertebrates")
faciesNames <- c("Tidally influenced channel bar", "Fluvial channel bar", "Fluvial
channel lag", "Floodplain sand", "Floodplain mud", "Pond/Lake", "Mire")

color <- columnKey[order(columnKey$legendOrder, decreasing=TRUE), ]
color <- color$color

CItaxaProbComb <- pocDataOrder(CItaxaProbComb, plotFaciesFactorOrder, faciesNames,
plotFossilsFactorOrder)

nTaxa <- length(levels(CItaxaProbComb$fossilType))
nFacies <- length(levels(CItaxaProbComb$facies))
yAxisLen <- nrow(CItaxaProbComb) + nTaxa #calculates total length needed
yposition <- 1:yAxisLen
spaces <- seq(from=nFacies + 1, to=yAxisLen, by=nFacies + 1) #calculates space
between clusters
yposition <- yposition[-spaces] #creates a vector of positions for plotting means

par(mai=c(1, 1.5, .5, 1))
plot(0, 0, type="n", ylim=c(0, yAxisLen), xlim=c(0, 100), xlab="Probability of
occurrence", ylab="", yaxt="n", bty="n", main="Judith River Formation")

ybottom <- 8
ytop <- 16
rect(ybottom=ybottom, ytop=ytop, xleft=0, xright=100, col="snow2", border=NA)
points(CItaxaProbComb$probCol, yposition, pch=16, col=color)
segments(y0=yposition, x0=CItaxaProbComb$lowerCI, x1=CItaxaProbComb$upperCI,
col=color)

text(y=yposition, x=CItaxaProbComb$upperCI + 1.5, labels=faciesNames, cex=0.5,
adj=0.1)
mtext(text=plotFossilsFactorOrder, side=2, at=c(4, 12, 20), las=2)

#-----
#Probabilities of occurrence for LAST vs. HAST
color2points <- c("#EEF2DF", "#EEF2DF", "#F2BE7D", "#F2BE7D", "#A7A9AC", "#A7A9AC",
"#C1B47E", "#C1B47E", "#A4A591", "#A4A591", "#C0D6D8", "#C0D6D8", "#434343",
"#434343")

CIhastTaxaProbComb$systemTract <- "HAST"
CIlastTaxaProbComb$systemTract <- "LAST"
hastVlastTaxa <- rbind(CIlastTaxaProbComb, CIhastTaxaProbComb)

```

```

hastVlastTaxa <- pocDataOrder(hastVlastTaxa, plotFaciesFactorOrder, faciesNames,
plotFossilsFactorOrder)
hastVlastTaxa$systemTract <- as.factor(hastVlastTaxa$systemTract)

nSysTract <- length(levels(hastVlastTaxa$systemTract))
nTaxa <- length(levels(hastVlastTaxa$fossilType))
nFacies <- length(levels(hastVlastTaxa$facies))

yAxisLen <- nFacies * (nSysTract + 1) * nTaxa #calculates total length needed
yposition <- 1:yAxisLen
spaces <- seq(from=nSysTract + 1, to=yAxisLen, by=nSysTract + 1) #calculates space
between clusters
yposition <- yposition[-spaces] #creates a vector of positions for plotting means

par(mai=c(1, 1.5, .5, 1))
plot(0, 0, type="n", ylim=c(0, yAxisLen), xlim=c(0, 100), xlab="Probability of
occurrence", ylab="", yaxt="n", bty="n", main="HAST versus LAST")
rect(ybottom=21, ytop=42, xleft=0, xright=100, col="snow2", border=NA)

points(hastVlastTaxa$probCol, yposition, pch=16, col=color2points)
segments(y0=yposition, x0=hastVlastTaxa$lowerCI, x1=hastVlastTaxa$upperCI,
col=color2points)

text(y=yposition, x=hastVlastTaxa$upperCI + 1.5, labels=hastVlastTaxa$systemTract,
cex=0.5, adj=0.1)
mtext(text=faciesNames, side=2, at=seq(from=1.5, to=61.5, by=3), cex=0.65, las=2)
mtext(text=plotFossilsFactorOrder, side=4, at=c(12, 34, 54), cex=0.75, las=2)

#-----
#Probabilities of occurrence for updip vs. downdip HAST- split by individual facies

CIstaffordComb$systemTract <- "Updip"
CIwoodhawkComb$systemTract <- "Downdip"

upVdownTaxa <- rbind(CIwoodhawkComb, CIstaffordComb)
upVdownTaxa <- pocDataOrder(upVdownTaxa, plotFaciesFactorOrder, faciesNames,
plotFossilsFactorOrder)
upVdownTaxa$systemTract <- factor(upVdownTaxa$systemTract, levels=c("Updip",
"Downdip"))

nSysTract <- length(levels(upVdownTaxa$systemTract))
nTaxa <- length(levels(upVdownTaxa$fossilType))
nFacies <- length(levels(upVdownTaxa$facies))

yAxisLen <- nFacies * (nSysTract + 1) * nTaxa #calculates total length needed
yposition <- 1:yAxisLen
spaces <- seq(from=nSysTract + 1, to=yAxisLen, by=nSysTract + 1) #calculates space
between clusters
yposition <- yposition[-spaces] #creates a vector of positions for plotting means

par(mai=c(1, 1.5, .5, 1))
plot(0, 0, type="n", ylim=c(0, yAxisLen), xlim=c(0, 100), xlab="Probability of
occurrence", ylab="", yaxt="n", bty="n", main="Updip HAST versus Downdip HAST")
ybottom <- c(21)

```

```
ytop <- c(42)
color <- columnKey$color
rect(ybottom=ybottom, ytop=ytop, xleft=0, xright=100, col="snow2", border=NA)

points(upVdownTaxa$probCol, yposition, pch=16, col=color2points)
segments(y0=yposition, x0=upVdownTaxa$lowerCI, x1=upVdownTaxa$upperCI,
col=color2points)

text(y=yposition, x=upVdownTaxa$upperCI + 1.5, labels=upVdownTaxa$systemTract,
cex=0.5, adj=0.1)
mtext(text=faciesNames, side=2, at=seq(from=1.5, to=61.5, by=3), cex=0.65, las=2)
mtext(text=plotFossilsFactorOrder, side=4, at=c(10.5, 32.5, 52.5), cex=0.75, las=2)
```

APPENDIX I

R CODE FOR HELPER FUNCTIONS

R code for helper functions used in calculations, model simulation, and figure creation.

Referred to as 'markovModelFunctions.R' in Appendix H.

```
#Function that converts fossil counts to probabilities of occurrence per facies.

obsToProbs <- function(observations, categories, systemTract=NULL, cutoff) {
  facies <- levels(observations$facies)
  if (!is.null(systemTract)){
    observations <- observations[observations$SystemTract == systemTract, ]
  }
  counts <- sapply(facies, function(x) sapply(observations[observations$facies
== x, categories], function(y) sum(y>cutoff)))
  numberRows <- sapply(facies, function(x) nrow(observations[observations$facies
== x, ]))
  probabilities <- sweep(counts, 2, numberRows, FUN = '/')
  probabilities <- round(probabilities, digits=3)
  probabilities <- as.data.frame(probabilities)
  probabilities <- t(probabilities)
  code <- rownames(probabilities)
  probabilities <- cbind(probabilities, sampleSize=numberRows)
  probabilities <- cbind(code, data.frame(probabilities, row.names=NULL))
  #changing rownames to a new column for facies code

  probabilities
}

#-----
#Function that calculates the upper and lower confidence intervals for the
probabilities of occurrence of different taxa. Probabilities is a dataframe with the
columns "code", "sampleSize", and various taxa. It produces a dataframe with facies,
sample size, taxa, and upper and lower confidence intervals

probabilityConfInt <- function(probabilities, fossilCategories) {
  facies <- probabilities$code
  sampleSize <- probabilities$sampleSize
  taxa <- probabilities[ ,c(fossilCategories)] * 100
  confInt <- data.frame(facies=character(), fossilType=character(),
probCol=numeric(), upperCI=numeric(), lowerCI=numeric(), sampleSize=numeric())

  for (i in 1:length(taxa)) {
    column <- taxa[i]
```

```

fossil <- names(column)

for (j in 1:length(facies)) {
  currentFacies <- facies[j]
  percentage <- column[j, ]
  currentSampleSize <- sampleSize[j]
  if (percentage == 0 | percentage == 100 | is.nan(percentage) ) {
    lowerCI <- NA
    upperCI <- NA
  } else {
    CI <- binomialCI(percentage=percentage,
sampleSize=currentSampleSize)
    lowerCI <- round(CI[1], digits=3)
    upperCI <- round(CI[2], digits=3)
  }
  confInt[nrow(confInt)+1, ] <- c(currentFacies, fossil,
percentage, upperCI, lowerCI, currentSampleSize)
}
}
confInt
}

```

```

#-----
#Function that adds a base to the system tracts in a column. This allows for
calculating the sampling units. A new base is added when the system tract changes
within one measured column (section number remains the same).

```

```

addBase <- function(allColumns, baseCode) {
  lastRow <- nrow(allColumns)
  row <- 1
  while (row < lastRow) {
    systemTractHasChanged <- allColumns[row, "systemTract"] !=
allColumns[row+1, "systemTract"]
    sectionUnchanged <- allColumns[row, "section"] == allColumns[row+1,
"section"]
    if (systemTractHasChanged && sectionUnchanged) {
      newSection <- allColumns[row,1]
      newTop <- allColumns[row, "top"]
      newSysTract <- allColumns[row+1, "systemTract"]
      newSamplingUnit <- allColumns[row+1, "samplingUnit"]
      newRow <-list(newSection, 0, baseCode, newTop, newSysTract,
newSamplingUnit)
      allColumns <- rbind(allColumns[1:row, ], newRow, allColumns[-
(1:row), ])
      lastRow <- nrow(allColumns)
    }
    row <- row + 1
  }
  allColumns
}

```

```

#-----
#Function that adds sampling units. These can be used for future metric calculations.
"col1" and "col2" are the columns that define individual sampling units.

```

```

addSamplingUnits <- function(rawData, col1, col2) {
  rawData$samplingUnit <- NA
  samplingUnit <- 1
  rawData$samplingUnit[1] <- samplingUnit
  for (i in 1:(nrow(rawData) - 1)) {
    col1HasChanged <- rawData[i, col1] != rawData[i+1, col1]
    col2HasChanged <- rawData[i, col2] != rawData[i+1, col2]
    if (col1HasChanged || col2HasChanged) {
      samplingUnit <- samplingUnit + 1
    }
    rawData$samplingUnit[i + 1] <- samplingUnit
  }
  rawData$samplingUnit <- factor(rawData$samplingUnit)
  rawData
}

#-----
#Function that splits data based on the system tract and stores it as a list

splitData <- function(allColumns, sysTractList) {
  sysTractData <- list()
  for (i in 1:length(sysTractList)) {
    rows <- which(allColumns$systemTract == sysTractList[i])
    sysTractData[[i]] <- allColumns[rows, ]
    names(sysTractData)[i] <- sysTractList[i]
  }
  sysTractData
}

#-----
#Function that calculates the thickness distribution of the systems tracts

sysTractThickness <- function(allColumns, sysTract, thicknessCutoff=0) {
  subset <- allColumns[allColumns$systemTract == sysTract, ]
  base <- which(subset$thickness == 0)
  thickDist <- rep(0, length(base))
  base <- c(base, nrow(subset))
  for (i in 1:(length(base) - 1)) {
    bottom <- base[i]
    top <- base[i + 1]
    sysTractThick <- sum(subset$thickness[bottom:top])
    thickDist[i] <- sysTractThick
  }
  thickDist <- thickDist[thickDist >= thicknessCutoff]
  thickDist
}

#-----
#Function which adds a column ("thickness") to the measured stratigraphic column with
the calculated thickness of each unit in meters. The argument x is a data frame. "x"
requires a column named top.

thickness <- function(x) {
  base <- 0 #initializes base
  top <- x$top
}

```

```

        x$thickness <- c(base, diff(top))      #calculates thickness
        x$thickness <- ifelse(x$thickness < 0, 0, x$thickness)  #replaces negative
thickness values with 0
        x
    }

#-----
#Function that calculates a transition matrix on a strata object. The strata argument
should be a stratigraphic column. "strata" needs to have a column named "facies".
"del" is a vector of facies names that you want to exclude from the calculation such
as "base", "covered" etc. "digits" is a fixed value for rounding.

transitionMatrix <- function(strata, del, digits=3) {
    transitions <- table(head(strata$facies, -1), tail(strata$facies, -1))
    #totals transitions
    transitions <- as.data.frame.matrix(transitions)
    toDelete <- which(!is.na(match(rownames(transitions), del)))  #creates
vector of rows and columns to delete
    transitions <- transitions[-toDelete, -toDelete]
    transitions <- round(transitions/rowSums(transitions), digits=digits)
    #calculates transition probabilities
    transitions[is.na(transitions)] <- 0 #replaces NaN values with 0
    transitions
}

#-----
#Function that calculates the system tract transition matrix

systemTractTransitionMatrix <- function(sysTractTransData, digits=3) {
    transitions <- table(head(sysTractTransData$systemTract, -1),
tail(sysTractTransData$systemTract, -1))  #totals transitions
    transitions <- as.data.frame.matrix(transitions)
    transitions <- round(transitions/rowSums(transitions), digits=digits)
    #calculates transition probabilities
    transitions
}

#-----
#Function that returns a list of vectors containing the thickness distribution of
each facies. Requires a strata object that contains the columns "thickness" and
"facies". "del" is a vector of facies you do not want to include in the simulated
column (i.e. base, covered)

faciesThicknessDist <- function(strata, del) {
    toDelete <- which(!is.na(match(strata$facies, del)))
    strata <- strata[-toDelete, ]
    strata$facies <- factor(strata$facies)

    allFaciesThick <- list() #initializes list of vectors
    strata <- strata[ , c("facies", "thickness")]
    fLevs <- levels(strata$facies)
    for (i in 1:length(fLevs)) {          #loops over the number of distinct
facies
        oneFaciesThick <-strata[which(strata$facies == fLevs[i]), "thickness"]
#creates a vector of thickness for one facies

```

```

        allFaciesThick[[i]] <- oneFaciesThick
        names(allFaciesThick)[[i]] <- fLevs[i]
    }
    allFaciesThick
}

#-----
#Function to generate a synthetic column. "transitions" is a transition matrix.
#"faciesThickDist" is a list of vectors containing the thickness distribution of each
#facies. "maxThick" is the total desired thickness of the column

columnGenerator <- function(faciesTransitions, faciesThickDist, maxThick ) {
    maxbeds <- rep(-1, 10000)
    facies <- maxbeds #initializes vector of facies to fill
    thickness <- maxbeds #initializes vector of thicknesses to fill

    sampleLevels <- names(faciesTransitions)
    baseFacies <- sample(sampleLevels, size=1)
    facies[1] <- baseFacies

    baseThicknessDist <- faciesThickDist[[which(names(faciesThickDist) ==
baseFacies)]]
    baseThickness <- sample(baseThicknessDist, size=1)
    thickness[1] <- baseThickness

    total <- baseThickness
    unit <- 1
    while (total < maxThick) {
        startingFacies <- facies[unit]
        weightedProb <- as.numeric(faciesTransitions[which(sampleLevels
== startingFacies), ])
        nextFacies <- sample(sampleLevels, size=1, prob=weightedProb)
        facies[unit+1] <- nextFacies

        thicknessDist <- faciesThickDist[[which(names(faciesThickDist) ==
nextFacies)]]#pulls thickness distribution for specified facies
        nextThickness <- sample(thicknessDist, size=1)
        thickness[unit+1] <- nextThickness
        total = total + nextThickness
        unit = unit + 1
    }

    #deletes unused rows and levels
    newColumn <- data.frame(facies, thickness)
    newColumn <- newColumn[!(newColumn$facies == -1 & newColumn$thickness == -1),
]
    newColumn$facies <- factor(newColumn$facies)

    #caps thickness to maxThick
    if (sum(newColumn$thickness) > maxThick) {
        cap <- sum(newColumn$thickness) - maxThick
        newColumn$thickness[nrow(newColumn)] <-
newColumn$thickness[nrow(newColumn)] - cap
    }
}

```

```

        newColumn
    }

#-----
#Function that randomly generates system tracts and their thickness from a transition
matrix and thickness probability distribution

columnGenerator_systemTractSharp <- function(faciesTransitions, sysTractTransitions,
faciesThickDist, sysTractThickDist, maxHeight, sysTractForce=NULL,
sysTractThickForce=NULL) {
    if (is.null(sysTractForce) && is.null(sysTractThickForce)) {
        sysTractDF <- columnGenerator(sysTractTransitions, sysTractThickDist,
maxHeight)
        colnames(sysTractDF)[1] <- "systemTract"
    } else {
        sysTractDF <- data.frame(systemTract=sysTractForce,
thickness=sysTractThickForce)
    }

    fullColumnList <- list()

    for (i in 1:nrow(sysTractDF)) {
        sysTract <- sysTractDF$systemTract[i]
        sysTractThickness <- sysTractDF$thickness[i]

        simulatedColumn <- columnGenerator(faciesTransitions[[sysTract]],
faciesThickDist[[sysTract]], maxThick=sysTractThickness)
        simulatedColumn$systemTract <- rep(sysTract, nrow(simulatedColumn))
        fullColumnList[[i]] <- simulatedColumn
    }
    simulatedColumn <- Reduce(rbind, fullColumnList)
    returnList <- list(simulatedColumn=simulatedColumn, sysTractDF=sysTractDF)
    returnList
}

#-----
#Function that interpolates between two end member transition matrices

interpolateTransitionProbabilities <- function(low, high, fraction) {
    intermediate <- low + fraction * (high - low)
    intermediate
}

#-----
#Function that calculates the fractional distance from the base- used in the
interpolation functions

fractionFromPosition <- function(base, top, position) {
    frac <- (position - base) / (top - base)
    frac
}

#-----
#Function that interpolates the thickness of a given facies from the end member
systems tracts

```

```

interpolateFaciesThickness <- function(low, high, facies, fraction) {
  highThicknessDist <- high[[which(names(high) == facies)]]
  lowThicknessDist <- low[[which(names(low) == facies)]]

  highThickness <- sample(highThicknessDist, size=1)
  lowThickness <- sample(lowThicknessDist, size=1)

  intermediateThickness <- lowThickness + fraction * (highThickness -
lowThickness)
  intermediateThickness
}

#-----
#Function that generates a column with a gradational change between two end member
systems tracts.

columnGenerator_systemTractGradual <- function(faciesTransitions, faciesThickDist,
startSysTract, endSysTract, maxThick) {
  sysTractDF <- data.frame(systemTract="Gradual", thickness=maxThick)
  maxbeds <- rep(-1, 10000) #vector of a size larger than I would need, with -1
to filter results
  facies <- maxbeds #initializes vector of facies to fill
  thickness <- maxbeds #initializes vector of thicknesses to fill

  lowTmatrix <- faciesTransitions[[startSysTract]]
  lowFaciesThickDist <- faciesThickDist[[startSysTract]]
  highTmatrix <- faciesTransitions[[endSysTract]]
  highFaciesThickDist <- faciesThickDist[[endSysTract]]

  baseFacies <- sample(names(lowTmatrix), size=1)
  facies[1] <- baseFacies

  baseFaciesMatch <- which(names(lowFaciesThickDist) == baseFacies)
  baseThicknessDist <- lowFaciesThickDist[[baseFaciesMatch]]
  baseThickness <- sample(baseThicknessDist, size=1)
  thickness[1] <- baseThickness

  currentPosition <- baseThickness
  unit = 1

  while (currentPosition < maxThick) {
    fraction <- fractionFromPosition(0, maxThick, currentPosition)
    currentTmatrix <- interpolateTransitionProbabilities(lowTmatrix,
highTmatrix, fraction)
    startingFacies <- facies[unit]
    probStartFacies <- names(currentTmatrix) == startingFacies
    weightedProb <- as.numeric(currentTmatrix[probStartFacies, ])
    nextFacies <- sample(names(currentTmatrix), size=1, prob=weightedProb)
    nextFaciesThickness <- interpolateFaciesThickness(lowFaciesThickDist,
highFaciesThickDist, nextFacies, fraction)

    facies[unit+1] <- nextFacies
    thickness[unit+1] <- nextFaciesThickness
    currentPosition = currentPosition + nextFaciesThickness
  }
}

```

```

        unit = unit + 1
    }

    #deletes unused rows and levels
    newColumn <- data.frame(facies, thickness)
    newColumn <- newColumn[!(newColumn$facies == -1 & newColumn$thickness == -1),
]
    newColumn$facies <- factor(newColumn$facies)

    #caps thickness to maxThick
    if (sum(newColumn$thickness) > maxThick) {
        cap <- sum(newColumn$thickness) - maxThick
        newColumn$thickness[nrow(newColumn)] <-
newColumn$thickness[nrow(newColumn)] - cap
    }
    returnList <- list(simulatedColumn=newColumn, sysTractDF=sysTractDF)
    returnList
}

```

```

#-----
#Function that prepares a strata object (generated column or natural column) for
plotting using a key. The key should contain columns for the facies code, grainSize,
isSurface, and color.

```

```

plottingStrata <- function(strata, strataKey) {
    strata$top <- cumsum(strata$thickness)
    strata$bottom <- c(0, strata$top[-length(strata$top)])
    strata$left <- rep(0, nrow(strata))

    right <- rep(0, nrow(strata))
    for (i in 1:nrow(strataKey)) {
        right[which(!is.na(match(strata$facies, strataKey$code[i])))] <-
strataKey$grainSize[i]
    }
    strata$right <- right

    color <- rep(0, nrow(strata))
    for (i in 1:nrow(strataKey)) {
        color[which(!is.na(match(strata$facies, strataKey$code[i])))] <-
strataKey$color[i]
    }
    strata$color <- color
    strata
}

```

```

#-----
#Function that draws strata. Requires the product of the plottingStrata function and
a key. The x and y axis labels can be changed. The order of the legend is specified
in the strataKey by a legendOrder column

```

```

drawStrata <- function(plottingStrata, strataKey, plotLegend=FALSE,
yaxisLabel="Stratigraphic Position (m)", xaxisLabel = "Grain size", main="",
yScale=simulatedColThickness) {
    thickness <- plottingStrata$thickness
    facies <- plottingStrata$facies

```

```

grainSize <- list(clay=1, mud=2, silt=3, sand=4, cong=5)
boundaries <- strataKey$code[which(strataKey$isSurface == TRUE)]
boundaries <- plottingStrata[facies %in% boundaries, ]

strataKey <- strataKey[which(!is.na(match(strataKey$code,
plottingStrata$facies))), ]
strataKey <- strataKey[order(strataKey$legendOrder, strataKey$name), ]

dev.new()
plot(0, 0, xlim=c(0,10), ylim=c(0,yScale + 1), type="n", yaxs="i", xaxs="i",
xlab=xaxisLabel, ylab=yaxisLabel, xaxt="n", bty="n", las=2, main=main)
axis(side=1, at=grainSize, labels = names(grainSize))
if (plotLegend == TRUE) {
  legend(x=max(unlist(grainSize))+0.5, y=yScale, legend=c(strataKey$name),
pch=15, pt.cex=1.5, cex=0.8, bty="n", col=c(strataKey$color))
}

#drawing units as rectangles
rect(ybottom=plottingStrata$bottom, ytop=plottingStrata$top,
xleft=plottingStrata$left, xright=plottingStrata$right, col=plottingStrata$color)
rect(ybottom=boundaries$bottom, ytop=boundaries$top, xleft=boundaries$left,
xright=boundaries$right, col=boundaries$color, border=boundaries$color)
}

#-----
#Function that adds colored bars to the plot to delineate systems tracts

plotSystemTract <- function(plottingStrata, sysTractColors) {
  plottingStrata$systemTract <- factor(plottingStrata$systemTract)
  nSysTracts <- length(levels(plottingStrata$systemTract))
  for (i in 1:nSysTracts) {
    currentTract <- levels(plottingStrata$systemTract)[i]
    row <- sysTractColors[sysTractColors$systemTract == currentTract, ]
    barColor <- row$barColor
    sysTract <- plottingStrata[plottingStrata$systemTract == currentTract, ]
    rect(ybottom=sysTract$bottom, ytop=sysTract$top, xleft=5.1, xright=5.3,
col=barColor, border=barColor)
  }
}

#-----
#Function that generates the occurrence of fossils at each "sampleInterval" based on
the probability of occurrence. Requires a strata object, and a matrix with the
probability of occurrence of each taxa per each facies ("taxaProbability").

fossilGenerator <- function(strata, taxaProbability, sampleInterval) {
  strata$unitTops <- cumsum(strata$thickness)
  if (ncol(strata) == 4) {
    strata <- rbind(c(NA, 0, NA, 0), strata) #start column at 0
  } else if (ncol(strata) == 3) {
    strata <- rbind(c(NA, 0, 0), strata) #start column at 0
  }

  nSamples <- round(max(strata$unitTops) / sampleInterval)
  taxa <- names(taxaProbability[2:ncol(taxaProbability)])

```

```

test <- matrix(data=rep(0, ncol(taxaProbability) * nSamples),
ncol=ncol(taxaProbability), nrow=nSamples)
occurrence <- data.frame(test)
colnames(occurrence) <- c("stratPosition", taxa)
stratPosition <- seq(sampleInterval, max(strata$unitTops), by=sampleInterval)
occurrence$stratPosition <- stratPosition
for (horizon in 1:nrow(occurrence)) {
  index <- min(which(strata$unitTops >=
occurrence$stratPosition[horizon]))
  row <- which(!is.na(match(taxaProbability$code, strata$facies[index])))
  for (taxon in 2:ncol(taxaProbability)) {
    prob <- taxaProbability[row, taxon]
    if (prob > runif(1)){
      occurrence[horizon, taxon] <- 1
    }
  }
}
occurrence
}

#-----
#Function that plots the occurrences of fossils. "color" is a vector of color names
that should be the same length as the number of taxa you want to plot. The
"guideLine" argument can be set to "none", for no lines, or "bold", for bold lines.
The default is light guidelines and black dots indicating a taxon occurred.

plotFossils <- function(occurrences, plottingStrata, strataKey, color=c("black"),
guideLine=c("light", "bold", "none"), yScale=simulatedColThickness, plotLegend=TRUE)
{
  colorCheck <- length(color)
  if (colorCheck != 1) {
    if(colorCheck != (length(occurrences) - 1)) {
      stop("Error: Number of colors given is not equal to the number of
taxa")
    }
  }

  guidelineCheck <- guideLine %in% c("light", "bold", "none")
  if (any(guidelineCheck == FALSE)) {
    stop(paste(guideline, "not valid argument for guideline: must be
'light', 'bold', or 'none'"), call.=FALSE)
  }
  guideline <- match.arg(guideline)

  ntaxa <- ncol(occurrences) - 1 #figuring out horizontal spacing of fossils on
plot
  edge <- 5.5 + (ntaxa - 1) * 0.25
  location <- seq(5.5, edge, 0.25)

  strataKey <- strataKey[which(!is.na(match(strataKey$code,
plottingStrata$facies))), ]
  strataKey <- strataKey[order(strataKey$legendOrder, strataKey$name), ]

  if (plotLegend == TRUE) {

```

```

        legend(legend=c(strataKey$name), x=edge + 0.5, y=yScale + 1, pch=15,
pt.cex=1.5, cex=0.8, bty="n", col=c(strataKey$color))
    }

    for (i in 2:ncol(occurrences)) {
        mtext(text=names(occurrences[i]), side=1, line=0, at=location[i-1],
cex=.7, las=2)
        fossilOccured <- which(occurrences[ , i] == TRUE)
        if (guideLine == "light") {
            abline(v=location[i-1], col="grey90")
        } else if (guideLine == "bold") {
            abline(v=location[i-1], col="grey60")
        }

        if (color[1] == "black") {
            points(x=rep(location[i-1], length(fossilOccured)),
y=occurrences$stratPosition[fossilOccured], pch=16, cex=.75, col=color)
        } else {
            points(x=rep(location[i-1], length(fossilOccured)),
y=occurrences$stratPosition[fossilOccured], pch=16, cex=.75, col=color[i-1])
        }
    }
}

```

```

#-----
#Function to calculate the channel to floodplain ratio in each sampling unit

```

```

percentFaciesThick <- function(allColumns, facies) {
    samplingUnits <- levels(allColumns$samplingUnit)
    faciesPercent <- rep(0, length(samplingUnits))
    for (i in 1:length(samplingUnits)) {
        group <- allColumns[allColumns$samplingUnit == samplingUnits[i], ]
        totalThick <- sum(group$thickness)

        faciesOfInterest <- which(!is.na(match(group$facies, facies)))
        faciesThickness <- group[faciesOfInterest, "thickness"]

        percentThick <- sum(faciesThickness) / totalThick
        faciesPercent[i] <- percentThick
    }
    faciesPercent <- round(faciesPercent, 3)
    faciesPercent
}

```

```

#-----
#Function to calculate the proportional thickness of a facies for each sampling unit

```

```

propFaciesThickness <- function(allColumns, facies){
    samplingUnits <- levels(allColumns$samplingUnit)
    propThick <- rep(0, length(samplingUnits))
    for (i in 1:length(samplingUnits)) {
        group <- allColumns[allColumns$samplingUnit == samplingUnits[i], ]
        totalThick <- sum(group$thickness)
        faciesThick <- sum(group$thickness[group$facies == facies])
        propThickFacies <- faciesThick / totalThick
    }
}

```

```

        propThick[i] <- propThickFacies
    }
    propThick <- round(propThick, 3)
    propThick
}
#-----
#Function that creates a new data frame to tabulate stratigraphic column metrics

createMetricsTable <- function(allColumns) {
    samplingUnits <- levels(allColumns$samplingUnit)
    metrics <- data.frame("samplingUnit"=samplingUnits, "section"=NA,
"systemTract"=NA)

    for (i in 1:length(samplingUnits)) {
        subset <- allColumns[allColumns$samplingUnit == samplingUnits[i], ]
        section <- subset$section[1]
        metrics$section[i] <- as.character(section)

        systemTract <- subset$systemTract[1]
        metrics$systemTract[i] <- as.character(systemTract)
    }
    metrics
}

#-----
#Function that counts the number of each facies and divides by the total number of
facies for that systems tract. Used for making a comparative bar plot

proportionalFaciesCounts <- function(sysTractData, del){
    nFacies <- count(sysTractData, facies)
    nFacies <- nFacies[!nFacies$facies == del, ] #gets rid of base as facies
    totalBodies <- sum(nFacies$n)
    nFacies$n <- nFacies$n / totalBodies #calculate proportional number of
bodies
    nFacies
}

#-----
#Function to transform transition matrix into ggplot dataframe for Judith River data

JRtMatrixFigure <- function(transitions) {
    list <- c()
    for (i in 1:length(transitions)) {
        list[[i]] <- t(transitions[i,])
    }

    x <- do.call(rbind, list)
    tmatrixPlot <- as.data.frame(x, make.names=NA)
    tmatrixPlot$To <- rownames(x)
    colnames(tmatrixPlot)[1] <- "Probability"
    tmatrixPlot$From <- rep(NA, 49)
    tmatrixPlot$From[1:7] <- "Fluvial channel bar"
    tmatrixPlot$From[8:14] <- "Floodplain mud"
    tmatrixPlot$From[15:21] <- "Floodplain sand"
    tmatrixPlot$From[22:28] <- "Fluvial channel lag"
}

```

```

tmatrixPlot$From[29:35] <- "Mire"
tmatrixPlot$From[36:42] <- "Pond/Lake"
tmatrixPlot$From[43:49] <- "Tidally influenced channel bar"

tmatrixPlot
}

#-----
#Function that gets confidence interval data into the correct order for plotting

pocDataOrder <- function(confIntData, plotFaciesFactorOrder, faciesNames,
plotFossilsFactorOrder) {
  confIntData$fossilType <- factor(confIntData$fossilType,
levels=plotFossilsFactorOrder)
  confIntData$facies <- factor(confIntData$facies, levels=plotFaciesFactorOrder)
  fossilTypes <- levels(confIntData$fossilType)
  orderedTaxa <- list()

  for (i in 1:length(fossilTypes)) {
    taxa <- confIntData[confIntData$fossilType == fossilTypes[i], ]
    taxa <- taxa[order(taxa$facies), ]
    orderedTaxa[[i]] <- taxa
  }

  orderedTaxa <- do.call("rbind", orderedTaxa)
  orderedTaxa$fossilType <- as.factor(orderedTaxa$fossilType)
  orderedTaxa$probCol <- as.numeric(orderedTaxa$probCol)
  orderedTaxa$upperCI <- as.numeric(orderedTaxa$upperCI)
  orderedTaxa$lowerCI <- as.numeric(orderedTaxa$lowerCI)
  orderedTaxa[is.na(orderedTaxa)] <- 0

  orderedTaxa
}

#-----
#Functions to check data for errors

surfacesToDeleteCheck <- function(rawData, surfacesToDelete) {
  checkToDeleteS <- !is.na(match(surfacesToDelete, levels(rawData$facies)))
  if (any(checkToDeleteS == FALSE)) {
    error <- surfacesToDelete[which(checkToDeleteS == FALSE)]
    warning(paste(error, "is not in rawData facies. Check spelling of
'baseCode' or 'coveredCode' inputs.\n"), call.=FALSE)
    return(1)
  } else {
    return(0)
  }
}

rawDataStructureCheck <- function(rawData) {
  columnNames <- c("top", "facies")
  columnCheck <- columnNames %in% colnames(rawData)
  if (any(columnCheck == FALSE)) {
    index <- which(columnCheck == FALSE)
    missingCols <- columnNames[index]
  }
}

```

```

        warning(paste("Column named", missingCols, "is missing from your
rawData.\n"), call.=FALSE)
        return(1)
    } else{
        return(0)
    }
}

strataKeyStructureCheck <- function(strataKey) {
    columnKeyNames <- c("code", "name", "color", "grainSize", "isSurface",
"legendOrder")
    columnKeyCheck <- columnKeyNames %in% colnames(strataKey)
    if (any(columnKeyCheck == FALSE)) {
        index <- which(columnKeyCheck == FALSE)
        missingCols <- columnKeyNames[index]
        warning(paste("Column named", missingCols, "is missing from your
columnKey.\n"), call.=FALSE)
        return(1)
    } else{
        return(0)
    }
}

keyDataMatchCheck <- function(rawData, strataKey, surfacesToDelete) {
    dataFacies <- levels(rawData$facies)
    keyFacies <- strataKey$code
    checkFacies <- is.na(match(dataFacies, keyFacies))
    mismatch <- dataFacies[which(checkFacies)]
    checkMismatch <- mismatch %in% surfacesToDelete
    if (any(checkMismatch == FALSE)) {
        error <- mismatch[which(checkMismatch == FALSE)]
        warning(paste(error, "is in the rawData but not in the columnKey. Fixing
spelling of 'baseCode' or 'coveredCode' could solve this error.\n"), call.=FALSE)
        return(1)
    } else{
        return(0)
    }
}

taxaProbDataMatchCheck <- function(rawData, taxaProbability, surfacesToDelete) {
    dataFacies <- levels(rawData$facies)
    taxaProbFacies <- taxaProbability$code
    checkFacies <- is.na(match(dataFacies, taxaProbFacies))
    mismatch <- dataFacies[which(checkFacies)]
    checkMismatch <- mismatch %in% surfacesToDelete
    if (any(checkMismatch == FALSE)) {
        error <- mismatch[which(checkMismatch == FALSE)]
        warning(paste(error, "is in the rawData but not taxaProbability. Fixing
spelling of 'baseCode' or 'coveredCode' could solve this error.\n"), call.=FALSE)
        return(1)
    } else {
        return(0)
    }
}

```

```

anomalousThicknessCheck <- function(rawData, stratSurfaces, stratSurfaceThickness) {
  data <- thickness(rawData)
  surfaces <- which(!is.na(match(data$facies, stratSurfaces)))
  checkThickness <- data$thickness[surfaces] >= stratSurfaceThickness
  if (any(checkThickness == TRUE)) {
    row <- surfaces[checkThickness == TRUE]
    warning(paste("Thickness of surface in row", row, "of rawData is
anomalous.\n"), call.=FALSE)
    return(list(1, row))
  } else {
    return(0)
  }
}

highProbabilityCheck <- function(taxaProbability) {
  taxaProbs <- taxaProbability[, 2:ncol(taxaProbability)]
  check <- taxaProbs > 1
  if (any(check == TRUE)) {
    trueMatrix <- which(check == TRUE, arr.ind=TRUE)
    row <- trueMatrix[, "row"]
    warning(paste("Probability in row", row, "of taxaProbability is greater
than 1. Probabilities greater than 1 are not allowed.\n"), call.=FALSE)
    return(list(1, row))
  } else {
    return(0)
  }
}

lowProbabilityCheck <- function(taxaProbability) {
  taxaProbs <- taxaProbability[, 2:ncol(taxaProbability)]
  check <- taxaProbs < 0
  if (any(check == TRUE)) {
    trueMatrix <- which(check == TRUE, arr.ind=TRUE)
    row <- trueMatrix[, "row"]
    warning(paste("Probability in row", row, "of taxaProbability less than
0. Negative probabilities are not allowed.\n"), call.=FALSE)
    return(list(1, row))
  } else {
    return(0)
  }
}

zeroThicknessCheck <- function(rawData, baseCode) {
  data <- thickness(rawData)
  zeroThickness <- data[data$thickness == 0, ]
  checkFacies <- !is.na(match(zeroThickness$facies, baseCode))
  if (any(checkFacies == FALSE)){
    row <- which(is.na(match(zeroThickness$facies, "AFbase")))
    warning(paste("Thickness of", zeroThickness$facies[row], "in column",
zeroThickness$section[row], "of rawData is zero.\n"), call.=FALSE)
    df <- zeroThickness[checkFacies == FALSE, ]
    return(list(1, df))
  } else {
    return(0)
  }
}

```

```

}

#-----
#Parent testing function

checkData <- function(rawData, strataKey, taxaProbability, stratSurfaces,
surfacesToDelete, stratSurfaceThickness) {
  errors <- rep(0, 10)
  errors[1] <- surfacesToDeleteCheck(rawData, surfacesToDelete)
  errors[2] <- rawDataStructureCheck(rawData)
  errors[3] <- strataKeyStructureCheck(strataKey)
  errors[4] <- keyDataMatchCheck(rawData, strataKey, surfacesToDelete)
  errors[5] <- taxaProbDataMatchCheck(rawData, taxaProbability,
surfacesToDelete)
  thicknessCheck <- anomalousThicknessCheck(rawData, stratSurfaces,
stratSurfaceThickness)
  errors[6] <- thicknessCheck[[1]]
  if (errors[6] == TRUE) {
    print(thickness(rawData)[thicknessCheck[[2]], ])
  }
  zeroThickness <- zeroThicknessCheck(rawData, surfacesToDelete[1])
  errors[7] <- zeroThickness[[1]]
  if (errors[7] == TRUE) {
    print(zeroThickness[[2]])
  }
  highProbs <- highProbabilityCheck(taxaProbability)
  errors[8] <- highProbs[[1]]
  if (errors[8] == TRUE) {
    print(taxaProbability[highProbs[[2]], ])
  }
  negativeProbs <- lowProbabilityCheck(taxaProbability)
  errors[9] <- negativeProbs[[1]]
  if (errors[9] == TRUE) {
    print(taxaProbability[negativeProbs[[2]], ])
  }

  if (any(errors == TRUE)) {
    message("Fix errors and re-run checkData function.")
  } else {
    message("There were no errors detected in your data. Proceed to
analysis.")
  }
}

```